



D1.1 Literature review on electrochemical suppression and electromagnetic decomposition of NOx

Lead beneficiary:	National Aerospace University "KhAI"
Author(s):	Leonid Bazyma, Dmytro Dolmatov, Vladimir Sorokin
Contributor(s):	Igor Rybalchenko
Date of issue:	29 March 2019
Dissemination level:	Public

Project information

Project full title:	Innovative Technologies of Electrochemical Suppression and Electromagnetic Decomposition for NOx Reduction in Aeroengines
Project acronym:	DENOX
Grant agreement:	831848
Project start date	01 January 2019
Duration:	48 months
Project website:	www.denox-project.eu



This project has received funding from the Clean Sky 2 Joint Undertaking (JU) under grant agreement No 831848. The JU receives support from the European Union's Horizon 2020 research and innovation programme and the Clean Sky 2 JU members other than the Union".

Document History

Version and date	Changes
1.0 – 05/02/2019	Report structure: prepared by Leonid Bazyma (Khal)
1.1 – 04/03/2019	Draft: technical inputs are provided by Leonid Bazyma, Dmytro Dolmatov, Vladimir Sorokin (KhAI)
2.0 – 15/03/2019	Draft: all inputs are harmonized by Leonid Bazyma (KhAI). Version ready for review.
2.1 – 21/03/2019	Revised version: Dmytro Dolmatov, Igor Rybalchenko (KhAI)
3.0 – 26/03/2019	Final version: prepared by Dmytro Dolmatov (KhAI)
3.1 – 29/03/2019	Final version: reviewed and approved by Mykola Lubiv (STCU)

Contents

Abbreviations	5
1. Introduction	7
1.1. About the DENOX project.....	7
1.2. Scope of this deliverable.....	7
2. Foreword.....	9
3. Nitrogen Oxides Generation Mechanism	14
3.1 Decomposition of NOx formation into slow and fast processes	16
3.2 Impact of operating conditions	16
4. Emission Controlling Mechanisms	17
5. Combustion Concepts.....	22
5.1 Classical Low Emission Combustors	22
5.2 Current Combustion Technologies	26
6. Different Variants to Gas Discharge Plasmas	28
6.1 Nanosecond Repetitively Pulsed Discharges	31
6.2 Comparison of various discharges.....	32
7. Gas Discharge Plasma Technologies	35
8. New Combustion Concepts Under Extreme and Non-Equilibrium Conditions	38
8.1 New FLame Regimes at Low Temperature and Non-Equilibrium Conditions	39
9. Nonequilibrium Plasma-Assisted Combustion	40
10. Mechanisms of Plasma Assisted Combustion	43
11. Combustion Modification by Non-Thermal Plasma	44
11.1 Flame stabilization	44
11.2 Experimental study plasma-assisted combustion in an aero-engine combustion chamber	45
12. Development of Kinetic Mechanisms for Plasma Assisted Combustion.....	49
12.1 The Chemistry of Nonequilibrium Discharges.....	49
12.2 Multiscale and Dynamic Adaptive Chemistry Modeling Using Reduced and Detailed Mechanism	54
12.3 Microwave plasma and catalytic decomposition of nitrogen oxides	57
13. Conclusion	62
References.....	65

APPENDICES	76
Appendix 1. Oxygen plasma kinetic scheme	76
Appendix 2. Reaction scheme for hydrogen oxidation involving electronically-excited oxygen molecules.....	77
Appendix 3. Influence of reactions rate on conversion NOx species	80

Abbreviations

AC	Alternating Current
ACARE	Advisory Council for Aviation Research and Innovation in Europe
AFR	Air Fuel Ratio
ASC	Axially Staged Combustors
CAEE	Committee on Aviation Engine Emissions
CAEP	Committee on Aviation Environmental Protection
CAN	Committee on Aircraft Noise
CC RF	Capacitively Coupled Radio-Frequency
CO ₂	Carbon Dioxide
CO	Carbon Monoxide
CMD	Continuous Microwave Discharge
DAC	Double Annular Combustor
DC	Direct Current
Da (I)	Damkohler number: ratio of chemical reaction rate to mass flow rate or relation between the transport time scale and the chemical time scale
Da (II)	Damkohler number: ratio of chemical heat liberation rate to advection heating value
Da (III)	Damkohler number: ratio of chemical reaction rate to diffusion
Da (IV)	Damkohler number: ratio of chemical heat to diffusive heat flow
Da (V)	Damkohler number: ratio of chemical rate to elutriation rate, used in fluidized bed combustion
DBD	Dielectric Barrier Discharge
DES	Detached Eddy Simulation
EASA	European Aviation Safety Agency
FAR	Fuel Air Ratio
FAA	Federal Aviation Administration
FC	Flameless Combustion
GE	General Electric
GT	Gas Turbine
GTE	Gas Turbine Engine
HC	Hydrocarbon
ICAO	International Civil Aviation Organisation

Ka	Kalovitz number: ratio between the chemical time scale and the Kolmogorov time scale
LDI	Lean Direct Injection
LEC	Low Emissions Combustors
LECC	Low Emission Combustion Chambers
LTE	Local Thermal Equilibrium
LPP	Lean Premixed Prevaporised
LT	Long Term
LTO	Landing take-off
MT	Mid Term
N2O	Nitrous Oxide
NO2	Nitrogen Dioxide
NOx	Nitrogen Oxides
NO	Nitrogen Monoxide
O*=O(1D)	Singlet D atomic oxygen
O ₂ [*]	Excited oxygen
O ₂ (¹ _a Δ _g)	Excited oxygen singlet delta
O ₂ (¹ _b Σ _g ⁺)	Excited oxygen singlet sigma
OPR	Overall Pressure Ratios
PAC	Plasma assisted Combustion
PERM	Partially Evaporating and Rapid Mixing
RF	Radio-Frequency
RQL	Rich-burn Quick-quench Lean-burn
SFC	Specific fuel consumption
SSC	Single annular combustors
TALON	Technology for Advanced Low NOx
TAPS	Twin Annular Premixing Swirler
TET	Turbine Entry Temperatures
TIT	Turbine inlet temperatures
TVC	Trapped Vortex Combustor
UHC	Unburned Hydrocarbons

1. Introduction

1.1. About the DENOX project

DENOX project aims to develop and experimentally prove two breakthrough technology concepts and their optimal combination for drastic reduction of NO_x emissions in aeronautic gas-turbine engines (GTEs).

Technology concept 1 is electrochemical suppression of NO_x generation in primary combustion zone. It consists in generation of modulated discharge(s) in combustion chamber to initiate chemical reactions competitive to conventional NO_x generation mechanisms.

Technology concept 2 is electromagnetic decomposition of NO_x molecules in engine exhaust. It consists in application of multi-frequency electromagnetic fields to the exhaust flow to ensure resonance excitation of chemical bonds in NO_x molecules up to their dissociation.

DENOX technology concepts are underpinned by the theoretical investigations and numerical studies of high-temperature high-pressure low emission combustion processes, which demonstrated potential to decrease NO_x concentration in exhausting gases on 20-95% without decreasing of engine efficiency.

The project will combine analytical studies and numerical simulations with experimental investigations and multilevel testing campaign to translate proposed technology concepts from TRL1 to TRL3 and to assess full potential of their combination for the next-generation GTEs.

DENOX outcomes will contribute to the advancement of aircraft engines in both (i) mid-term perspective (EIS 2035) through progress in understanding and modelling of high-temperature low emission combustion processes, and (ii) long-term perspective (EIS 2050) through the potential to drastically reduce NO_x emissions to meet Clean Sky 2 High Level Objectives and ACARE SRIA goals.

1.2. Scope of this deliverable

This deliverable provides a comprehensive review of low emissions combustion technologies for modern aero gas turbines, which is a primary focus of the DENOX project. However, analysis will not be limited to aeronautic applications. The focus of the review is placed on working principles, a review of the key technologies, technology application and emissions mitigation potential, on electrochemical suppression and electromagnetic decomposition of NO_x.

As Dickson reported for the Long-Term 2026 goal it was demonstrated that no entire engine family has yet to meet the goal. The trends and goals in aviation engines are paradoxical in relation to NO_x emissions. Turbine inlet temperatures and overall pressure ratios have been increasing over time in the pursuit of increasing thermal efficiency and thereby reducing the fuel consumption and CO₂ emissions. While on the other hand, NO_x emissions have to be reduced, in spite of their tendency to increase with both turbine inlet temperatures and overall pressure ratios.

A few approaches have been investigated and attempted as new combustion concepts for aeronautical gas turbines, such as the Trapped Vortex Combustor and Lean Direct Injection. However, these concepts are not likely to be able to meet the ambitious ACARE and NASA emission reduction goals for aero engines as the pressure ratio and operating temperatures are being increased in the pursuit of increasing efficiency. Therefore alternative combustion concepts like flameless combustion or plasma assisted combustion have to be explored.

The research papers and patents reviewed for plasma combustion have shown better understanding of nonthermal and thermal enhancement effects, kinetic modelling and validation, diagnostics of excited species, plasma temperature combustion, flame regime transition, dynamics of the minimum ignition energy in gas turbine engines, scramjets, and other lean burn combustion systems. However, there are only few research papers on effect of different plasma conditions on the combustion and ignition processes. The data on plasma low temperature are also limited. There are inadequate kinetic models and tools to adequately simulate plasma combustion and ignition processes. Thus, further research studies on the application of plasma in wide range of engine operations are still required and will be implemented in the frame of the DENOX project

2. Foreword

Over the past 40-50 years, the aviation industry has been capable of reducing fuel consumption by 70% while also limiting noise and reducing gaseous CO and Hydrocarbon (HC) emissions by approximately 50 and 90%, respectively [1]. This is mainly due to technology improvement in materials and cooling that enable engines to operate at higher Overall Pressure Ratios (OPRs) and Turbine Entry Temperatures (TET) to increase thermal efficiency which in turn reduces the engine specific fuel consumption (SFC) for economic benefit. This leads to high combustor inlet temperature and pressure. These wide environmental benefits (e.g. CO₂ reduction) achieved through higher OPR and TET therefore also led to an increase in NO_x emission. Until 1970s, when larger OPR engines were developed less attention was paid to NO_x emissions until serious concerns were raised by the general public on the effects of NO_x on human health and climate.

The emissions regulations for aircraft are established by the International Civil Aviation Organisation (ICAO) adopting a standard landing take-off (LTO) cycle intended to simulate the aircraft operation below 3000 feet altitude. For subsonic civil aero engines, it is composed of four operating modes (idle, take-off, climb-out and approach) measured at sea level, static and standard day conditions. Emissions are measured as a part of the airworthiness certification process under the supervision of a national airworthiness authority (e.g. European Aviation Safety Agency – EASA or the U.S Federal Aviation Administration – FAA). The standards for gaseous emissions are based on calculated D_p for each species divided by the maximum sea level static rated thrust F_{00} to take account of engine size. The ICAO Emissions Standards set maximum limits on D_p / F_{00} of each gaseous emission. The standards apply to the subsonic aircraft engines whose F_{00} is above 26.7kN (6000 lb).

The first ICAO standard was regulated by the ICAO Committee on Aviation Engine Emissions, (CAEE) in 1981. Later, the CAEE was combined with Committee on Aircraft Noise (CAN) and the Committee on Aviation Environmental Protection (CAEP) was established in 1983. Later ICAO adopted a standard that applied to all in-production engines in 1986, namely the CAEP/1 or ICAO 1986 standard. In order to reduce the impact of aircraft emissions on the environment, CAEP meets every three years to continually formulate and update the emission standards [2]. As NO_x has been considered as a primary issue, ICAO adopted a more stringent standard for NO_x emissions at the 2nd, 4th, 6th and 8th meetings of CAEP. (i.e. CAEP/2 1993, CAEP/4 1999, CAEP/6 2005, CAEP/8 2011). The NO_x emission currently remains at the CAEP/8 standard.

During the CAEP/10 meeting in 2016, recommendations have been made for the two complementary new standards for the emissions. Additionally, attention is also been accorded to address the impact of emissions at high altitude (i.e. NO_x at climb and cruise) [3].

The Clean Sky 2 initiative (2014-2024), part of the EU Horizon 2020 programme, is a Joint Undertaking of the European Commission and the European aeronautics industry. It builds on the original Clean Sky 1 programme (2008-2017), and contributes towards achieving the “Flightpath 2050” environmental objectives set out by the Advisory Council for Aviation Research in Europe (ACARE). It set out the two challenging goals for emissions reduction to be achieved by the time frame 2020 and 2050 relative to year 2000 technology: Vision 2020 and Flightpath 2050. LTO NO_x emissions goals are: 80% reduction relative to CAEP/2 that is

equivalent to -60% CAEP/6 (Vision 2020) and 90% reduction of NO_x (e.g. -75% CAEP/6) for Flightpath 2050. The cruise NO_x targets were also incorporated with the same reduction level as for LTO NO_x [4].

Clean Sky 1 envisioned technologies and procedures that would reduce CO₂ emissions per passenger kilometre by 75%, NO_x emissions by 90%, and perceived noise by 65% relative to the capabilities of a typical new aircraft in the year 2000. The objectives of Clean Sky 2 are to reduce CO₂, NO_x and noise emissions by 20 to 30% compared to “state-of-the-art” aircraft entering into service as from 2014. The Programme aims to accelerate the introduction of new technology in the 2025-2035 timeframe. By 2050, 75% of the world’s fleet now in service (or on order) will be replaced by aircraft that can deploy Clean Sky 2 technologies.

Figure 1 illustrates certified NO_x emissions data of aircraft engine models above 89 kN thrust in relation to the ICAO CAEP NO_x limits [6]. The current ICAO technology goals for NO_x are also shown. These goals, which were agreed in 2007, represent the expected performance of expected ‘leading edge’ technology in 2016 (mid-term) and 2026 (long term).

Each point in Figure 1 represents EASA certified data for an engine model, and the different colours provide insight into the trend over time. The dataset represents engine models typically fitted to single-aisle aircraft (e.g. A320, B737) and larger aircraft (e.g. A350, B777, A380). No further versions of the leading edge GENx engines (lower green dots) have been certified since 2015. However, the most recent data (purple diamonds) illustrate that other manufacturers on different product development cycles have optimised new and existing combustor designs.

Based on experience from European funded research since the 4th framework, the development of low NO_x combustion systems is very difficult and takes a long time. A wide range of technological strategies has been investigated and a lot of effort was spent. These programmes were very successful in identifying and assessing the potential of low emission combustion improvements. Out of the variety of today’s different low emission technology approaches there will be only a few having the potential to eventually meet future NO_x reduction targets while offering the ability to maintain lean combustion stability, operability and safety with competitive cost and weight and airworthiness [5].

As reported in [3] for the Long-Term (LT) 2026 goal it was demonstrated that **no entire engine family has yet to meet the goal**.

The trends and goals in aviation engines are paradoxical in relation to NO_x emissions. Turbine inlet temperatures (TIT) and overall pressure ratios (OPR) have been increasing over time in the pursuit of increasing thermal efficiency and thereby reducing the fuel consumption and CO₂ emissions [8]. While on the other hand, NO_x emissions have to be reduced, in spite of their tendency to increase with both TIT and OPR.

A few approaches have been investigated and attempted as new combustion concepts for aeronautical gas turbines, such as the Trapped Vortex Combustor (TVC) and Lean Direct Injection (LDI). However, these concepts are not likely to be able to meet the ambitious ACARE and NASA emission reduction goals for aero engines as the pressure ratio and operating temperatures are being increased in the pursuit of increasing efficiency. Therefore alternative combustion concepts like Flameless Combustion (FC) or Plasma Assisted Combustion (PAC) have to be explored. A qualitative comparison of different types of combustors with FC is shown in Table 1 [9], in which the advantages of FC are clear: the well-distributed reactions that

characterise the FC regime often yield low temperature gradients, low NO_x emissions, high stability and low acoustic oscillations. It is worth pointing out that the level of readiness for application of FC-based combustors is lower than that of the other types, therefore the characteristics stated in Table 1 are based on its potential [9].

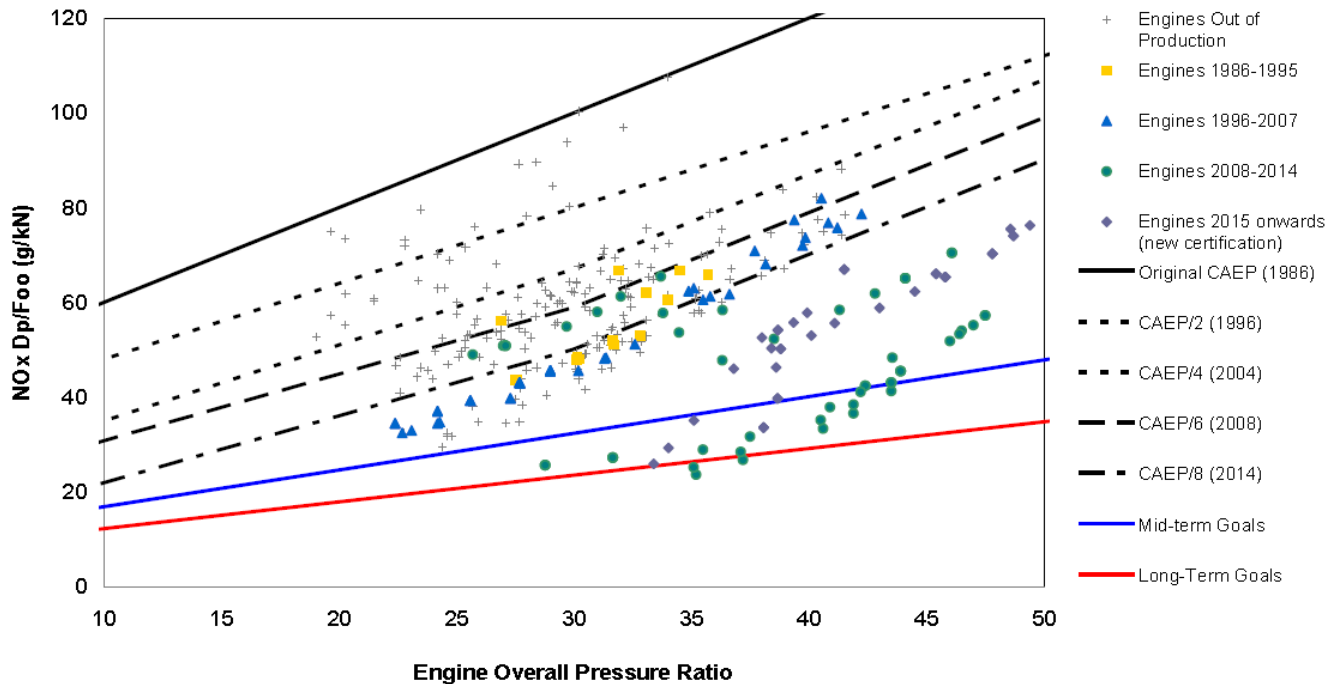


Figure 1. Aircraft engine NO_x emissions vs. CAEP limits (engines with rated thrust > 89 kN) [6, 7]

The literatures reviewed for plasma combustion have shown better understanding of nonthermal and thermal enhancement effects, kinetic modelling and validation, diagnostics of excited species, plasma temperature combustion, flame regime transition, dynamics of the minimum ignition energy in gas turbine (GT) engines, scramjets, and other lean burn combustion systems. However, there are few information on effect of different plasma conditions on the combustion and ignition processes. The data on plasma low temperature are also limited. There are inadequate kinetic models and tools to adequately simulate plasma combustion and ignition processes. Thus, further research studies on the application of plasma in wide range of engine operations are still required.

Table 1 – Qualitative comparison of different combustor types [9].

	Combustor type			
	Lean premixed	Lean direct Injection(LDI)	Rich-burn Quick-mix Lean burn (RQL)	Flameless based
Combustion efficiency	High	High	High	High

Combustion instability	High	Low	Low	Low
Fuel flexibility	Moderate	High	High	Moderate
Integration into engine	Moderate	Moderate	Easy	Difficult
Mechanical complexity	Moderate	High	Moderate	Moderate
NOx emission	Low	Low	Moderate	Ultra-low
Operating range	Moderate	High	High	Low
Soot emission	Very Low	Low	Moderate	Low
Volume requirement	Moderate	Low	Low	High

The resume of the previous reviews (A. Starikovskiy 2013 [10]; Sun W, Ju Y 2013 [11]; D. Dolmatov 2016 [12]; Ju Yiguang 2014, 2017 [13]; Alrashidi, A.M. 2018 [14]) the following:

- Nonequilibrium plasma demonstrates an ability to control flames for a wide range of applications, including aviation GTEs, piston engines, ramjets, scramjets, etc.
- Although many previous studies have demonstrated the effectiveness of plasma to enhance combustion properties *phenomenologically*, the detailed enhancement mechanisms remain largely unknown.
- There is no detailed review on recent advances in the application of plasma in engines, particularly GTs.

Problems to be solved

1) The principal mechanisms of plasma-assisted ignition and combustion have been established and validated for a wide range of plasma and gas parameters.

- High pressure volumetric discharge
- Selective excitation (electronic and vibrational)
- Selective species/radicals production
- Plasma properties: Electric field, electron number density, excitation states, non-equilibrium temperatures
- Plasma physics: Energy transfer processes between different excited states
- Plasma chemistry: Low temperature kinetic pathways, non-equilibrium kinetics
- Kinetic process: Key species, reaction rates, and cross-section areas for large fuel molecules
- Multi-dimensional modelling tools

2) These results provide a basis for improving various energy-conversion combustion systems, from automobile to aircraft engines, using nonequilibrium plasma methods.

This deliverable provides a comprehensive review of low emissions combustion technologies for modern aero gas turbines. However analysis will not be limited to aeronautic applications.

The focus of review is placed on working principles, a review of the key technologies, technology application and emissions mitigation potential, as well as on electrochemical suppression and electromagnetic decomposition of NO_x, which are the key technology concepts to be developed in the frame of the DENOX project.

3. Nitrogen Oxides Generation Mechanism

Nitrogen oxides are a primary air pollutant which is linked to tropospheric ozone O_3 : (i.e. ozone formation in the troposphere) and has an adverse impact on human health. The formation mechanisms are:



Nitrogen oxides (NO_x) are also linked to ozone layer depletion in the stratosphere whose relevant formations are:



The NO produced at the end of reaction will in turn further deplete the ozone layer and chain reaction takes place. The ozone layer depletion in the Stratosphere will increase the ground level UV radiation and cause skin cancer and eye diseases. NO_x is also linked to photochemical smog, acid rain and global warming [15].

The thermal NO is one of the major sources of NO_x produced in practical gas turbine combustors. It is produced in the post flame region where the flame temperature is above 1800 K. The chemical reaction is endothermic (i.e. atomic dissociation occurs when diatomic oxygen O_2 gains enough energy through heat absorption to break into two oxygen atoms). The set of reactions is known as the Zeldovich mechanism and details are shown below:



Nitrogen Oxide (NO) is produced when nitrogen reacts with oxygen atoms via (5) at high temperatures. A chain reaction is then initiated as the nitrogen atom which is produced in (6) can react with molecular oxygen O_2 (7) and OH radical in (8) to form NO with O and H atoms. The concentration of atomic oxygen in the flame front is largely an exponential function of temperature, and NO formation via the Zeldovich mechanism has a similar relationship with flame temperature. Therefore, the thermal NO is increased exponentially with flame temperature for both premixed and diffusion systems.

The prompt NO route was initially suggested by Fenimore [16, 17], who observed that high NO concentrations were found close to the flame region that could not be attributed to the slow thermal route alone. Prompt NO formation is an attribute of hydrocarbon flames where hydrocarbon radicals such as CH react with molecular N_2 [18]. This interaction was initially attributed to a reaction with CH to form HCN intermediate:



Formation of NO from chemically bound nitrogen is complex due to the varying structure of the nitrogen bonding to the parent molecule. According to Glarborg *et al.* [19] most of the fuel bound nitrogen is converted to HCN and NH₃ to react with combustion radical to form NO.

HCN reacts through various reactions to lead to the formation of NO, while the N radical directly promotes the thermal NO formation. Thus the thermal and prompt pathways are highly coupled in the flame reaction zone. This description of prompt NO via HCN has been retained in many detailed mechanisms. However, it was argued that the reaction between N₂ and CH violates the quantum mechanics principle of spin conservation, and thus cannot represent the true chemical process of prompt NO initiation. It is now accepted that the correct intermediate species is rather NCN [20] via the reaction



which conserves electron spin, and is now implemented in recently built detailed mechanisms [21].

The prompt NO process peaks at stoichiometric or slightly rich conditions, because it is enhanced by high flame temperature and large quantities of available hydrocarbon radicals. It plays also a significant role in the rich region of diffusion flames. Its contribution is generally negligible in the post-flame region where hydrocarbon radicals are no longer available [22].

In the N₂O route, N₂O intermediate is formed via the reaction of N₂ and O that leads to NO formation via the following reactions:



It is one of the major contributor to NO_x formation under lean premixed, high pressure conditions, that are typically found in modern gas turbine combustors [23]. It is also promoted by O superequilibrium concentrations in the fame region.

In the NNH pathway [24], N₂ and H react to form NNH intermediate, which is then oxidised by the O atom to form NO:



This process is significant for low flame temperatures. Similarly to the thermal pathway, it is promoted by possible superequilibrium O concentration in the flame front.

NO conversion in NO₂ is promoted by high pressure conditions. NO is also rapidly oxidised into NO₂ at moderate temperatures. However, NO₂ concentrations are generally small in the hot exhaust gases of gas turbine chambers [22].

High temperature NO, N₂O and N₂O₂ formation mechanisms in high gradient turbulent flames still is a matter to discover. The most problematic is the process of NO_x formation in flames with

abnormal distribution of chemical bond excitement level, common for plasma stimulated flames and electrochemical combustion which are the main research subject of the present project. Thereby the analytic studies of combustion mechanisms and reaction general balance filtration methods, numerical investigations of various flame structure and properties and physical experiments are crucial for better understanding of NO_x formation process and so for the project success.

3.1 Decomposition of NO_x formation into slow and fast processes

Fenimore [16] observed that the NO profile in burnt gases had a non-zero intercept when extrapolated to the flame front for rich mixtures. As exemplified in [22] on a rich premixed methane-air flame computation, rapid NO formation occurs in the reaction of zone, which was given the name “prompt NO” by Fenimore. To analyse NO_x formation in combustors, it is interesting to separate the overall NO_x production into the fast flame processes that are related to the fuel consumption and the local combustion regime, and the slower post-flame processes that are related to residence time and essentially driven by thermal NO pathway. This can be done in several manners:

- By chemical pathways:
 - The total NO source term can be decomposed into the contributions of the different pathways. However prompt and thermal pathways are highly coupled via N radical, so that there is no clear separation.
 - The subtraction method consists in removing one pathway from the mechanism to obtain an evaluation of its impact on NO production.
- By separating flame and post-flame processes:

As suggested by Biagioli et al. [25], the decomposition can be based on the analysis of chemical time scales. Another possibility is to measure NO concentration at a given arbitrary distance from the flame front to separate flame and post-flame processes. However, this definition is not applicable to turbulent flows. Instead, a threshold value of the progress variable can be used to separate flame and post-flame zones.

3.2 Impact of operating conditions

The temperature has a strong impact on NO_x formation rate. Increased combustor inlet temperature results in a higher flame and post-flame temperature, and in turns increased NO_x emissions mostly because of thermal NO. Prompt NO formation is also promoted by increased temperature, but to a smaller extent.

The influence of pressure on NO_x formation is more complex, because it differs for the different pathways. It is case dependent, and influenced by the combustion regime, the fuel-air stratification and the relevant NO_x chemical pathways. As a result, available data from the literature sometimes exhibit contradictory trends [22]. To summarise, the impact of pressure on NO_x depends on various parameters including combustor design and fuel considered. However, the clear global trend is that low flame temperature and efficient mixing of fuel and air prior to combustion always tend to decrease NO_x production [22].

4. Emission Controlling Mechanisms

Amongst all factors influencing the pollutant emissions from gas turbine combustors, the most important is the flame temperature in the combustor primary zone. Figure 2 indicates the emissions as function of flame temperatures: below 1670K significant CO is produced whereas when it is above 1900K, excessive amount of NO_x is produced. Between 1670K and 1900K, there is a narrow band where CO and NO_x emissions are relatively low (i.e. 25ppmv for CO and 15ppmv for NO_x). As previously stated, modern engines have higher OPR and TET in order to increase the thermal efficiency and reduce engine specific fuel consumption SFC; therefore, the 'low emissions band' may shift rightward to the plot. The basic strategy for limiting the pollutant emissions is therefore controlling the temperature of the primary combustion zone within this narrow band over the entire power ranges of the engine.

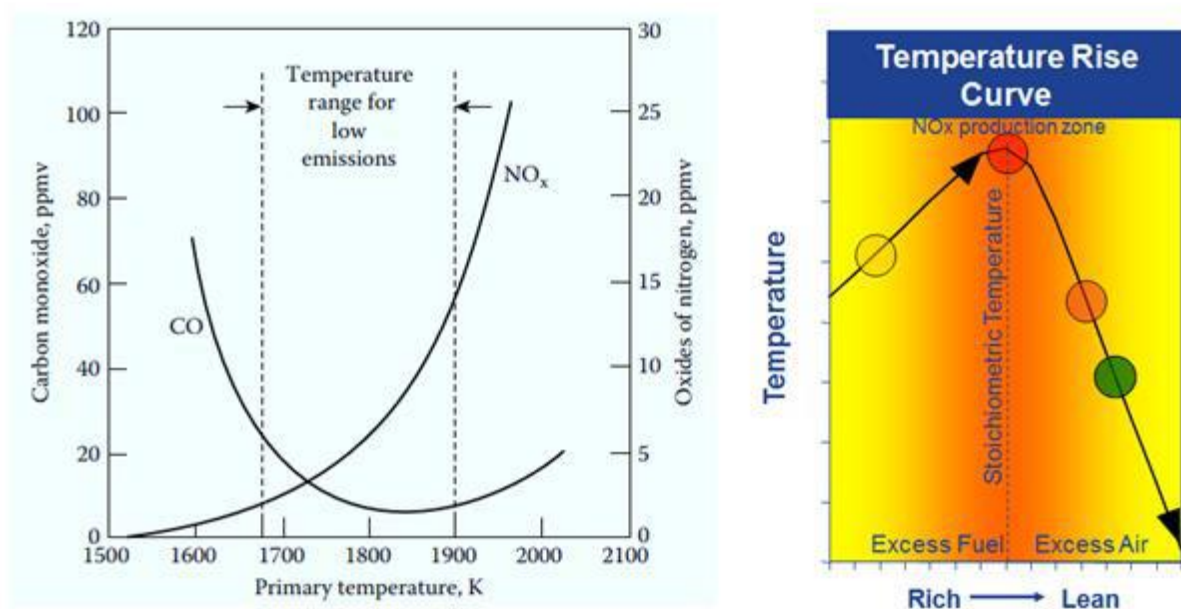


Figure 2. NO_x and CO emissions vs primary temperature and Temperature vs AFR [26]

The NO_x reduction is realized by moving the air fuel ratio AFR away from the stoichiometric value since maximum heat release hence highest flame temperature occurs close to that value. As shown in Figure 3 flame temperature and nitrogen oxide NO₂ formation against AFR. Peak NO₂ formation is at the stoichiometric ARF = 15:1, while peak flame temperature occurs at just below stoichiometric [27]. Therefore, combustion can be initiated with less air (rich burn) or excessive air (lean burn). In the latter case, a large fraction of the air flows through the combustion dome and is mixed with fuel so that a lower flame temperature can be achieved compared to rich burn. However, this poses a stability challenge at low power where the fuel-air ratio may approach the lean extinction limit.

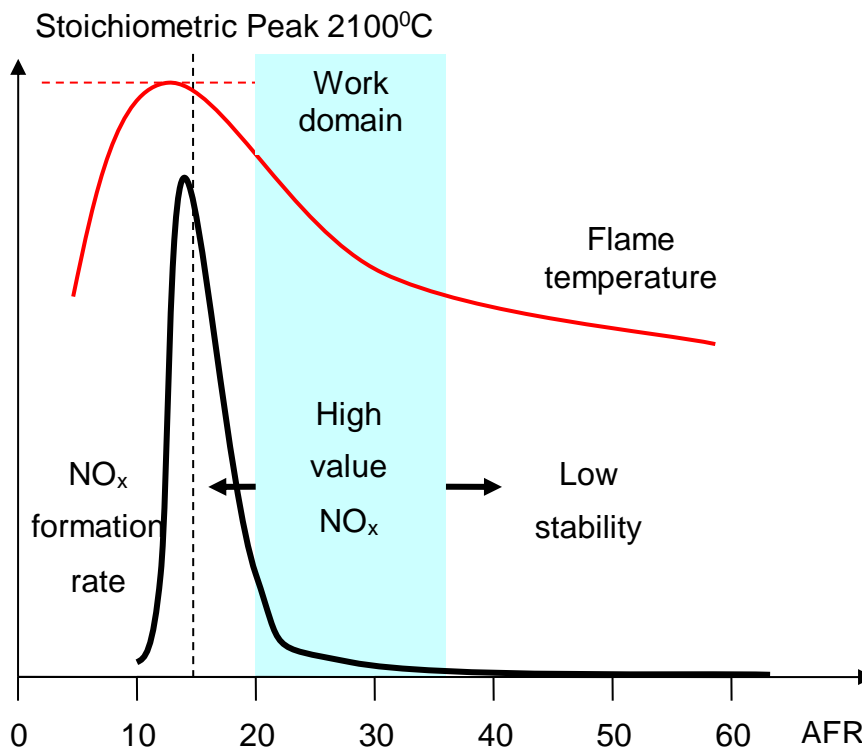


Figure 3. Flame temperature against air fuel ratio

Fuel staging is employed such that part of the fuel injectors is turned off at low power. In this manner, the local equivalence ratio is maintained close to the stoichiometric value at the operating fuel injection zones so as to maintain high combustion efficiency and stability. Figure 4 shows the NO_x distribution within the LTO cycle for rich and lean burn. Increased reduction in high power NO_x can be achieved by lean burn since the flame temperature gradient is higher for the lean side than the rich side. However, the low power emissions for both mechanisms show similar characteristics. This is primarily due to the increase in flame temperature via fuel staging, as previously described.

The bulk equivalence ratio either for rich burn or lean burn in the primary zone represents only a rough guide to emission reductions. The actual values are heavily dependent on the effective fuel-air mixing. Unsatisfactory mixing quality would produce a large variation in local fuel air distribution; the rich pocket yielding a local hot “spot” which would produce higher NO_x and smoke emissions. Therefore, good fuel atomization and fuel air mixing are vital for low emission reduction.

The flow residence time within the combustor zone is also a crucial factor that needs to be controlled. Sufficient residence time should be allowed for complete combustion to ensure that CO and UHC are reduced; on the other hand the residence time should not be long for excessive NO_x production.

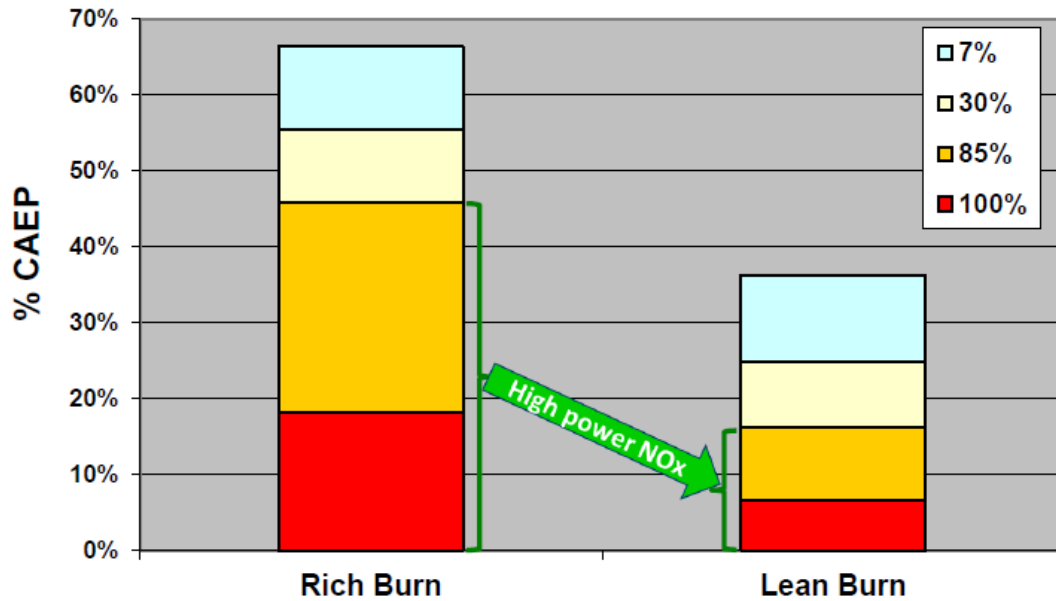


Figure 4. NOx distribution within LTO cycle for RQL vs Lean Burn [27]

In terms of combustor design, the need for higher OPR leads to higher inlet temperature and pressure as well as higher outlet temperature. As shown, these conditions strongly promote the formation of NOx. The main low-emission concepts used in modern aircraft combustors [28] and alternative combustion concepts [9] are summarized in Figure 5. Figure 6 illustrates more common low emissions combustion technologies for different practical application. Whereas combustion in conventional combustors is done at near-stoichiometric conditions, in most innovative concepts, the combustion process occurs away from stoichiometry. As shown in Figure 3, strong NOx reduction is achievable on both the lean and rich sides of stoichiometry. Conversely, CO concentrations are generally high in rich conditions or close to lean-blow of conditions, where the NOx emissions are the lowest. The residence time of the combustor must be sufficient so that CO can be fully burnt out into CO₂, but this will promote NOx in the post-flame region that is directly related to the residence time. Therefore a strong compromise must be found to obtain satisfactory emission levels at all regimes.

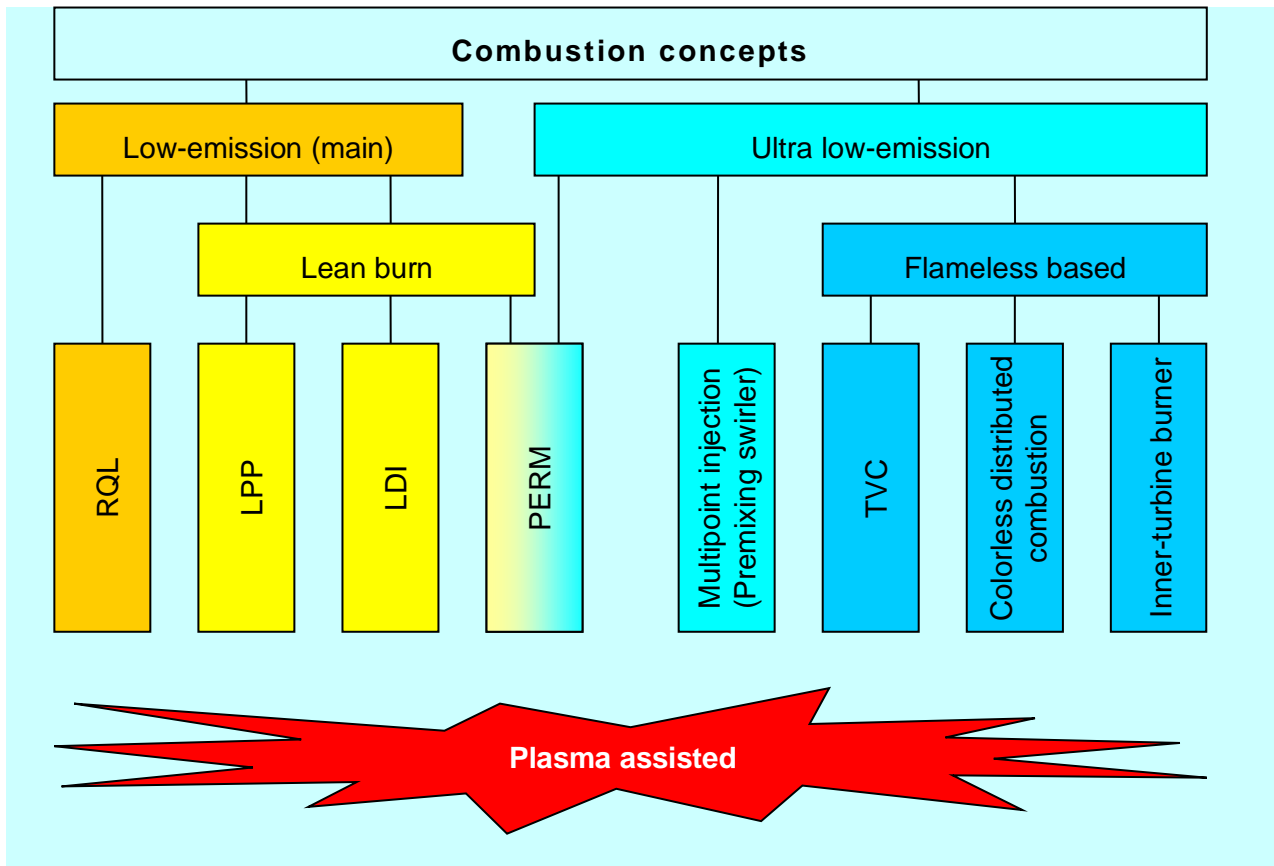


Figure 5. Combustion concepts

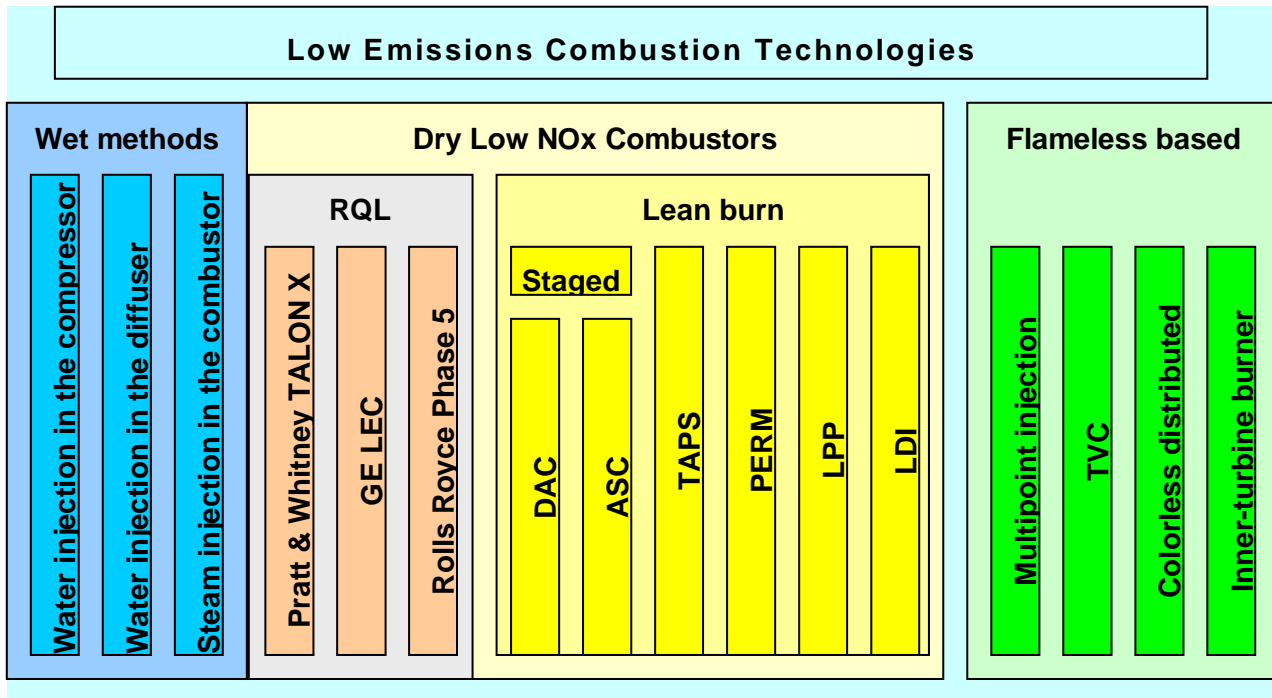


Figure 6. Low Emissions Combustion Technologies

Pratt & Whitney TALON family (Technology for Advanced LowNO_x): TALON I, TALON II, TALON X

GE's RQL technology named LEC (Low Emissions Combustors)

The high temperature operational zone, close to stoichiometric, is the most promising for mid-term and long-term gas turbine engine improvement programs because of significant increasing of engine efficiency and power in comparison with relatively low temperature combustion. But even most of RQL techniques shown on Figure 6 can't support stable low level of NO_x generation in primary combustion zone for flames with final temperatures (before turbine) above 1800K. The main problem of existing methods of NO_x reduction is the lack of direct management of the kinetic mechanisms of NO_x generation. Specific reaction stimulation, damping and restricting in multicomponent reacting flow are almost unattainable for conventional methods and need the focused electrochemical intervention in the chemical kinetic of combustion process.

5. Combustion Concepts

Now, the basic way of increase of fuel profitability and reduction in emissions in an atmosphere at gas turbine engines is transition to burning more and more poor fuel mixes with the big surplus of an oxidizer (AFR-air fuel rate). Value AFR is limited [29, 30] to area of unstable modes of a flame and vibrating burning (Figure 3). Ways of NO_x concentration reduction are reduced, basically, to reduction of temperature of burning of fuel, use lean burning, reduction of time of stay of products of combustion in the field of heats and "training" NO_x on the mechanism of fast cooling when speed of reaction of oxidation essentially decreases [31, 32].

These ways lead to the several technical decisions [33], allowing creating low emission combustion chambers (LECC): Rich-burn Quick-mix Lean burn (RQL); Lean Premixed Prevaporized/Lean Direct Injection (LPP/LDI). Traditional LECC have the big dimensions and rather difficult design providing multistage burning. Therefore various ways of LECC sizes reduction and increases in combustion speed are considered.

Various other successful NO_x reduction technologies such as "catalytic combustion" "flameless combustion", etc. have not proved suitable for aero engine use as a result of problems such as weight, size, stability, etc.

5.1 Classical Low Emission Combustors

Up to now, the Rich Quench Lean (RQL) technology represents the state of the art in aero-engines (Figure 7). In this concept, a rich burning primary region is generated to ensure the flame stability. Then, a rapid mixing takes place and finally a lean zone is created to burn out smoke. In this way, NO_x levels are controlled [34].

A reduction of the residence time inside the combustor, the use of more advanced injection strategies together with a more rapid air-jet mixing have been realized to achieve a drastic reduction of NO_x, without compromising the operability and the manufacturing technology. In this manner, the Pratt & Whitney TALON X (Technology for Advanced Low NO_x) combustor is able to cut down emission levels below 55% with respect to CAEP/6 standards [34].

Figure 8 shows, schematically, the relationship between NO_x formation, flame temperature and AFR together with acceptable and unacceptable operating bands.

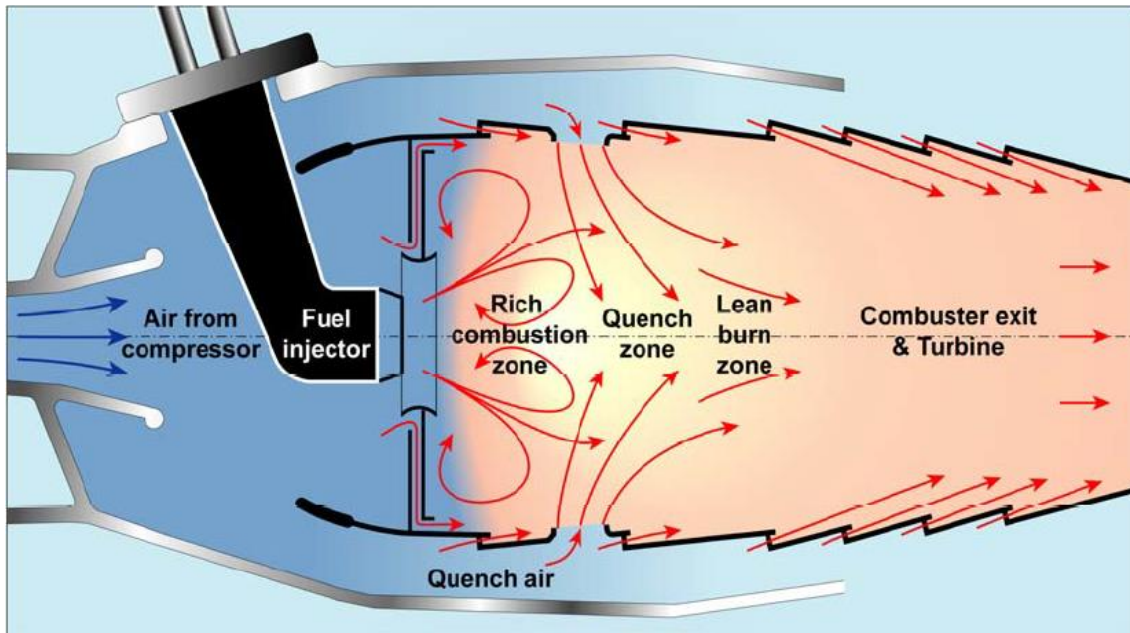


Figure 7. Schematic illustration of an RQL combustor [35]

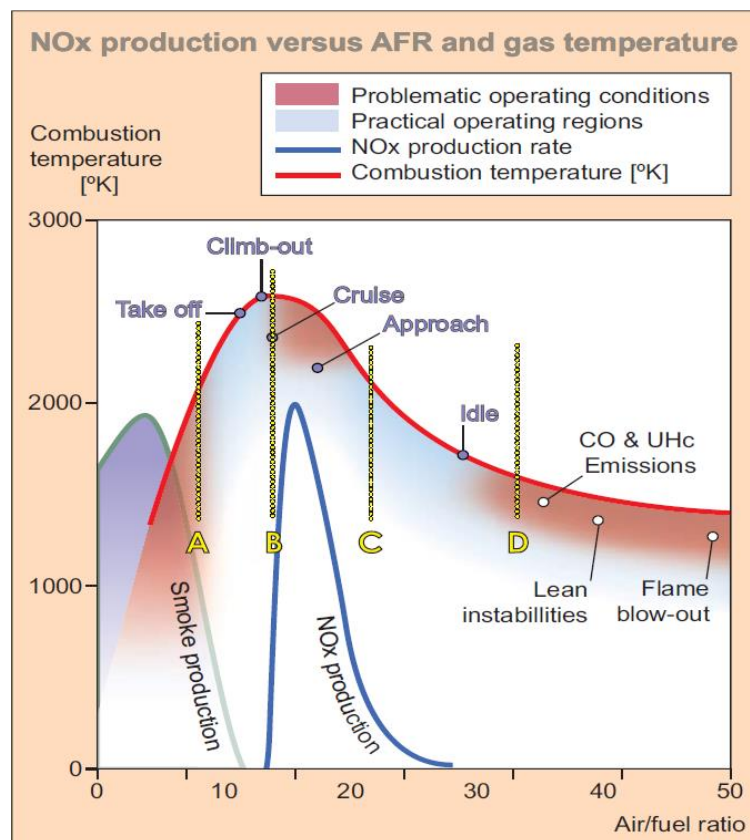


Figure 8. NOx production versus AFR and gas temperature [35]

In Cruise and Approach the primary zone may operate in or close to the NO_x production band. However because of the design features built in for LTO NO_x reduction, - good fuel preparation, short residence time - and because the combustion air temperature and pressure are low NO_x production at these conditions is also reduced. It should be expected that NO_x reduction technology designed for the take-off and climb conditions (where NO_x reduction is very challenging) would be at least as good at Cruise and Approach where, from a NO_x reduction perspective, conditions are much more benign [35].

After the primary zone, additional air is injected into the combustor to dilute the part-burned rich combustion products from the A-B zone (Figure 8) to somewhere in the C-D band to complete burning. Clearly, the mixing of the air with the primary zone products must be very fast and uniform so that NO_x production is minimized in passing through the B-C zone. Achieving this minimization is a considerable technical challenge because the NO_x production rate is very fast and the aerodynamic mixing process (which is not naturally very fast) has to be designed to be as efficient as possible and comparably fast [35].

Nevertheless, even if some potential improvements should be still expected from the RQL technology, the more and more stringent regulations pushed towards the development of alternative burning concepts, such as lean combustion. Here, the burner operates with an excess of air to significantly lower the flame temperature (e.g. up to 70% of total combustor air flow has to be premixed with the fuel) [34].

The development of lean combustion in the aero-engine framework is a long-time history started with fuel-staging. Dual Annular Combustors (DAC) employed this strategy and were designed with a pilot stage in the outer annulus and a main stage in the inner one. However, several issues related to the uniformity of the exit temperature profile during staging conditions, as well as CO and UHC emission levels, limited the application of this kind of technology [34].

Therefore, all the engine manufacturers focused the attention on Single Staged Combustors. One of the most relevant examples in this context is surely the GE-TAPS (Twin Annular Premixing Swirler), which currently represents the only lean burn combustion system employed on a certified aircraft engine (GENx family) [34] and which take advantage of premixed and lean-burn flames (i.e. Lean Pre-mixed Prevaporized (LPP) combustors).

Lean burn Premixed Prevaporized (LPP) technology is illustrated conceptually in Figure 9. This technology aims to emulate gas fuelled combustion in that the fuel spray is perfectly mixed with an excess of air and evaporated before entry to the combustor. In principle the technique could produce very low NO_x emissions than are currently being achieved in gas fired power plant applications where weight, complexity and passenger safety are not problems. However, in spite of considerable research activity in the 1980s and '90s the technology was best by numerous problems that appear to be insurmountable. Although NO_x reductions of better than 90% were demonstrated (at reduced combustor pressures) it was necessary to use non-premixed pilot combustion in order to ensure the safe operation of the combustor. This reduced the gains to ~60% only. Overall there were huge operability and flight safety issues [35].

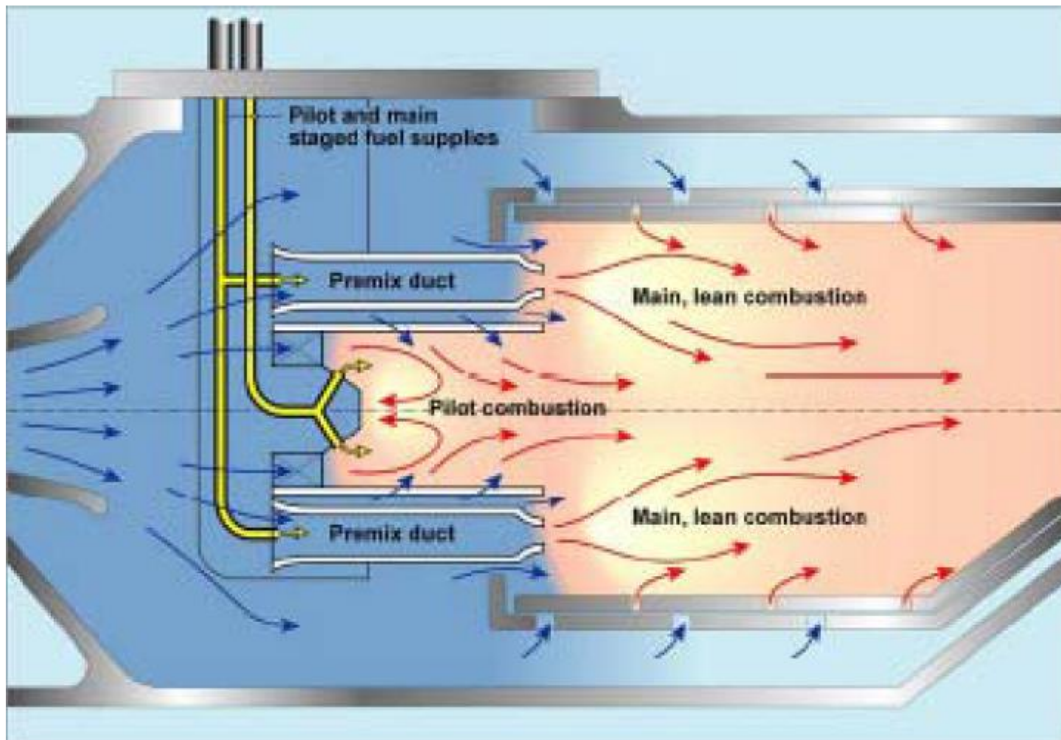


Figure 9. Schematic illustration of an LPP combustor [35]

In spite of the large NO_x reductions that have been achieved by RQL technology, rising pressure ratios and combustion air temperature are increasing the difficulty of making further large improvements, especially for the larger, high pressure ratio engines. After the LPP research programmes, possibilities of lean combustion, direct injection (i.e. fuel sprays) were investigated in combustors featuring novel aerodynamics that allow separate combustion zones to co-exist in the same combustion space (Figure 10). These separate zones allow staging for high power and low power duty to be achieved in order to optimize the combustion process [35].

This design approach requires that a very high percentage (in the region of 40 to 50%) of the combustor air passes through the airspray fuel injector. Therefore the fuel injector tends to become large and complex with some issues of cost and weight and problems of overheating. Excellent performance in terms of fuel spray placement and quality is required of the atomizer in order that the spray should be as much vaporized and mixed with the airflow as possible prior to the flame [35].

From the results of experiments with circumferential staging in the past it might be expected that this technology would require much work to meet low power efficiency/emissions targets. Also because of the staging it cannot, automatically, be assumed that Cruise/LTO NO_x relationship will be retained. Rather, Cruise NO_x will have to be optimized separately in its own right. On the other hand because of the additional flexibility offered by the more complex fuel injection system and the staging there must be prospects of achieving better Cruise NO_x than the current RQL technology [35]. And the main problem of high NO_x output from thermal mechanism for B-C zone of RQL combustors still is unresolvable without direct control of kinetic processes in high temperature zone.

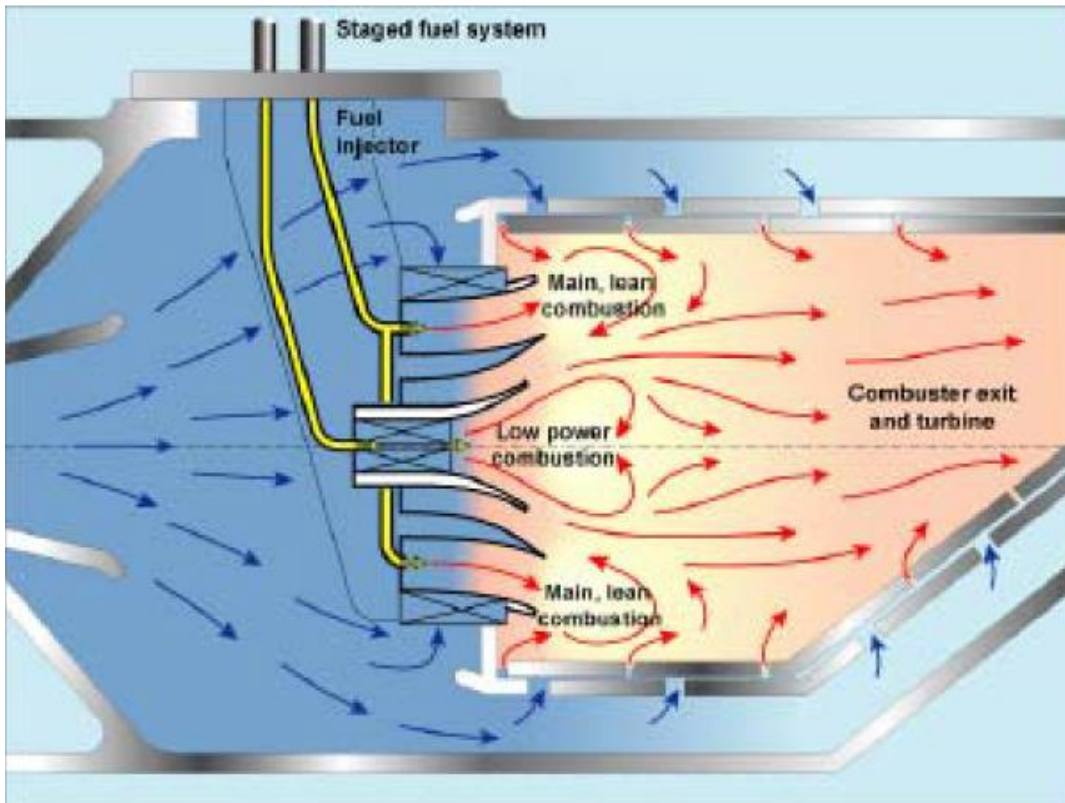


Figure 10. Schematic illustration of a DLI combustor [35]

5.2 Current Combustion Technologies

Recently, the TAPS II configuration has been developed leading to an additional reduction of emission levels [36]. The improvements achieved in terms of NO_x using this technology with respect to RQL are clearly shown in Figure 11.

Several other interesting injector configurations have been as well proposed in the lean combustion framework. As an alternative to the mentioned discrete jets atomization process, a common approach is to adopt liquid film breakup by means of prefilming airblast atomizers. An interesting solution, which employs this concept, is the so-called PERM (Partially Evaporating and Rapid Mixing) injection system developed by GE Avio Aero [38, 39]. The injector is a double swirler airblast atomizer designed in order to achieve partial evaporation inside the inner duct and rapid mixing within the combustor. In this manner, the location and the stability of the flame is optimized as sketched in Figure 12. A film of fuel is generated over the inner surface of the lip that separates the two swirled flows. As the film reaches the edge of the lip, through the action of the gas flow, primary atomization occurs: fine droplets and rapid mixing are promoted by the two co-rotating swirled flows generated by the double swirler configuration. Furthermore, in order to ensure a stable operation of the flame, especially at low power conditions, the airblast injector is coupled with a hollow cone pressure atomizer. It is located at the centre of the primary swirler and generates a pilot flame in a configuration similar to a piloted airblast atomizer.

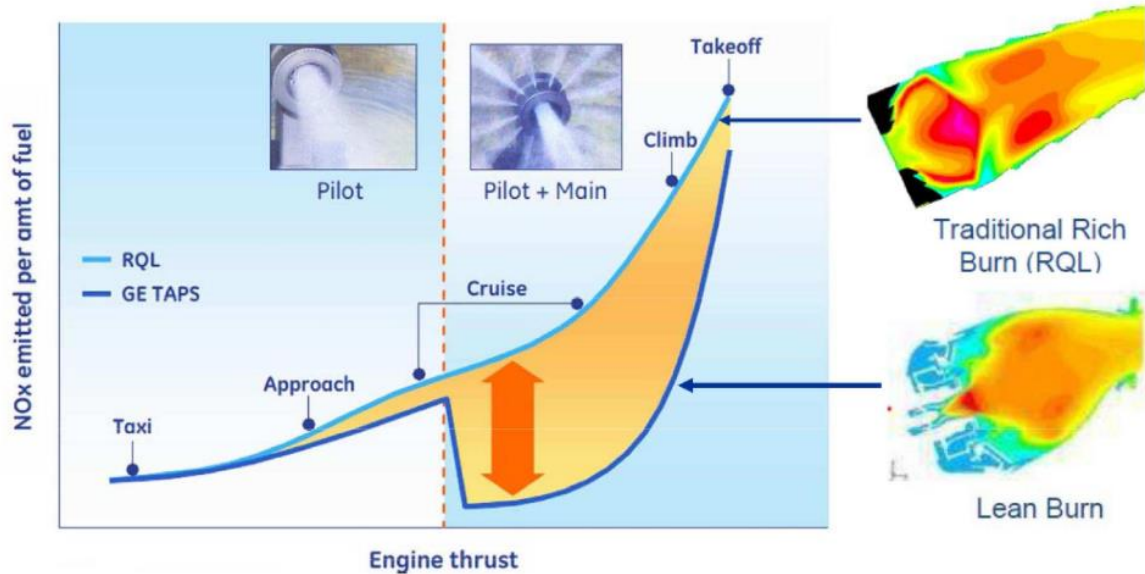


Figure 11. NOx emission levels between conventional RQL and TAPS combustor [37].

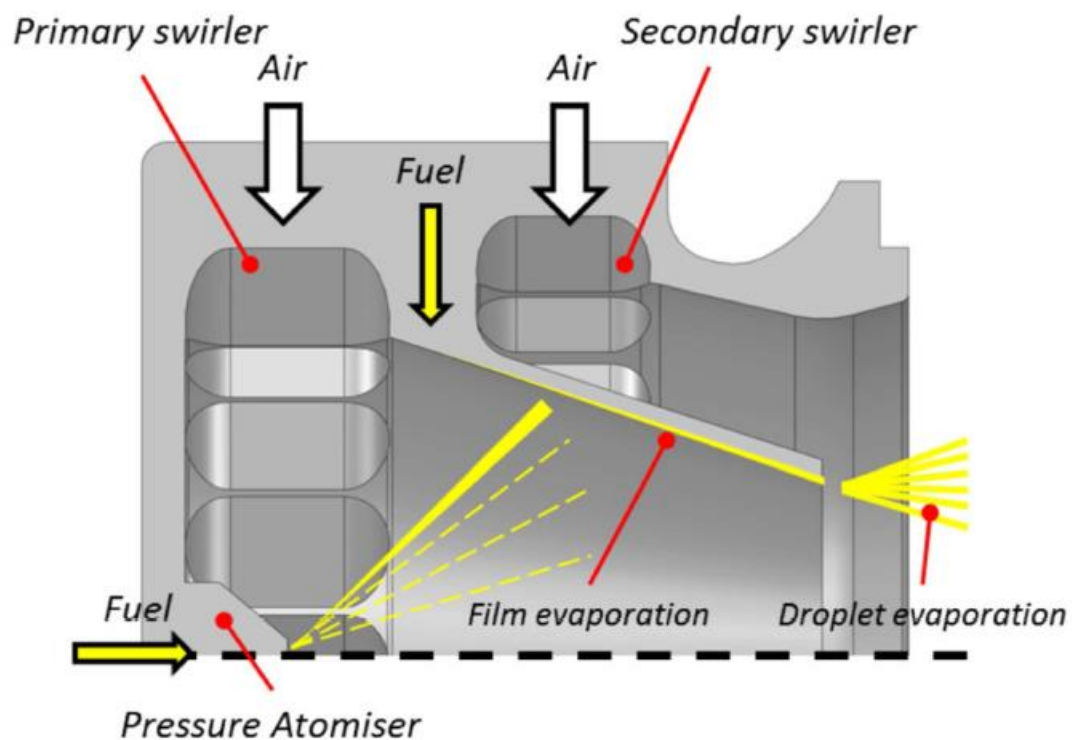


Figure 12. PERM functioning concept [40]

Nonetheless, beyond the specific adopted solution, from these observations it should be clear that one of the biggest challenges in lean devices is surely represented by the design of the injection system and how it affects the reacting flow-field [34].

6. Different Variants to Gas Discharge Plasmas

Plasmas are ionized gases. Hence, they consist of positive (and negative) ions and electrons, as well as neutral species. The ionization degree can vary from 100% (fully ionized gases) to very low values (e.g. 10^{-4} – 10^{-6} ; partially ionized gases).

In general, a subdivision can be made between plasmas which are in thermal equilibrium and those which are not in thermal equilibrium. Thermal equilibrium implies that the temperature of all species (electrons, ions, neutral species) is the same. High temperatures are required to form these equilibrium plasmas, typically ranging from 4000 K (for easy-to-ionize elements, such as cesium) to 20 000 K (for hard-to-ionize elements, like helium) [41]. Often, the term “local thermal equilibrium” (LTE) is used, which implies that the temperatures of all plasma species are the same in localized areas in the plasma. The term “non-LTE” means that the temperatures of the different plasma species are not the same; more precisely, that the electrons are characterized by much higher temperatures than the heavy particles (ions, atoms, molecules) [42].

The gas discharge plasmas can also be classified into LTE and non-LTE plasmas. This subdivision is typically related to the pressure in the plasma. Indeed, a high gas pressure implies many collisions in the plasma (i.e. a short collision mean free path, compared to the discharge length), leading to an efficient energy exchange between the plasma species, and hence, equal temperatures. A low gas pressure, on the other hand, results in only a few collisions in the plasma (i.e. a long collision mean free path compared to the discharge length), and consequently, different temperatures of the plasma species due to inefficient energy transfer. Of course, there are some exceptions to this rule, e.g. dielectric barrier discharges or atmospheric pressure glow discharges. The reason is that, as suggested above, not only does the pressure play a role, but also the discharge length or the distance between the electrodes (which is very small in the above-mentioned exceptions). In general, it is the product of both (typically denoted as pD) which classifies the plasmas into LTE and non-LTE [42].

Exists a large variety of gas discharge plasmas, employed in a large range of applications. LTE discharges, which are characterized by rather high temperatures, are typically used for applications where heat is required, such as for cutting, spraying, welding, etc. Non-LTE plasmas, on the other hand, are typically used for applications where heat is not desirable[42].

For a basic direct current (DC) glow discharge, three main regions can be distinguished from each other, dark discharge, glow discharge and arc discharge. The Figure 13 is a typical V/I plot of a glow discharge [43]. The main characteristics of the discharge such as the breakdown voltage, the voltage current characteristic and the structure of the discharge depend on the geometry of the electrodes, the gas used, the pressure and the electrode material.

The glow discharge can be called the “basic version”. In this DC glow discharge, a continuous potential difference is applied between cathode and anode, giving rise to a constant current. However, this set-up gives problems when one of the electrodes is non-conducting, as is the case in some applications. Indeed, due to the constant current, the electrodes will be charged up, leading to burn-out of the glow discharge [42].

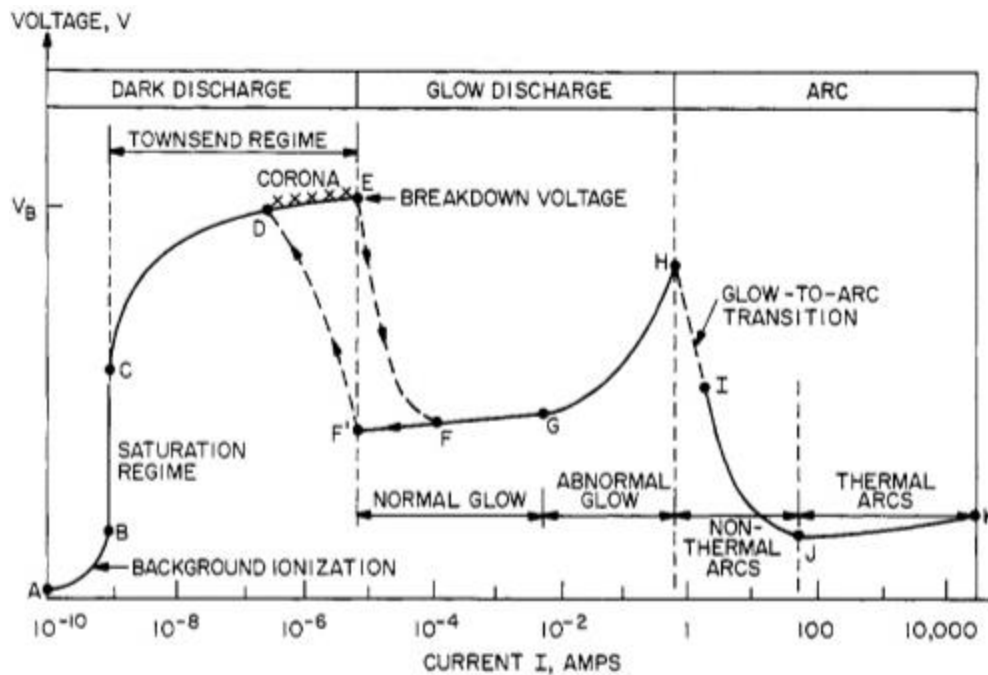


Figure 13. Electric discharge regimes [43]

This problem is overcome by applying an alternating voltage between the two electrodes, as in the capacitively coupled radio-frequency (cc rf) glow discharge. Indeed, the charge accumulated during one half of the cycle, will be neutralized by the opposite charge accumulated during the next half-cycle [42].

Beside a time-dependent rf voltage, an alternating voltage can also be applied in a lower frequency range, giving rise to an alternating current (ac) glow discharge. This can be considered as a consecution of short discharges, in which the two electrodes alternately play the role of cathode and anode. An important type of ac glow discharge, operating at atmospheric pressure, is the dielectric barrier discharge (DBD), where the electrodes are typically covered by a dielectric barrier [42].

A variation to the ac discharge is the pulsed glow discharge, which also consists of short glow discharges (with lengths typically in the milli- or microsecond range), followed by an afterglow, which is generally characterized by a longer time-period. The advantage is that high peak electrical powers can be reached for a low average power, resulting in high peak efficiencies for various applications [42].

In addition to applying an electric field (or potential difference), a magnetic field can also be applied to a glow discharge. The most well-known discharge type with crossed magnetic and electric fields is the magnetron discharge. The electrons circulate in helices around the magnetic field lines and give rise to more ionization. Hence, magnetron discharges are typically operated at lower pressures and higher currents than conventional glow discharges [42].

There exist also other discharge types characterized by low pressure and high plasma densities, which have their main application in the semiconductor industry and for materials technology. The major difference with the conventional glow discharge is that the electrical

power is not applied through a potential difference between two electrodes, but through a dielectric window. The two most important “high-density sources”, are the inductively coupled discharge, where the rf power is inductively coupled to the plasma, and the electron cyclotron resonance reactor, where microwave power and a magnetic field are applied [42].

Microwave power can also be applied in so-called microwave induced plasmas. Various discharge types can be classified under this name, among others the resonance cavity plasmas, free expanding plasma torches and surface wave discharges [42].

The various kinds of gas discharge plasmas is presented in Figure 14.

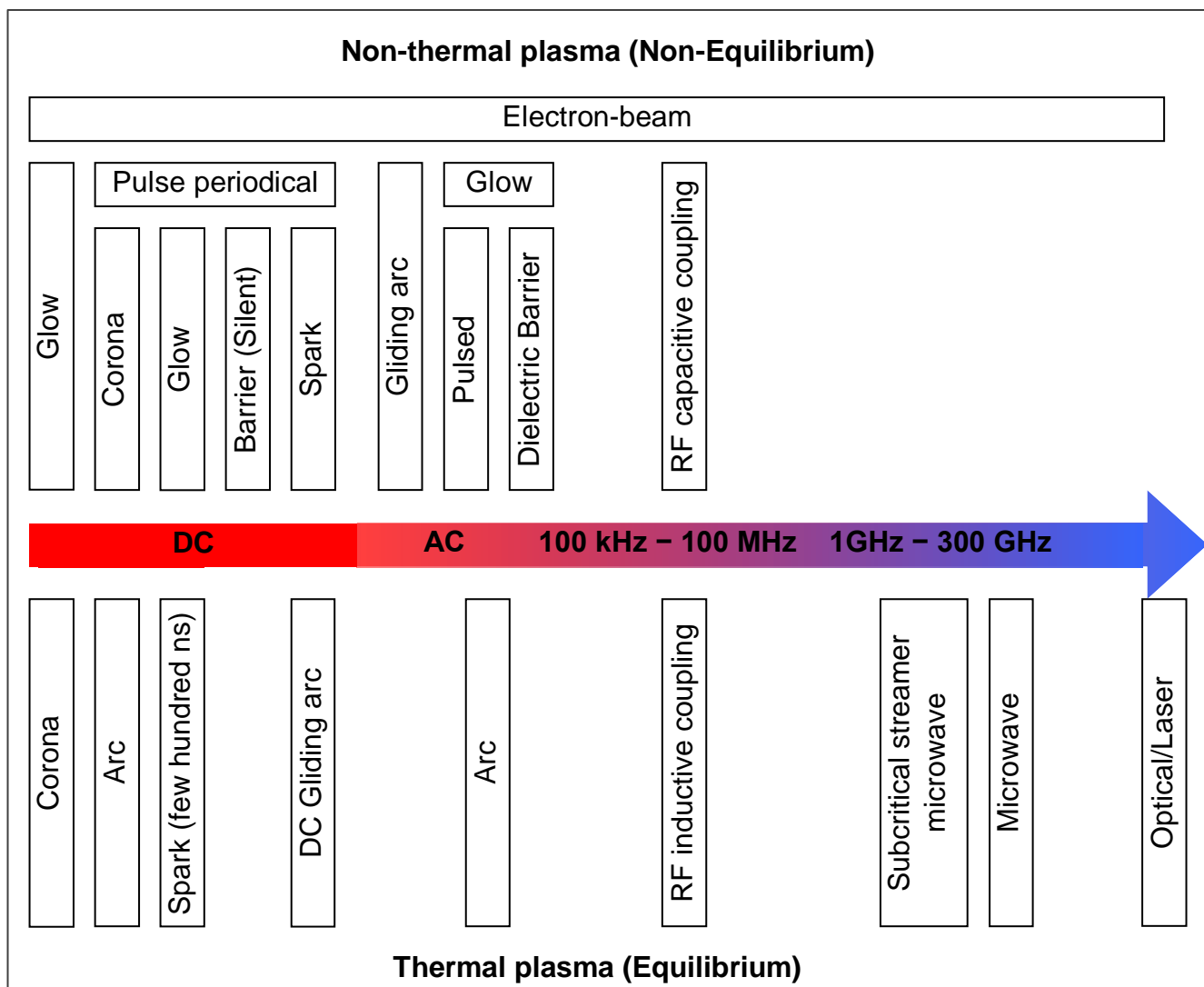


Figure 14. Discharge types

Corona, glow and spark discharges have been investigated for various conditions [44]–[47] and have been applied to combustion [48], [80], nanomaterial synthesis [49], [50] and flow control [51]–[53]. Typical parameters of these discharges are presented in Table 2 [54]. The corona and the glow discharges are non-thermal plasmas in non-equilibrium and the electrical energy deposited in the gas is spent mainly on electronic and vibrational excitation of N₂. A description

of the glow regime can be found in [47]. In the spark regime a quick transfer of the electrical energy into the thermal energy occurs, but is still out of equilibrium plasma [44]. The transition between these non-equilibrium regimes of nanosecond discharges were investigated by Pai et al. [46].

One can see from Table 2 that the transition to the arc increases the electron number density and the gas temperature. It has been demonstrated recently [55] that this transition occurs for nanosecond plasmas in less than 5 ns.

Physical and chemical properties of the flow can dramatically affect the discharge and plasma parameters for different discharge types. Practical application of plasma and microwaves for gas turbine engine needs a lot of preliminary research in the related science fields.

Table 2 – Typical parameters of corona, glow [47], spark [44], [45] and arc nanosecond discharges at ambient conditions ($p = 1$ bar, $T = 300$ K). The deposited electrical energy is valid if the extension of the plasma is in the mm scale

Parameter	Corona	Glow	Spark	Arc
State	Non-equilibrium	Non-equilibrium	Non-equilibrium	Equilibrium
Total Deposited Electrical Energy	~1-10 μ J	~10 μ J	~1 mJ	~1 mJ
Dominant Emission	Molecular (N_2)	Molecular (N_2)	Molecular (N_2) and Atomic (O)	Atomic (N, O) and Ionic (N^+ , O^+)
Electron Number Density	$<10^{13}$ cm^{-3}	10^{13} cm^{-3}	10^{15} cm^{-3}	10^{19} cm^{-3}
Gas Temperature Increase	~0 K	~200 K	~1000-2000 K	~40,000 K

6.1 Nanosecond Repetitively Pulsed Discharges

This technique is based on the use of Nanosecond Repetitively Pulsed (NRP) discharges. The principle is to apply short (about 10 ns), high voltage (~10 kV) pulses to ionize the gas efficiently, and at repetition rates high enough (10-100 kHz) so that the electron density does not decay too much between two consecutive pulses.

Figure 15 summarizes the power reductions afforded by NRP discharges relative to DC discharges [56]. The experimental point represents the measured power requirement of the NRP experiment presented in the foregoing. Power budget reductions by an additional factor of about 5 are possible with repetitive pulses of 1 nanosecond duration. Such repetitive pulsers are already commercially available. Therefore, power budget reductions by a factor of 250-1000 relative to the DC case at 10^{12} electrons/ cm^3 can be readily obtained with a repetitively pulsed technique.

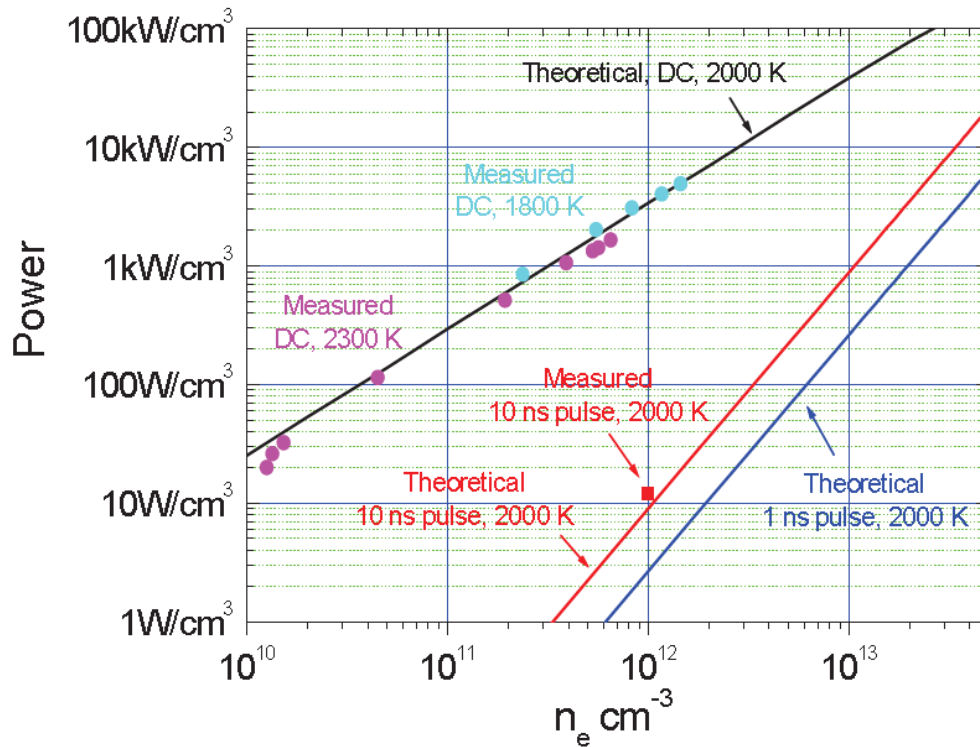


Figure 15. Power requirements vs. electron number density for DC and pulsed discharges in air at 1 atm, 2000 K [56].

6.2 Comparison of various discharges

In his thesis Pai [57] compared the power requirements of the various types of discharges used to produce air plasmas, as well as the temperature range of operation of these discharges. The results are shown in Figure 16 and Figure 17.

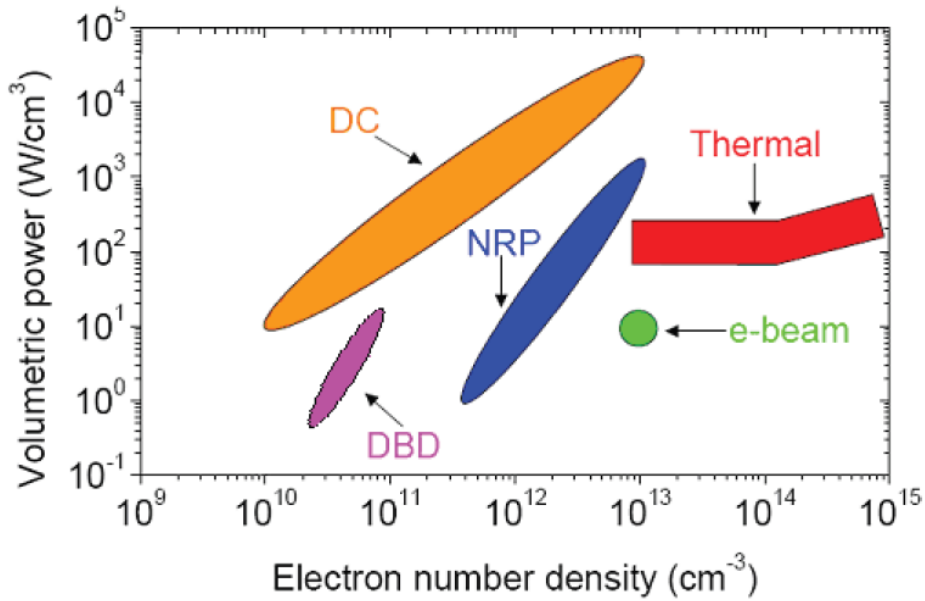


Figure 16. Power budgets of plasmas produced by different plasma sources as a function of electron number density [57].

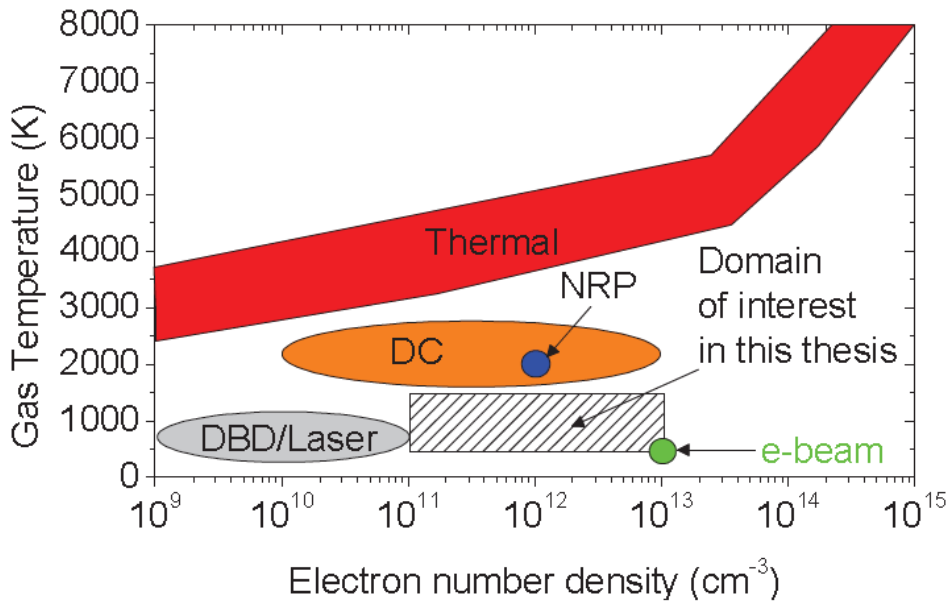


Figure 17. Gas temperatures of plasmas generated by various plasma discharges as a function of electron number density [57].

Pai demonstrated that three NRP regimes can be obtained at atmospheric pressure. In order of increasing voltage, these regimes can be defined as the NRP Corona, NRP Glow, and NRP Spark. Their main characteristics are summarized in Table 3.

Table 3 – Classification and measured thermal and electrical characteristics of observed NRP discharge regimes ($T_g = 1000$ K, $PRF = 30$ kHz, $d = 5$ mm, $v = 2$ m/s). Taken from [47, 58]

Regime name	Appearance	Energy deposited per pulse	Gas Heating ($+\Delta T_g$)	Conduction current
Corona	Corona	$< 1 \mu\text{J}$	< 200 K	< 2 A
Glow	Diffuse	$1-10 \mu\text{J}$	< 200 K	< 2 A
Spark	Filamentary	$>100 \mu\text{J}$	>1000	

The NRP glow regime is found to allow a higher energy deposition than the corona regime, without heating the gas. The spark regime provides even higher energy deposition, but it may significantly heat the gas. These characteristics make the glow an interesting regime for applications where gas heating is not tolerable. In the plasma-assisted combustion application only the spark regime is found to have a significant effect [57].

7. Gas Discharge Plasma Technologies

The electric-field/flame interaction as known from the early 20th century (Figure 18). To satisfy the requirements of future environmental protection legislation, many new de-NO technologies have been developed in the past decades, among which the discharge process turns out to be one of the promising routes for direct decomposition of NO. Many interesting results have been observed in chemical reactions using discharge technology.

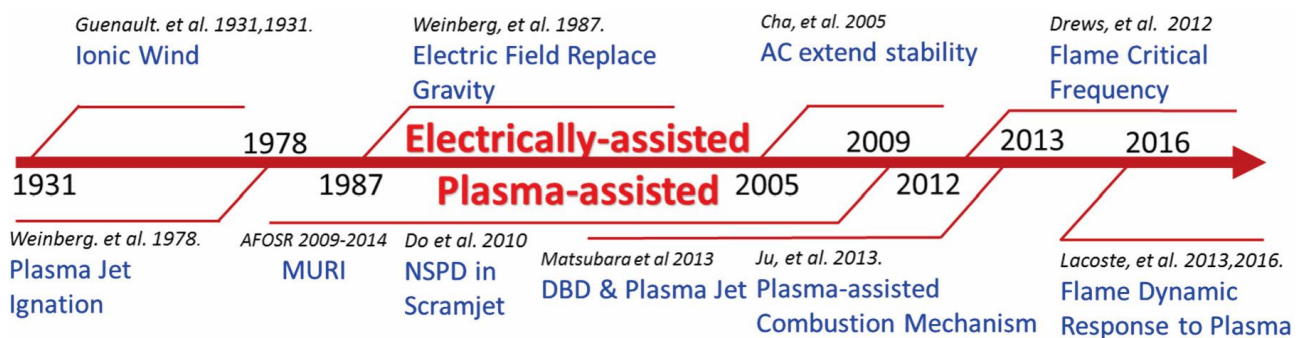


Figure 18. Time line marking the relationship between combustion and the electric/plasma field [59]

Discharges are capable of activating gaseous species, and in certain cases, nonthermodynamic equilibrium can be attained during the selective activation of stable small molecules [60]. Various types of energy and radiation, such as microwave [61, 62, 63] radio frequency [64] and electricity [65, 66, 67, 68, 69, 70, 71, 72] can be used to generate discharge.

Mok and Ham, Kim et al., and Broer and Hammer [68, 71, 72] investigated NO conversion using a pulse discharge in the first two cases and nonthermal plasma in the latter. They found that NO was mainly converted to NO₂. However, only a limited number of studies in microwave and radio-frequency discharge are available because of problems associated with the use of low pressure, the erosion of electrodes, and so on [66]. Authors [73] have developed a continuous microwave discharge (CMD) process at atmospheric pressure that does not require the use of any electrodes [62, 63]. Applying this CMD process in environmental chemistry, they are aiming at the direct decomposition of NO, which is a novel and environmentally friendly process free from the drawbacks of conventional catalytic processes, such as the use of high temperatures and the deactivation of catalysts.

CMD is a nonequilibrium discharge process characterized by a low gas temperature but a high electron temperature, i.e., it produces high-energy electrons in the gas while leaving the temperature of the bulk gas very low [62, 63]. Compared to other discharge technologies, such as AC (alternating current) and DC (direct current) discharge, CMD is energy-efficient because a large amount of energy goes into the production of energetic electrons rather than into gas heating [61]. In work [73], authors explored NO decomposition with three kinds of feed gas, i.e., NO + O₂, NO + O₂ + He (denoted as “dry gas”), and NO + O₂ + H₂O + He (denoted as “wet gas”). The effects of selective excitation of the reactants, input power, reactant concentrations, and flow rate on product distributions were also investigated. The reaction rate of NO

conversion, the energy efficiencies of these reactions, and possible mechanisms are discussed as well [73]

Last years, researches in a direction of stabilization of burning of a poor mix are actively conducted by means of cold non-equilibrium plasma [74, 75]. Application of super high-frequency discharges (MICROWAVE) allows to expand usually very narrow range of parameters of steady lean burning [76, 77]. For this purpose use a series of the following one after another in a quasi-continuous mode of pulses [78] or continuously burning coronary discharges [79] Review of works in the field of plasma assisted combustion is resulted in [10, 80].

Excitation of atoms of oxygen in cold non-equilibrium plasma increases speed of flame distribution that allows not only to stabilize a flame and to expand limits of burning [81], but also to increase speed and completeness of combustion of fuel, that also positively influences formation of oxides of nitrogen NO_x [82]. The MICROWAVE discharges are rather steady and do not die away in high-speed streams [83] that does perspective their application in systems of stabilization of burning [84], combustion chambers of aviation engines.

The main disadvantage of methods of the organization of burning at the presence of plasma is high expenses of energy on electromagnetic breakdown and environment ionization. Used for ignition micro and nanosecond pulses of microwave and laser radiation consume huge capacities because of low efficiency of sources and high threshold values of gas environment breakdown [85]. Direct use of laser breakdown differs also low efficiency of the process of evaporation of a drop of fuel and plasma formation [86]. Therefore try to unit subcritical discharges with laser pulses [87]. In work [88] the method of initiation streamer discharges in conditions of a resonance is used at subcritical level of a field. This method on one - two order is more economic, than the methods which are listed above. Authors [88] approve that the suggested way of burning of especially poor mixes due to the profitability, the big speed and completeness of combustion can apply for use at creation of a new class compact a low emission and high economic combustion chambers of. However, for this purpose problems of a radiation MICROWAVE introduction in the combustion chamber should be solved.

The streamer discharge looks as a chaotic structure of plasma channels (filaments). Their characteristic diameter is about a fraction of millimetre, and a characteristic distance between the channels is a fraction of wavelength. A streamer filament divides itself into several branches that connect to each other, forming a net of thin plasma filaments, whose characteristic length is related to electrodynamic resonance effects. A local initiation of such a discharge is provided by special facilities. The streamer discharge spreads in a considerable volume, and power is much smaller than the critical one (subcritical microwave discharge). The diameter of the plasma channels is a key parameter that determines ignition. If it is too large, ignition becomes more difficult or even impossible, whatever the energy released. It is more efficient for ignition to increase the power by varying the thickness of the plasma channels than by releasing more energy [89].

The more rapid combustion with streamer discharges could be exploited in practical combustion devices. Increase in flame surface, caused by the large ignition area, is one of the potential methods in improving combustion efficiency by reducing the burning time in the propulsion systems. These results suggest improved ignition devices for internal combustion engines, premixed gas turbines and pulse detonation engines [89]. Chemical kinetic of plasma-stimulated

combustion in MICROWAVE discharge can be modified in favor of NO_x generation reduction, but it's difficult to prejudice the effect of stimulation of multicomponent medium without additional fundamental studies of cold non-equilibrium plasma in hydrocarbon flames.

8. New Combustion Concepts Under Extreme and Non-Equilibrium Conditions

To enable the above new engine technologies and to achieve low emissions, fuel lean and high speed combustion, various new combustion concepts such as partially premixed and stratified combustion [90] (Dec, 2009), plasma assisted combustion [10], [91], [11] (Starikovskiy 2012, Uddi et al. 2009, Sun et al. 2010), cool flames [92] (Won et al. 2014), microscale combustion [93], [94] (Ju et al. 2011, Fernandez-Pello 2002), and pulsed and spinning detonation engines [95], [96] (Schott 1965, Bykovskii et al. 2006), and nanopropellants [97], [98] (Ohkura et al. 2011, Sabourin 2009) have been developed. These new combustion concepts involve in multi-physical interactions of non-equilibrium chemical and transport processes, and lead to many new combustion regimes. For example, for high pressure stratified combustion, the flame regimes arising from ignition to flame and ignition to detonation transitions at low temperature conditions are very complicated and have not been well examined (Ju et al. 2011, Sun et al. 2014, Dai et al. 2014) [99]. Understanding of cool flame chemistry is extremely important to control engine knocking and to avoid stochastic engine failure. Although cool flames have been observed for many decades (Barnard 1969, Griffiths 1992, Oshibe et al. 2010, Nayagam et al. 2012) [100], establishment of a stable cool flame in laboratories has not succeeded despite numerous attempts. As such, the dynamics, chemical kinetics, and kinetics-transport coupling as well as the cool flame regime diagram remain poorly understood. For example, to date we still do not know how fast a cool flame can propagate and how lean it can burn. On the other hand, for plasma assisted combustion, the highly non-equilibrium energy transfer between electrons, electronically and vibrationally excited molecules, and neutral molecules are not well known (Sun et al 2011, Stancu et al. 2009, Uddi et al. 2009) [91], [101], [102]. Moreover, the low temperature fuel oxidation chemistry of large hydrocarbon transportation fuels activated by plasma discharge is also poorly understood (Sun et al. 2014) [103]. For microscale energy conversion, the strong thermal and kinetic coupling via flame-wall interaction significantly modified the flame regimes (Ronney 2003, Ju et al. 2003, Maruta et al. 2005, Ju et al. 2005, Xu et al. 2009) [104]. In nano-propellant design, functional groups including hydrogen, oxygen, and nitrogen bonds are added to nanoparticles and graphene sheets (Ohkura et al. 2011, Sabourin 2009) [97], [98] to enhance ignition and combustion properties via non-equilibrium photo-chemical and thermal chemical reaction processes. For spinning detonation, the wall curvature and fuel/air mixing have significant impacts on the detonation initiation and propagation modes (Sugiyama et al. 2013) [105]. Therefore, the third challenge in combustion is the lack of fundamental understanding of combustion phenomena and flame regimes under extreme and non-equilibrium conditions [13]. For successful application of electrochemical high temperature combustion and non-equilibrium cold plasma assistance for near stoichiometric flames, the modelling of vibrationally and transitionally excited radicals, electron and ion kinetic are absolutely necessary.

8.1 New FLame Regimes at Low Temperature and Non-Equilibrium Conditions

To achieve higher engine efficiency and lower emissions, new combustion technologies such as ultra-lean, thermal and fuel stratifications, pressure gain combustion, micro combustion, flameless combustion, and plasma assisted combustion have attracted great attention. These new combustion techniques often operate at near-limit conditions and the combustion processes are more kinetically dominated by the chemistry with strong coupling to flame dynamics. In this review, we limit our focus on the impact of how combustion chemistry affects flame regimes at highly non-equilibrium conditions with thermal and concentration stratifications, plasma activation, and low temperature oxidation.

9. Nonequilibrium Plasma-Assisted Combustion

Nonequilibrium plasma assisted combustion has drawn significant attention for its great potential to enhance combustion performance in pulsed detonation engines, gas turbines, scramjets, internal combustion engines, and other lean burn combustion systems. The physical and chemical kinetic processes in plasma assisted combustion involve strong coupling between combustion kinetics and the active radicals, excited species, ions/electrons, and other intermediate species produced specifically by the plasma. In recent years, extensive efforts have been made to develop new combustion techniques using non-equilibrium plasma, as well as new experimental platforms, advanced diagnostic methods, kinetic models, and quantitative experimental databases to understand the underlying interaction between the plasma and combustion mechanisms.

Although many previous studies have demonstrated the effectiveness of plasma to enhance combustion properties phenomenologically, the detailed enhancement mechanisms remain largely unknown. Previous reviews which focused more on the plasma processes and kinetics can be found in [79, 10, 11].

9.1 Flame regimes of plasma assisted combustion

Non-equilibrium plasma is another method to enhance ultra-lean combustion and flame stabilization. Plasma assisted combustion (PAC) has a great potential to enhance combustion performance in pulsed detonation engines, gas turbine engines, scramjets, internal combustion engines, and other lean burn combustion systems. Over the last decade, the applications of plasma to improve the performance of combustion have drawn considerable attention for its great potential to enhance combustion in internal combustion engines, gas turbines, pulsed detonation engines, scramjet engines, and lean burn combustion systems (Pilla et al. 2006, Ombrello et al. 2010a, 2010b, Sun et al. 2012, 2013, Starikovskaia 2006, Starikovskiy 2013, Singleto et al. 2011, Matsubara et al. 2011, Leonov et al. 2010, Little et al. 2010, Lacoste et al. 2013) [106], [107, 108], [11], [79, 10], [109], [110], [111, 112, 113].

Towards the development of advanced gas turbines, plasma is also used as a new technology to increase energy efficiency, reduce emissions, and improve stability of flames in the combustion chamber. Serbin et al. (2011) [114] showed that a gas turbine combustor with piloted flame stabilization by non-equilibrium plasma can provide better performance, wider turndown ratios, and lower emissions of carbon and nitrogen oxides.

However, the physical and chemical kinetic processes in plasma assisted combustion involve strong couplings (Figure 19) between combustion kinetics and the active radicals, excited species, ions/electrons, and other intermediate species produced specifically by the plasma. In recent years, extensive efforts have been made to develop new combustion techniques using non-equilibrium plasma, as well as new experimental platforms, advanced diagnostic methods, kinetic models, and quantitative experimental databases to understand the underlying interaction between the plasma and combustion mechanisms.

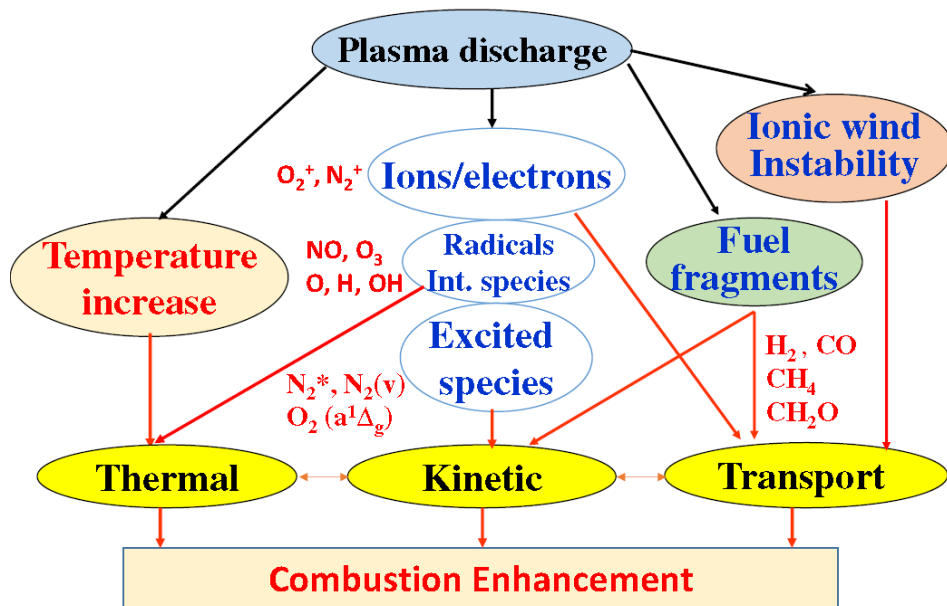


Figure 19. Possible enhancement pathways of plasma on combustion systems (Sun and Ju 2013) [11]

In order to fundamentally understand the physics of plasma enhanced ignition and flame stability, a non-equilibrium in situ plasma discharge integrated with a counter flow flame was developed (Sun et al. 2011, 2013) [11, 101].

In order to understand the elementary kinetic process of plasma-assisted combustion, advanced species diagnostics have been carried to quantify the effect of plasma generated radicals and intermediate species such as O, N_2^* , O_3 , $O_2\left({}^1\Delta_g\right)$, and NOx on ignition and flame propagation. Uddi et al. (2009) and Sun et al. (2010), [91], [115] measured the atomic O concentration in nanosecond pulsed discharges using the Two Photon Laser Induced Fluorescence (TALIF) technique, respectively, in a flow reactor and in a counter flow diffusion flame. It was found that the discharge can generate significant amounts of atomic O and the consumption of atomic O by fuel was very fast. To further understand the formation pathways of atomic oxygen production by excited N_2^* (known as $N_2(A)$, $N_2(B)$ and $N_2(C)$), the absolute number density of $N_2(A)$ was measured by Cavity Ring Down Spectroscopy (CRDS) and the densities of $N_2(B)$ and $N_2(C)$ were measured by Optical Emission Spectroscopy (OES) in a nanosecond pulsed discharge at atmospheric pressure in air (Stancu et al. 2009) [102]. The results show that in air plasaoxygen collisions with $N_2(B)$ and $N_2(C)$ are major reaction pathways to product atomic oxygen in addition to direct electron impact oxygen dissociation.

By using Integrated Cavity Output Spectroscopy (ICOS) (Williams et al. 2004, Ombrello et al. 2010b) [116, 108] measured the absolute concentrations of excited oxygen ($O_2\left({}^1\Delta_g\right)$) in a microwave generated plasma by using the (1,0) band of the $\sum_g^+ - {}^1\Delta_g$ Noxon system. Several thousand ppm level of $O_2\left({}^1\Delta_g\right)$ was reported and its effect on flame propagation was

then investigated. The effect of O_3 and $O_2(^1\Delta_g)$ on flame propagation speed was studied in a lifted flame (Ombrello et al. 2010a, 2010b) [107, 108]. The experiments demonstrated that both O_3 and $O_2(^1\Delta_g)$ increased the flame propagation speed by a few percentage. The effects of NOx production by plasma on ignition and flame extinction were also studied by Ombrello et al. (2006, 2008) [117, 118]. The results showed that NOx production by plasma also reduced the ignition temperature and extended the extinction limits of hydrogen and methane-air mixtures.

The above studies significantly advanced the understanding of the elementary processes of plasma chemistry. However, the experimental diagnostics was limited to small species and radicals at high temperature. In order to understand the kinetic processes of plasma activated low temperature combustion, in situ diagnostics of intermediate species produced by plasma assisted fuel oxidation is necessary. This information is necessary to understand the elementary process of plasma assisted combustion and to develop validated kinetic mechanisms [13].

Also crucial is the understanding of resonance mechanisms of nitrogen - oxygen intermediate excited states evolution and relaxation under the influence of modulated electromagnetic field.

10. Mechanisms of Plasma Assisted Combustion

Plasma has the potential to enhance combustion by being a source of heat, radicals, excited species, electrons/ions, fuel fragments, and perturbation of flow simultaneously. These many different enhancement pathways are coupled together to cause thermal enhancement, kinetic enhancement, and even transport enhancement via the ionic wind effect, as shown in Figure 19. In addition, the plasma chemistry has very different characteristics compared to the combustion kinetics. As shown in Figure 20, plasma chemistry happens in a time scale on the order of a few to several hundred nanoseconds and at low temperatures (from room temperatures and above). However, the combustion kinetics can only happen at high temperatures at a much longer time scale, from microseconds to milliseconds. If the reactions introduced by the plasma can play an important role in fuel oxidation, the combustion process can be accelerated significantly. The key process in plasma assisted combustion is the kinetic coupling between plasma produced long lifetime species with fuel and oxygen at low temperature. As shown in Figure 20, this process bridges the fast plasma chemistry process and the high temperature combustion process. Understanding this coupling process is critical to developing an efficient method for plasma assisted combustion [11].

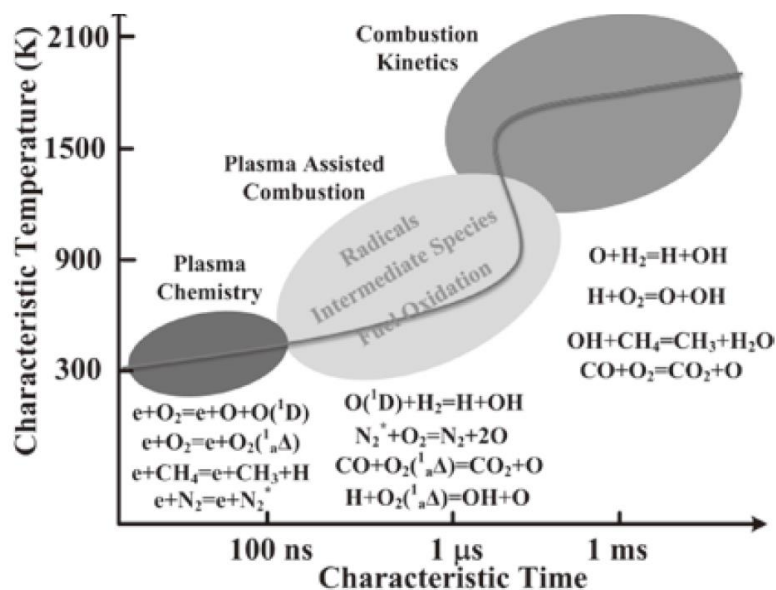


Figure 20. Kinetic regimes and time scales of a typical plasma assisted combustion process [11].

Another important feature for a well-defined plasma assisted combustion experimental platform is simplicity for kinetic modelling. Since many species generated by the non-equilibrium plasma are not well known and difficult to be quantified, the detailed modelling of plasma assisted combustion is very important to improve our understanding and elucidate the underlying enhancement mechanisms [11]. One of the possible way of model improvement is the focused experiments of specific components excited states chemical kinetic research, what is the important part of DENOX project and let significantly improve the detailed mathematical model of plasma assisted combustion.

11. Combustion Modification by Non-Thermal Plasma

11.1 Flame stabilization

1. Pilot flame stabilization

Reducing NO_x emissions from combustion chambers is a major challenge. One approach has been to operate at lean mixtures in order to reduce flame temperature, which in turn, reduces the production of NO_x. However, lean burning can lead to serious combustion instabilities, which can result in flame extinction [119]. Various stabilization methods have been implemented for both diffusion and premixed flames. These include pilot flames, recirculation flow via bluff bodies, swirl, electric fields, and plasmas. [120]

The first technique concerns the use of a rich pilot flame to reattach the combustion process. To attach a hydrocarbon flame to a burner lip, Han and Mungal [121], Muñiz and Mungal [122] and Carter et al. [123] used a hydrogen pilot flame in a coflow jet diffusion flame. Moreover, Prakash et al. [124] increased premixed flame stability by controlling the flow rate split between a bypass line and the main fuel line. Tachibana et al. [125] investigated the effect of secondary fuel injection location on premixed combustion instability. Typical examples of bluff body and swirl stabilization can be found in [126], [127], and [128]. However, these methods have an intrinsic limit in that the main energy transfer occurs predominantly in the form of thermal energy, which implies that a portion of energy is lost. Moreover, this technique significantly increases the level of NO_x generated. Electric field stabilization is then an interesting alternative [129].

2. Electric field stabilization

Flame stability can be obtained by controlling flow convection in the flame reaction zone with electric fields. The stabilization effect is caused by an “ionic wind” between the applied electric field and the “chemiionized” species in the flame reaction zone. In particular, Calcote et al. [130, 131] observed flame deflection and blowout limit extension of a Bunsen burner exposed to a DC electric field. The blowout limit of a premixed methane/air flame is then increased by a factor 4. More marginal in comparison to studies with DC fields, investigations of blowout limit and burning velocity under alternating current (AC) were also reported in [132-134].

Work regarding the interaction between flames and plasma discharges can be found for example in [135-137]. Within these papers, plasma jets are used to increase flame speed and expand the flammability limit of premixed flames.

Finally, an alternative possibility is the use of an electric discharge (in the form of an arc or a HF spark [119]) to reattach a flame and to keep the NO_x levels acceptable.

3. Nonequilibrium plasma stabilization

Recent activity to investigate novel flame stabilization approaches has included the use of nonequilibrium discharges for combustion enhancement (extended flammability limits and reduced ignition delay times), such as dielectric barrier discharges (DBDs) and nanosecond pulsed discharges for premixed flames [138-141]. In this case, the typical added energy is 0.1 to 1% compared to that of typical hydrogen pilot flames. Corresponding studies on the stability of diffusion flames are relatively rare. Kim et al. [142] found that a coflow lifted methane jet flame is stable under application of a nanosecond pulsed discharge in coflow velocities of up to 20 times

the laminar flame speed. They determine the optimal discharge placement in a methane jet in cross flow [129].

Furthermore, the use of pulsed and continuous plasma jets, for the ignition of a lean mixture and the stabilization of the flame in a supersonic flow is promising. An example of application is the flame stabilization in a gas turbine under conditions which tend to extinguish the flame [120]

Plasma-assisted combustion and stabilization of a turbulent premixed flame using nanosecond repetitively pulsed discharges is studied in [106]. A related study of Galley et al. [140] concerns the extension of the flammability of a lean mixture. Moreover, pulsed nanosecond plasma has been shown to stabilize lean premixed atmospheric pressure propane-air flames [140]. A nanosecond repetitively pulsed plasma generator capable of delivering an electric pulse of 10 kV during 10 ns at a frequency of up to 30 kHz is used to stabilize and improve the efficiency of a 25 kW lean premixed propane/air flame at atmospheric pressure. The plasma significantly extends the region of flame stability, in a much wider range of fuel equivalence ratios and flow rates. This example demonstrates the possibility of increasing the combustion efficiency with the addition of a 75 W discharge (0.3%). Also, the spontaneous emission of OH and CH radicals increases by at least 40% in the presence of the discharge [120].

4. Arc-type plasma stabilization

Other research activities study flame sustained by an arc type electric discharge to stabilize the combustion. For example, arc-type plasma stabilization of supersonic H₂/O₂ combustion mixtures is used within the framework of scramjet combustors.

In the same goal, but with a different electric discharge, Choi et al. [119] studied the stabilization of lean propane/air premixed flames. Low power arcs and high frequency sparks are used. Low power arcs significantly lowered the lean limits of flammability. The results showed that the lean flammability limit decreases from equivalence ratios of 0.62 to 0.55 at a flow rate of 330 cm³/s. Similar effects are observed with a spark discharge. In this study, the minimum equivalence ratio drops from 0.58 to 0.43 (~25% decrease) at a flow rate of 240 cm³/s. Finally, it is worth noting that similar reductions in the lean limit of combustion are observed at higher flow rates [120].

It has to be kept in mind that the plasma generates its own NO_x. The decrease in equivalence ratio, permitted by the presence of the discharge, can be compensated by the own plasma NO_x production [119]. However, in larger burners, this balance should be in favour of NO_x reduction [143]. The key technology in NO_x reduction is the better understanding of excited and ion mechanisms of NO_x generation and so the way to manage competing reactions for NO_x damping.

11.2 Experimental study plasma-assisted combustion in an aero-engine combustion chamber

Future aero-engines are expected to operate with a higher turbine inlet temperature than those of current technology engines. This increased turbine inlet temperature requires a combustor with a higher temperature rise capability than ever before [144]. There are many significant challenges for high-temperature rise combustors, among which operating stably in wider and

wider fuel/air ratio conditions and reducing inhomogeneity of the outlet temperature field are two primary challenges [145].

As a new combustion enhancement technology, Plasma-Assisted Combustion (PAC) has been extensively concerned. The air in the plasma actuator is ionized in the discharge process, and then additional energy and numerous chemically active species (O, O₃, ion, active groups, etc.) are injected to the combustor to reduce chemical reaction times and to achieve successful ignition, flame propagation, and flame stabilization [107].

PAC technology will have wider applications in the future due to its obvious advantages, and current research on PAC is mainly focused on the characteristics of the actuator and the mechanism of PAC, however, there is still insufficient research on PAC technology applications for aircraft engines.

In work [146] a plasma-assisted combustion (PAC) test platform for annular combustor (Figure 21) was developed to validate the feasibility of using plasma-assisted combustion actuation (cylindrical dielectric barrier discharge, see Figure 22) to reduce emission levels. Combustor outlet temperature and emission levels of O₂, CO₂, H₂, CO, and NO_x were measured by using a thermocouple and a Testo 350-Pro Flue Gas Analyzer respectively.

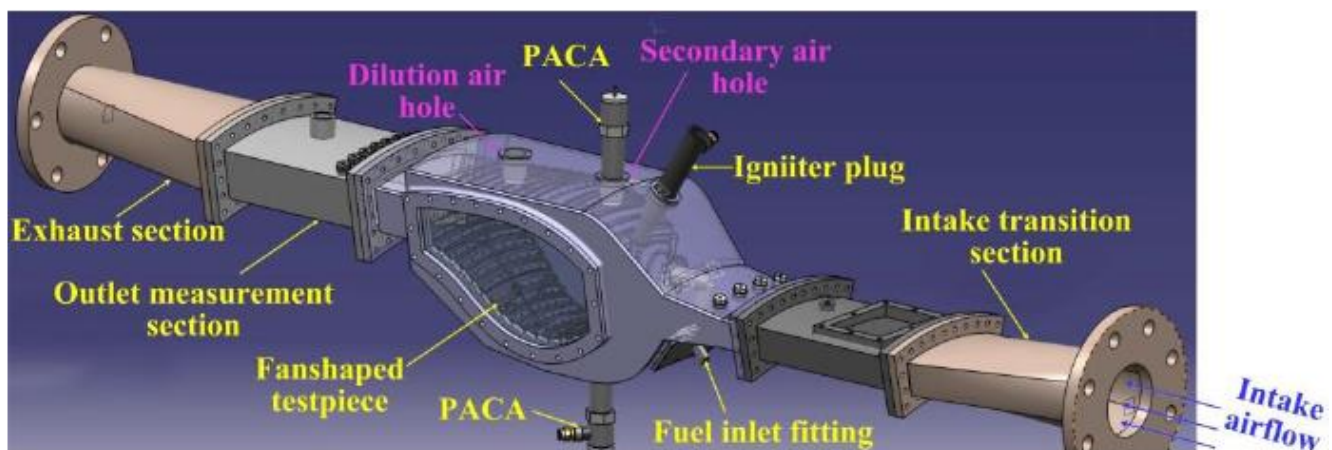


Figure 21. Schematic of plasma-assisted combustion test section [146]

The results [146] show that the target of CO and NO_x emissions reduction in plasma-assisted combustion could not be fully achieved for kerosene/air mixture with different combustor excessive air coefficients. It is also shown that PAC with dilution air hole actuation is superior to that of secondary air hole actuation for the combustion of liquid-kerosene fuel. Besides, plasma-assisted combustion effect is more obvious with an increase of duty ratio or feedstock airflow rate. These results are valuable for the future optimization of kerosene-fueled aero-engine when using plasma-assisted combustion devices to improve emission performance of annular combustor.

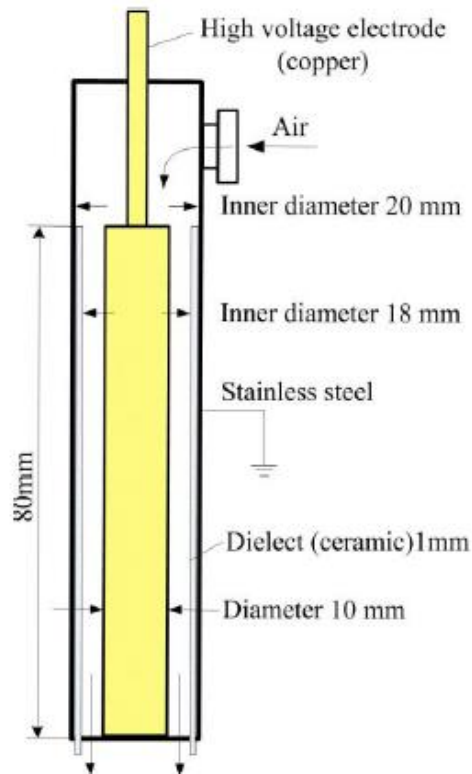


Figure 22. Geometry of plasma-assisted combustion actuator [147]

In work [148], a PAC test platform was developed to validate the feasibility of using PAC actuators (Figure 23) to enhance the annular combustor performance.

Two plans of PAC (rotating gliding arc discharge plasma) were designed, Assisted Combustion from Primary Holes (ACPH) and Assisted Combustion from Dilution Holes (ACDH), Figure 24.

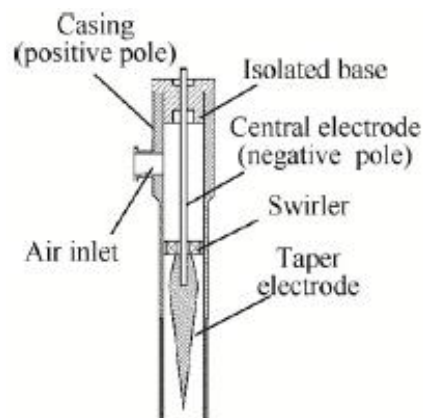


Figure 23 Geometry of PAC actuator [148]

Comparative experiments and analysis between conventional combustion and PAC were conducted to study the effects of ACPH and ACDH on the performances including average

outlet temperature, combustion efficiency, pattern factor under four different excessive air coefficients (0.8, 1, 2, and 4), and lean blowout performance at different inlet airflow velocities.

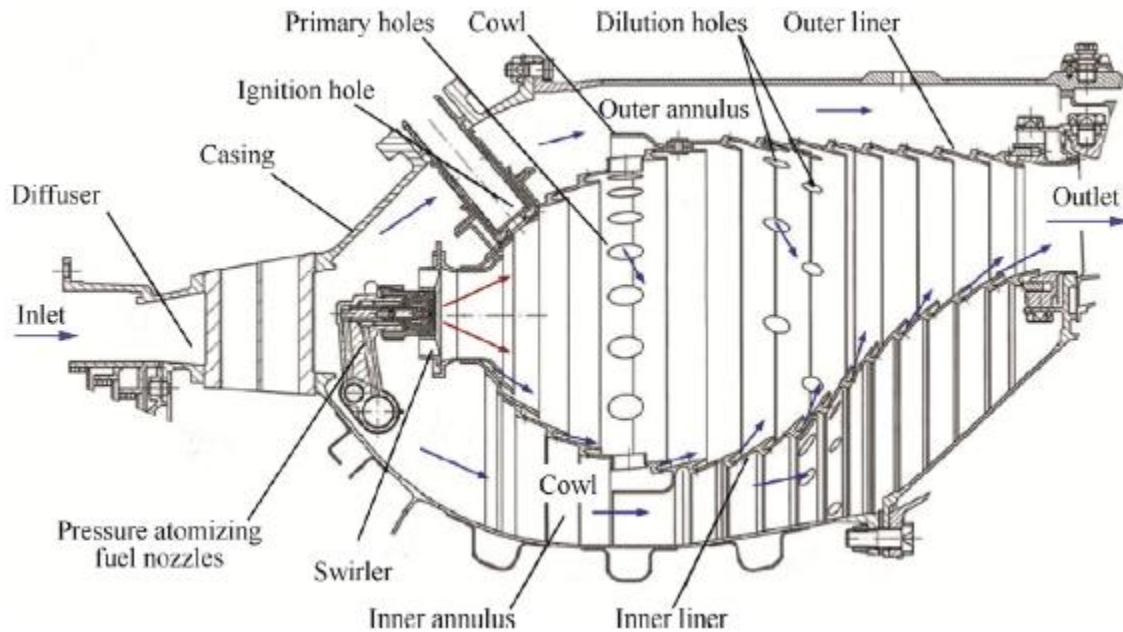


Figure 24 Sketch of annular combustion chamber [148]

The discharge is driven by a sinusoidal plasma power (CTP-2000S, Suman Electronics) with a frequency of 5–25kHz, a modulation frequency of 100Hz to 1000Hz, a maximum peak-to-peak voltage of 30kV, a duty ratio of 10% to 99%, and a maximum output power of 500W.

Experimental results [148] show that the combustion efficiency is improved after PAC compared with that in the normal conditions. The combustion efficiency of ACPH increases 2.45% in the rich condition, and increases 2.75% when PAC from dilution holes, because ACDH enhances the combustion in the after burning zone, and then, it improves the combustion completeness. The uniformity of the outer temperature field and lean blowout performance are improved after PAC. Especially for ACPH, the flame propagation is accelerated in the primary combustion zone, which is in favour of maintaining the fire sources. Experiments show that ACPH extends the lean blow out limit of 8.3%, 12.4%, 12.8%, and 25%, respectively, when the inlet velocity ranges from 60 m/s to 120 m/s.

12. Development of Kinetic Mechanisms for Plasma Assisted Combustion

The major challenge of modelling plasma assisted combustion is the lack of detailed kinetic mechanisms. A first step in this attempt is to combine the plasma kinetic mechanisms with combustion kinetic mechanisms and also include the known interactions between plasma generated species and species contained in the combustion kinetic mechanism.

12.1 The Chemistry of Nonequilibrium Discharges

The main types of reactions occurring in a volume plasma are listed in Table 4. The symbols A, B stand for atoms, A₂, B₂ for molecules, and e stands for an electron. M is a temporary collision partner, and species marked by + or - are ions. The excited species are marked by an asterisk (*).

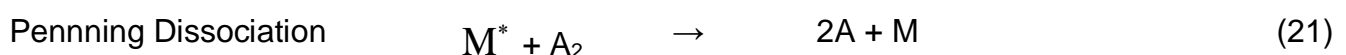
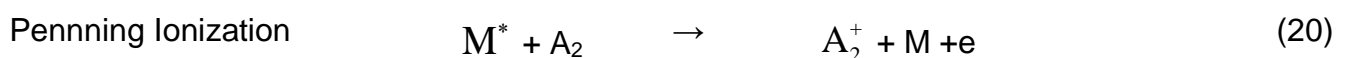
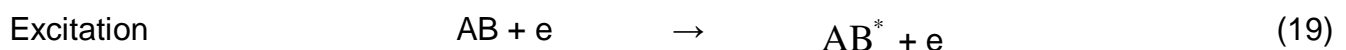
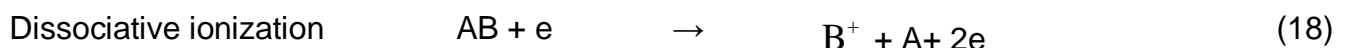
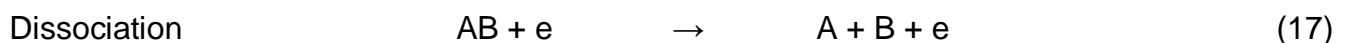
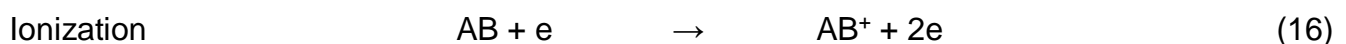
To describe the electron household of a nonequilibrium volume discharge, mainly four reactions are of importance. In a stationary situation, electron losses by attachment and recombination have to be balanced by ionization and detachment processes.

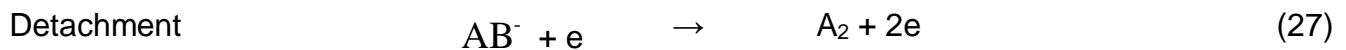
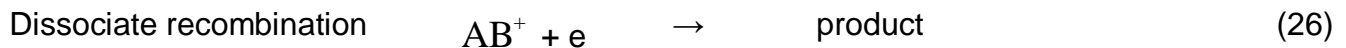
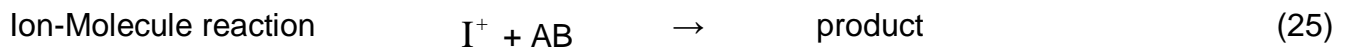
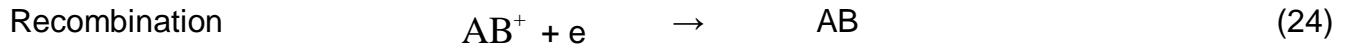
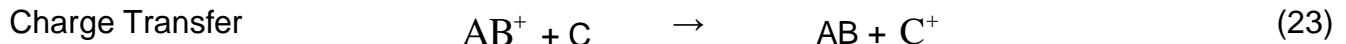
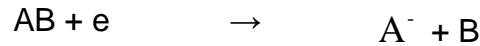
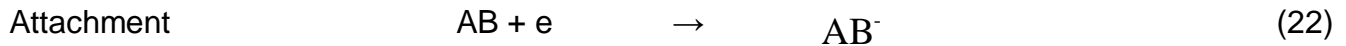
Table 4 – The main plasma reactions [149]

Electron/Molecular Reactions			
Excitation	$e + A_2$	\rightarrow	$A_2^* + e$
Dissociation	$e + A_2$	\rightarrow	$2A + e$
Attachment	$e + A_2$	\rightarrow	A_2^-
Dissociative attachment	$e + A_2$	\rightarrow	$A^- + A$
Ionization	$e + A_2$	\rightarrow	$A_2^+ + 2e$
Dissociative ionization	$e + A_2$	\rightarrow	$A^+ + A + 2e$
Recombination	$e + A_2^+$	\rightarrow	A_2
Detachment	$e + A_2^-$	\rightarrow	$A_2 + 2e$
Atomic/Molecular Reactions			
Penning Dissociation	$M^* + A_2$	\rightarrow	$2A + M$
Penning Ionization	$M^* + A_2$	\rightarrow	$A_2^+ + M + e$
Charge Transfer	$A^\pm + B$	\rightarrow	$B^\pm + A$

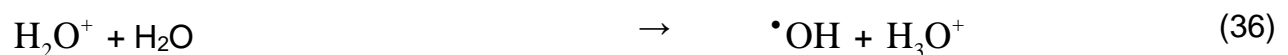
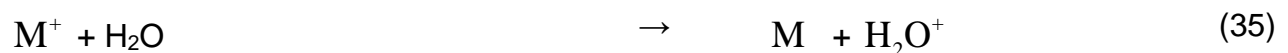
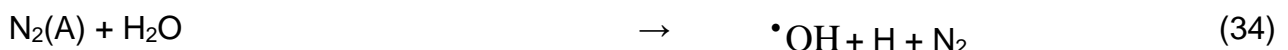
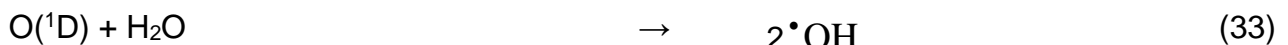
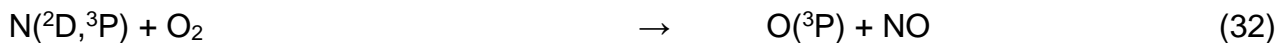
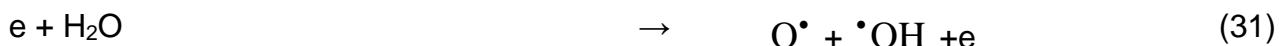
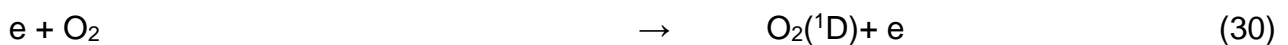
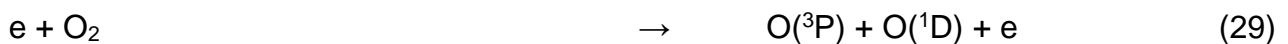
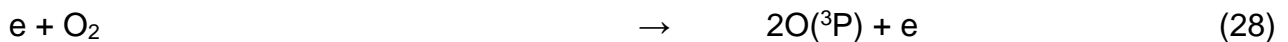
Ion Recombination	$A^- + B^+$	\rightarrow	AB
Neutral Recombination	$A + B + M$	\rightarrow	AB + M
Decomposition			
Electronic	$e + AB$	\rightarrow	$e + A + B$
Atomic	$A^* + B_2$	\rightarrow	AB + B
Synthesis			
Electronic	$e + A$	\rightarrow	$A^* + e$
	$A^* + B$	\rightarrow	AB
Atomic	$A + B$	\rightarrow	AB

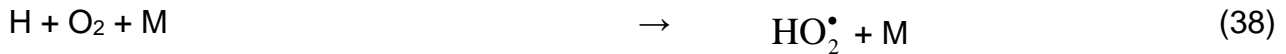
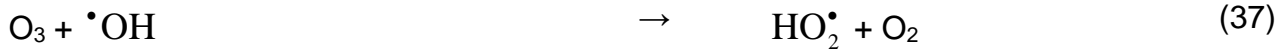
Chemical processes in non-thermal plasmas are based on non-thermal activation of particles via collisions. The quality and quantity of collisions is determined by the density and the kinetic parameters (e.g. mean velocity, collision frequency). In general three different phases has to be distinguished. The first phase is characterized by the electrical breakdown of the gas (e.g. in form of short-lived microdischarges as described above) where free electrons with high kinetic energies are produced via ionising collisions. These electrons undergo further electron-molecule collisions, namely ionisation (16), (18), dissociation (17), (18), excitation (19) and electron attachment (22). Furthermore Penning-ionisation and dissociation (20), (21); charge transfer (23) and ion reactions are possible. All mechanisms have quite different reaction rates due to its different energy thresholds. For example for dissociation energies between 3 and 10 eV are sufficient, while ionisation requires energies more than 10 eV and electron attachment happens at energies of some eV or lower. Indeed, the exact values are determined by the electronic configuration of the molecule being considered. The reaction rate further depends on the gas temperature which depends on the vibrational excitation level of molecules. The second stage of non-thermal plasma chemistry is the radical formation and removal stage, where a multitude of anorganic reactions takes place. In particular radicals are generated through direct electron impact molecule dissociation and ionization as well as ion-molecule reactions (25), dissociate recombination of ions and electrons (26), attachment and detachment reactions (27) (Chang, 2008) [150].



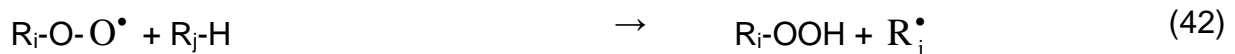
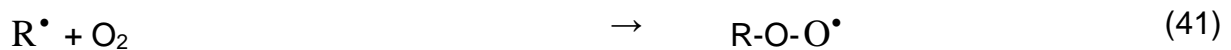
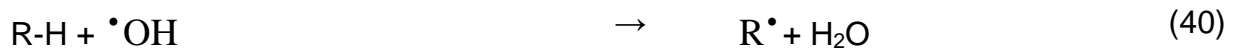
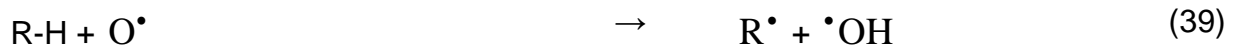


In air plasmas reactive oxygen species are generated by direct electron collisions (28)-(31), via Penning-processes (32)-(34) and charge exchange (35) with subsequent ion-molecule reaction (36) from O_2 and H_2O . Furthermore in non-thermal plasmas generated in oxygen containing atmospheres at low gas temperatures ozone, and other a strong oxidizing agents like O , $\cdot OH$ and HO^*_2 will be formed.

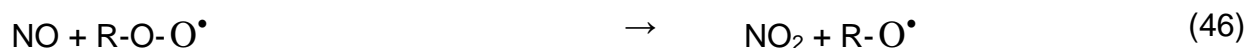
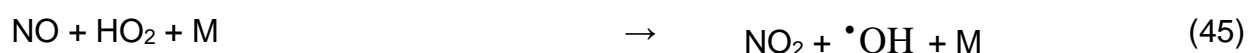
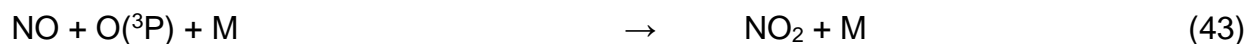




Many molecules are readily attacked by free radicals. Decomposition of hazardous compounds is achieved without heating of the flue or off-gas. Due to the presence of oxygen, water vapour and ozone, oxidizing reactions are dominant. The resulting chemistry is quite complex and depends on the gas mixture itself as well as the temperature. More detailed and comprehensive information the reader is referred to [151, 152, 153, 150] (Fridman, 2008; Penetrante & Schultheiss, 1993; H.H. Kim, 2004; Chang, 2008). Regarding the removal of saturated hydrocarbons (denoted as RH, e.g. alkane), the process starts with dehydrogenation reactions (39), (40) followed by the oxidation of the remaining organic radical R^\bullet (41). The latter reaction results in the formation of peroxy radicals RO_2^\bullet (41) which are further oxidized down to CO_2 and H_2O (total oxidation) or trigger a radical chain reaction with alkyl hydroperoxide radicals R-O-OH (42). In case of unsaturated hydrocarbons additionally radical addition following oxidation, radical chain reaction or polymerisation of hydrocarbons are taking place.



In plasma-based flue gas treatment for NO and SO₂ removal desired reductive reaction paths are of minor importance. Oxidative processes (43)-(45) lead to the formation of NO₂. The oxidation up to N₂O₅ is possible. If hydrocarbons are present (e.g. ethene, propene, propane) HO₂[•] and peroxy radicals become the dominant oxidizers (45), (46) and the energy required to oxidize NO molecule can be reduced. However, to remove NOx from the gas a heterogeneous chemical process for NO₂ reduction must follow the plasma treatment. In a similar way SO₂ oxidation to SO₃ by means of plasma treatment is possible, while SO₃ needs to be removed chemically.



Following the removal stage aerosol particles are formed through reaction of larger radicals with cluster ions and molecules. Aerosol formation is a quite important process since aerosol surface reaction rate is a few orders of magnitude higher than the electronic, ionic and radical reactions.

In work [154] is investigated the contribution of different chemical reactions that participate in NO_x creation or reduction in N₂/O₂/H₂O/CO₂ mixed gas induced by negative corona discharge under different reduced electric field levels: 100 - 200 Td (1Td=10⁻²¹ V.m²). The fundamental chemistry governing NO_x evolution developed in this paper is based on a full set of processes regrouped in 200 selected chemical reactions involving 36 molecular, excited, atomic, and charged species. The density was calculated using the continuity equation while not the diffusion term, and the time analysis varied from 10⁻⁹ to 10⁻³s. The results of simulations show the role played by different chemical reactions on NO_x conversion. It is shown that at 100 Td near 60% of NO can be removed by radical O₄⁻ through the reaction NO + O₄⁻ → NO₃⁻ + O₂ and near 20% of NO₂ and NO₃ could be removed by radicals O₃⁻ and O₂⁻ through NO₂ + O₃⁻ → NO₂⁻ + O₃ and NO₃ + O₂⁻ → NO₃⁻ + O₃.

Authors [154] have noticed that the evolution of one species can influence the evolution of another specie. They can be summarized as follows.

(i) The mechanism of NO creation occurs mainly by the reaction of N (²D) radicals with molecular oxygen:

N (²D) + O₂ → NO + O, and destruction by O₄⁻ radicals with: NO + O₄⁻ → NO₃⁻ + O₂. Authors [154] have obtained 29.33% at 100 Td against 28.93% at 200 Td for creation, and 59.13% at 100 Td against 49.50% at 200 Td for destruction.

(ii) The mechanism of NO₂ production is due mainly to the reaction of NO₃⁻ radicals with atomic nitrous:

N + NO₃⁻ → NO₂ + NO + e, and reduction by reaction: NO₂ + O₃⁻ → NO₂⁻ + O₃. At 100 Td authors have found 68.61% for production against 61.65% at 200 Td, and 19.30% at 100 Td against 27.61% at 200 Td for consumption.

(iii) About NO₃ it is shown that the creation is due to two radicals O₄⁺ and NO⁺ through reactions:

NO₃⁻ + O₄⁺ → NO₃ + 2O₂, and NO₃⁻ + NO⁺ → NO₃ + N + O, and reduction by reaction: NO₃ + O₂⁻ → NO₃⁻ + O₂.

Authors [154] note that at 200 Td, there is no reduction and the two reactions participated completely to the production of NO₃ (55.36% for R19 and 44.64% for R20, see Appendix 3, Table A3.1). This is the effect of transformation of NO and NO₂. For successful reduction of final NO_x rate, the additional, non-common for conventional flames, mechanisms should be developed and implemented by specific stimulation conditions.

12.2 Multiscale and Dynamic Adaptive Chemistry Modeling Using Reduced and Detailed Mechanism

To capture the physics of turbulence-chemistry interaction involving low temperature chemistry and different flame regimes for real fuels, a large kinetic mechanism involves hundreds of species and thousands of reactions is needed. The large number of species and the stiffness of the combustion kinetics results in a great challenge to combustion modelling (DOE report 2005). For a typical implicit method, the computation time is proportional to the cubic of the species number. Moreover, as shown in Figure 25, the timescales of the elementary reactions and physical processes have a disparity of more than 10 orders of magnitude. Even with the availability of petascale computation capability, direct numerical simulations with such large kinetic mechanisms remain to be difficult.

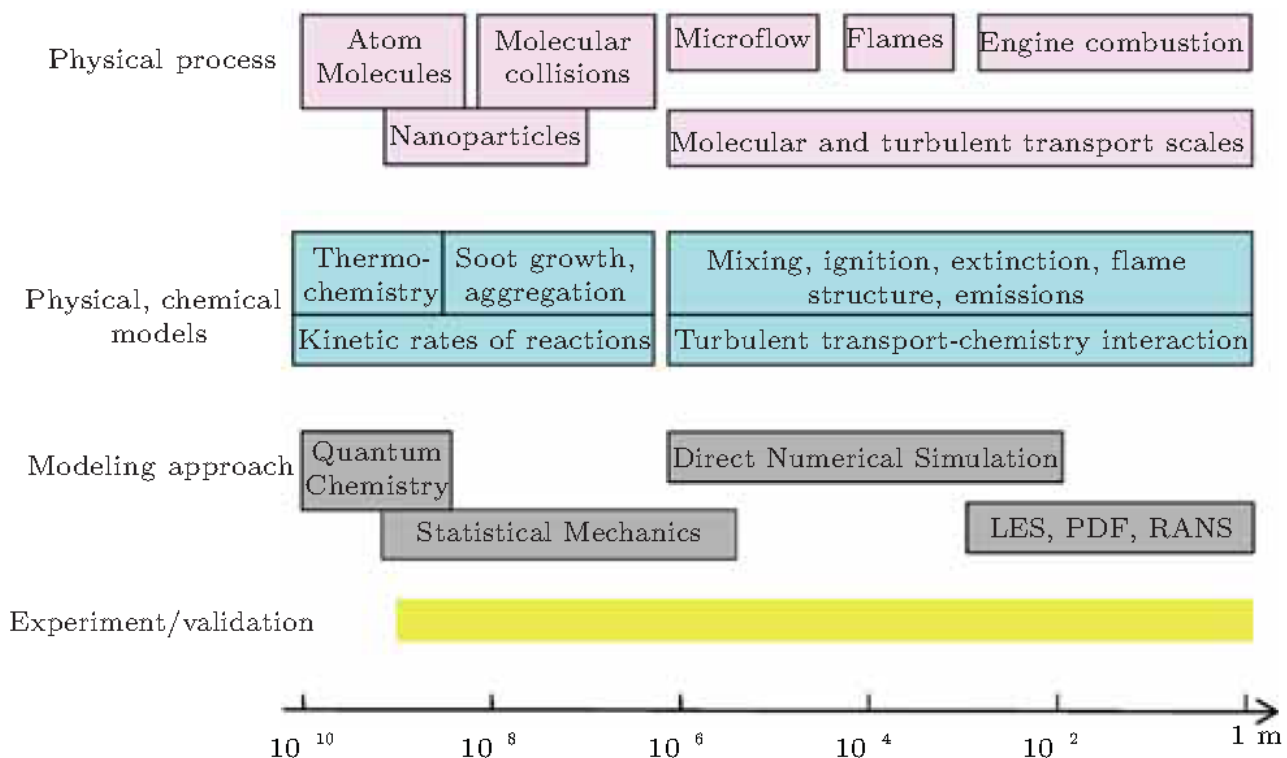


Figure 25. Multi-scale processes and multi-scale prediction models in combustion [115] (Gou et al. 2010)

It is extremely important to understand the mechanism by which non-equilibrium plasmas have an effect on the combustion of gaseous mixtures from both a fundamental and a technological standpoint. The issue here is that the plasma chemistry involved in contributing to these enhancements has very different characteristics compared to the combustion kinetics.

In Figure 26 it can be shown that plasma chemistry happens on a very small time scale (~ 100 ns) at relatively low temperatures, whereas the combustion chemistry normally occurs at higher temperatures and at longer time scales ($\sim \mu\text{s}$ to $\sim \text{ms}$). The key process in plasma enhanced

combustion involves the coupling of long-lived plasma species reacting with fuel and oxidizer at low temperatures. This essentially bridges the fast plasma chemistry with the high-temperature combustion processes. The role of different species in PAC has been widely discussed and despite increased interest in the problem, the kinetic mechanisms for plasma enhanced combustion are still not very well understood.

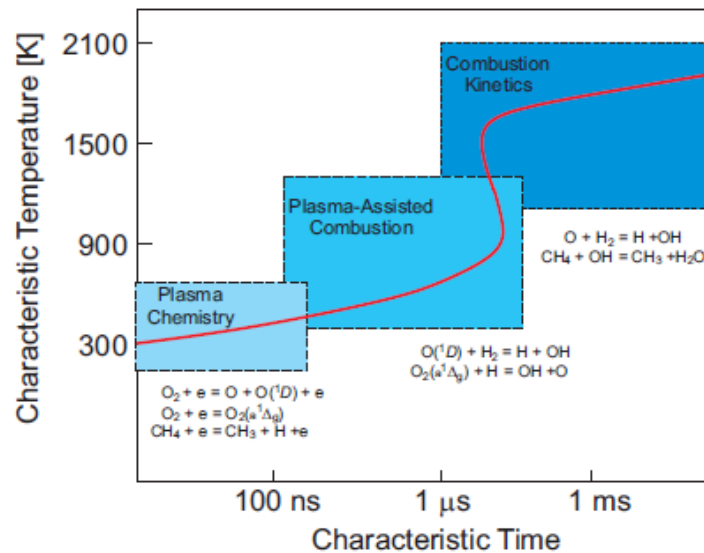


Figure 26. Comparison of characteristic time scales of different chemical processes [79].

Demuklar number (Da) is defined for the time scale turbulence on a scale chemical reaction time. If that number is very small Demuklar ($Da \ll 1$), confusion is much faster kinetics. Flow regime mixer as a good reaction, where the products and reactant were mixed together quickly. If the number is very large Demuklar ($Da \gg 1$), a chemical reaction occurs much faster than turbulence scales. The turbulent flame structure able to change and chemical reaction zone is in a comfortable position. Turbulent non-premixed combustion regime in Figure 27 is shown based on a function of the number Demuklar and Reynolds number turbulence.

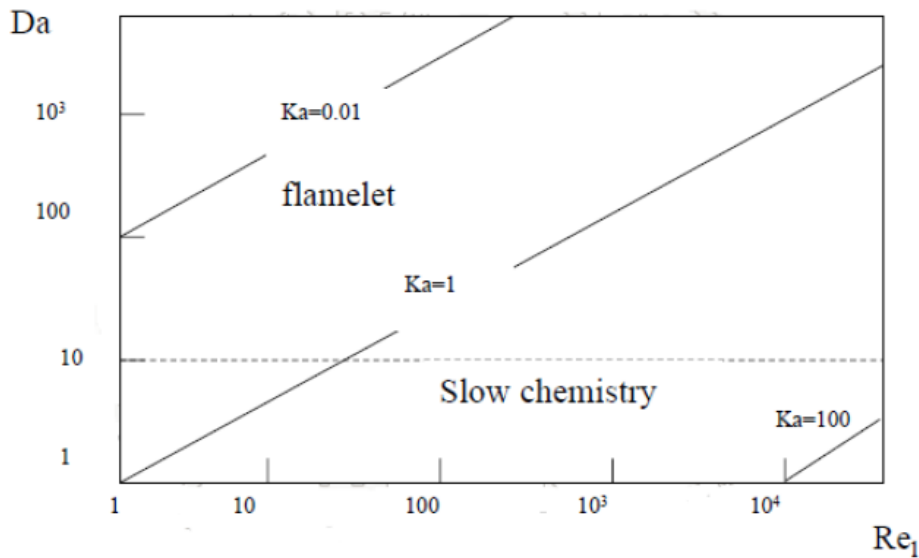


Figure 27. The non-premixed turbulent combustion regimes based on the Damköhler number and Reynolds number turbulence [155]

Chemical processes associated with plasma power, is studied by Hoon et al. [156] for NO_x emission control. Non-thermal plasma energy can produce NO₂ by combining NO and N₂ but it is enable in converted NO₂ to N₂. So chemical processes were developed with plasma force to be done to convert NO to NO₂ and NO₂ by using plasma reactors with minimal side effects. This method is able to analyze almost 100% NO_x with extremely low energy consumption and the formation of N₂O is the minimum amount.

In [155] study the combustion of methane - air in the combustion chamber has been made where the effects of fluid dynamics in a plasma actuator physics flow field. All steady state and transient simulation has been done in Fluent software and the application of appropriate turbulence model. The effects of plasma flow field force were investigated regardless any chemical reaction. The next step is non-premixed combustion of methane and air modeling and plasma energy applied to the system. Operators in places close to the area of the vortex flow field have been put in force so that the plasma tends to deactivate them. At the same time the flow is accelerated and it can be seen that the mixing of the reactants is increased. DES also a transient simulation to check for changes in the flow and combustion phenomena in plasma was performed by using force.

The results [155] show that the peak temperature of the plasma decreased after the application of force, which reduce emissions of NO_x and follow it. And the average temperature curve is flatter near the central axis of the combustion chamber suggests that it occurs more homogeneous combustion by mixing the turmoil. After setting up the plasma operations, an increase in the average axial velocity was observed in areas near walls. And then force the plasma, flame width is increased radially. According to the results, distribution of improved average fuel which could start up the engine when employing a diluted mixture induces.

Combustion kinetics of hydrocarbonic fuel (the reduced and detailed mechanisms) it has been investigated by the Dolmatov [12]. In [157] numerical experiments was carried out to predict the total temperature characteristics and formation of nitrogen oxide emissions and pattern factor in

an annular combustor liner based on geometrical parameters and location and rows of different air admission holes, for 6 various cases, using computational fluid dynamics.

12.3 Microwave plasma and catalytic decomposition of nitrogen oxides

There are several different approaches to microwave discharge and microwave fields using for reducing of nitrogen oxides and other pollutant emission level. The most common application of microwave discharge is the initiation of catalytic active surfaces increasing (the most useful for carbon and carbon-based surface catalysis) [162, 163]. Microwave discharge with frequency 0.8 - 3 GHz is ruining the surface of solid carbon, forming holes and micro fissures by typical thermal ruination mechanism and, possibly, partially by surface ionization with further destruction of smooth carbon surface. The sideboard surface reactions between solid carbon and oxygen (and other active gases, excluding main catalysis targets - nitrogen oxides and sulfure oxides, [162]) obviously take parts in surface ruination too, but the level of inner discharge carbon - oxygen direct reactions involvement into the process of carbon surface ruination and decomposition is still questionable. Thus, the molecular oxygen concentration has very low influence on the final level of catalytic desulfurization and denitrification according to experimental researches, and so it should has the same impact on surface ruination (see Figure 28). Nevertheless, the microwave discharge leads to significant increasing of carbon surface roughness and so to increasing of active catalytic surface for adsorption denitrification mechanism. On Figure 29 are presented the results of scanning electron microscopy of base carbon sample and carbon irradiated by microwaves with 2.45 GHz maximum frequency.

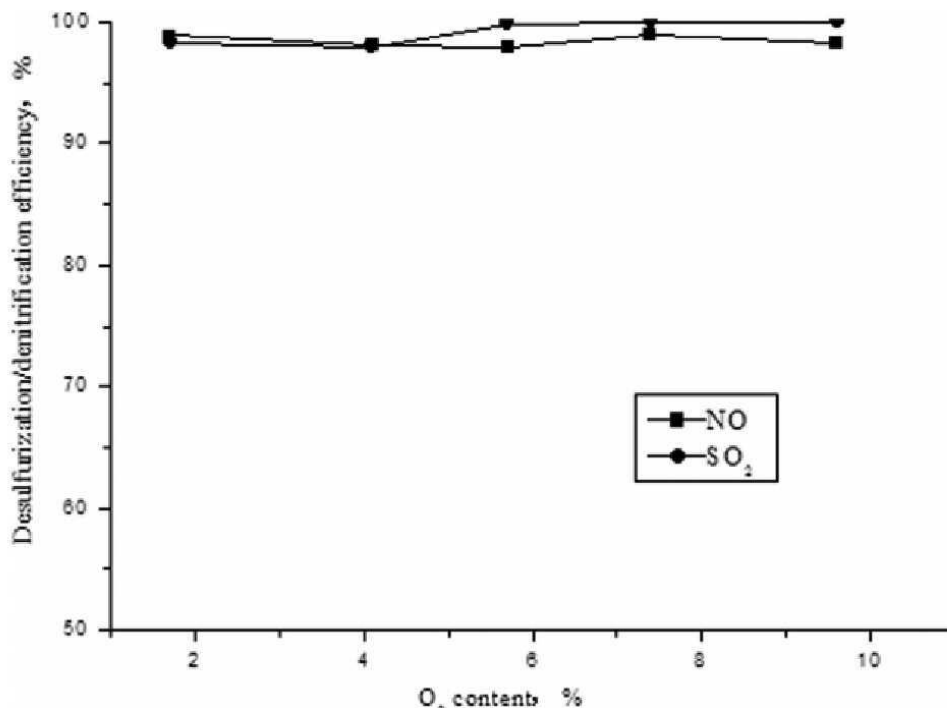
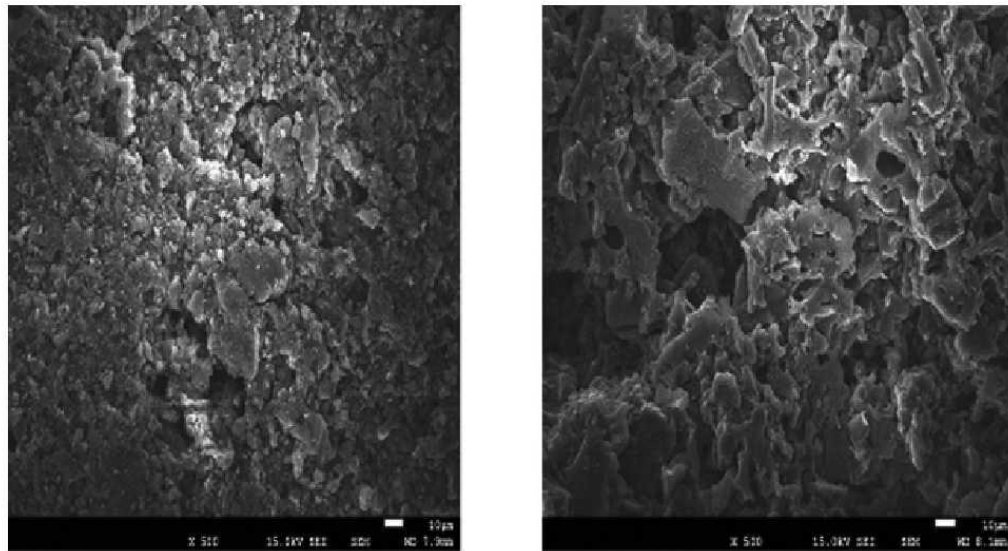


Figure 28. The influences of O₂ content on desulfurization and denitrification [162]

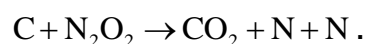
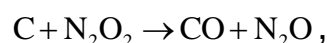
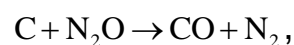
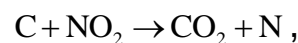
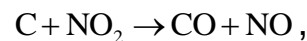
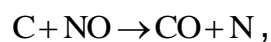


I base carbon

II activated carbon irradiated by microwave

Figure 29. SEM images of base carbon (I) and microwave-activated carbon (II) [162]

The basis of microwave initiated catalytic reduction of NO_x is the same to platinoid catalysis and is founded on the chemical reactions of carbon recovery of nitrogen by mechanism



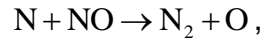
Activated carbon is a good microwave energy absorber [163] and so the recovery reactions rate is significantly increased by two reason - the additional surface area and reaction velocity constant rise.

The level of NO_x destruction for described method is very high and can reach 99% of initial concentration for start NO_x between 500 - 1100 mg/m³ [162]. Microwave carbon catalysis, on the contrary to platinoid catalytic NO_x reduction, is pretty cheap and applicable for ground-based facilities with wide range of gas mass flow rate. However, the method has some crucial shortcomings for gas turbine engines NO_x decomposition, including:

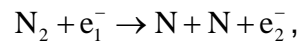
- the temperature limit: method is unapplicable for high temperature gases;
- gas velocity should be very low to provide enough time for contact with carbon for succesful recovery that makes it difficult for using on gas turbine engine;
- the microwave isn't involved in the NO_x decomposition process directly and so can't affect the high temperature mechanisms of NO_x creation;

- additional consumables (carbon) are necessary.

There is another approach based on low temperature plasma generation by microwave pulsed discharge [164, 165]. According to natural experiments, excited atomic nitrogen N can decrease an amount of NO by recovery reaction mechanism



and low temperature plasma generated in microwave pulsed discharge under specific circumstances can increase the concentration of N radical in N₂/NO mixture by simple percussive electron dissociation mechanism:



especially suited for vibrationally excited nitrogen molecules for vibrational temperature range 830 - 1080K and rotational temperature range 1170 - 1485K in the plasma core [159]. Figure 30 represents the dependence of vibrational and rotational temperature of N₂ in the plasma core and final concentration of NO depend on initial concentration of NO in N₂/NO mixture (energy deposition 30 mJ per pulse, pulse duration 50 μs, repetition frequency 2 kHz). Experimental device for pulsed microwave discharger is presented at Figure 31.

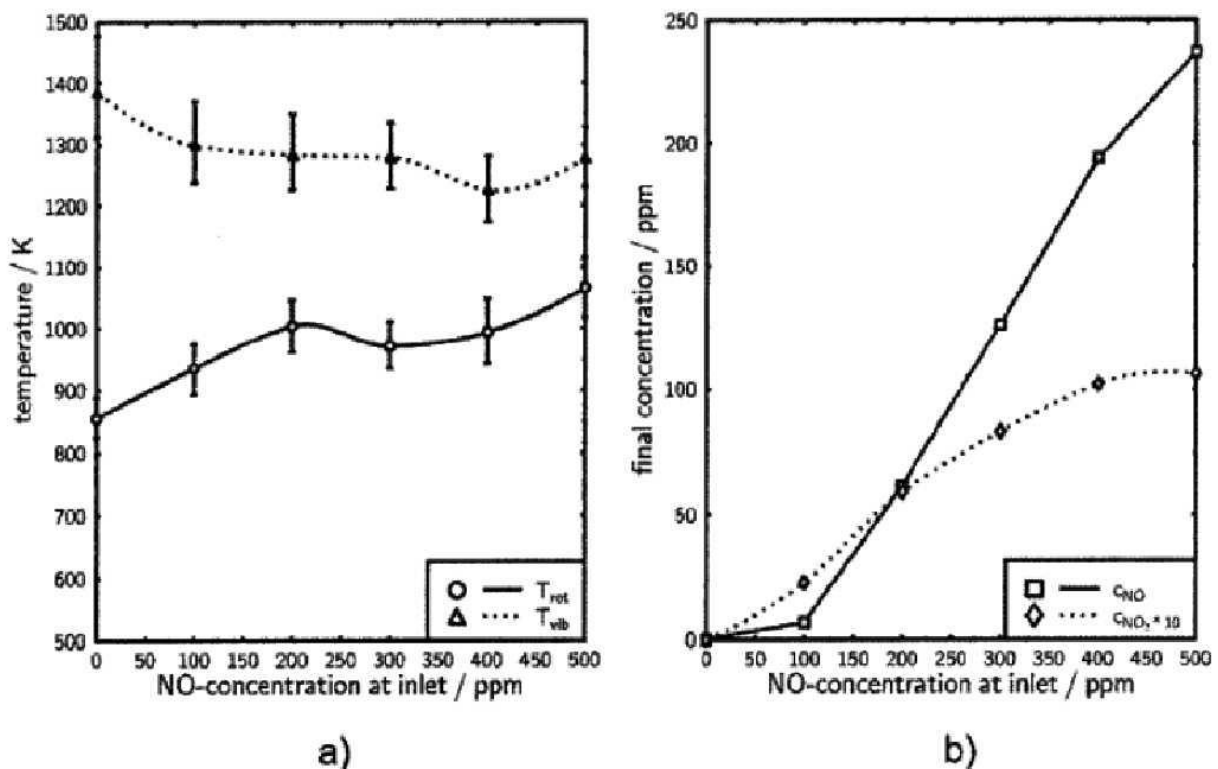


Figure 30. Measurements in N₂/NO mixtures [164]

- (a) Rotational and vibrational temperatures of N₂ in the plasma core;
 (b) concentrations of NO and NO₂ after exhaust gas treatment.

It's obvious that in N_2/NO mixture microwave discharge leads to significant (more than 50% maximum for inlet NO concentration 500 ppm) NO_x summary concentration decreasing because of lack of the oxygen-involved reactions of excited and ionized particles. Presence of additional recovery agents like CO , CH_x , H_2O (vapor) etc. provides additional decomposition of nitrogen oxides in the plasma core and attached regions [165]. However, the presence of oxygen in molecular and atomic form creates opportunities for competing reactions both radical and ion type which lead to increasing of NO producing. The results of microwave discharge in $N_2/O_2/NO$ mixture are presented at Figure 31.

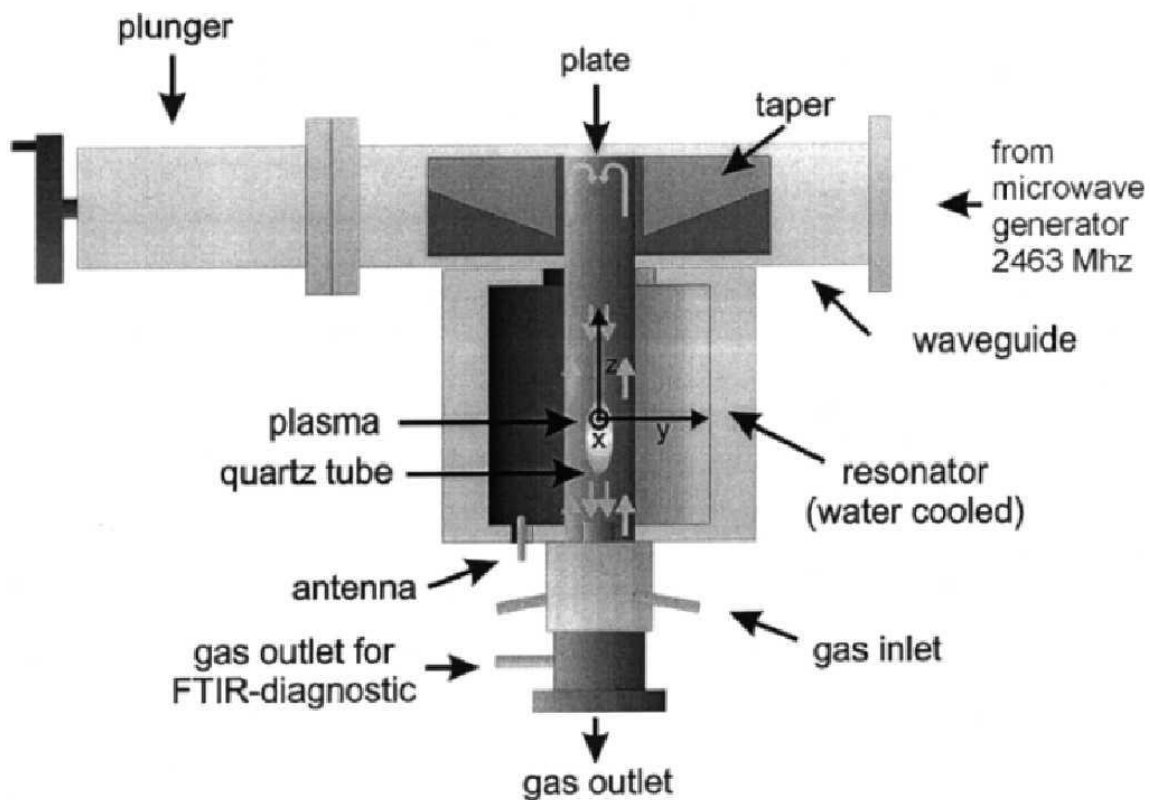


Figure 31. Experimental setup of the pulsed microwave discharge [164]

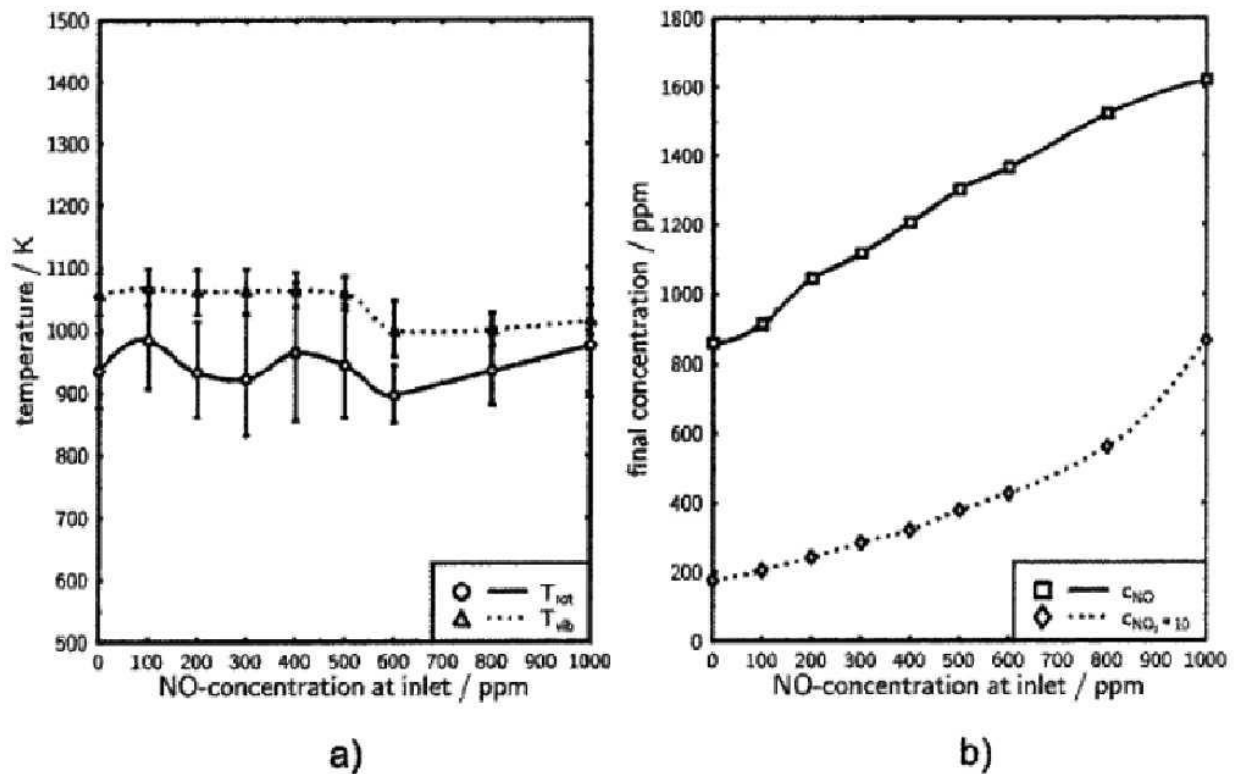


Figure 32. Measurements in N₂/10% O₂/NO mixtures [164]

- (a) Rotational and vibrational temperatures of N₂ in the plasma core;
 (b) concentrations of NO and NO₂ after exhaust gas treatment

It's clear that presence of oxygen (what is corresponding with real conditions in combustion chamber or exhausting nozzle of gas turbine engine or Diesel/Otto engine except stoichiometric and rich combustion) leads to dramatical increasing of summary NO_x production because of oxygen molecules and atoms aptitude to electron percussive exciting reactions (and, for high energy free electrons, percussive positive ionization). Created vibrationally excited and/or ionized particles have increased oxidation potential that affects the NO production rate.

Microwave pulsed discharge methods can be extremely useful for decomposition of NO and the rest of NO_x during low or near zero concentration of oxygen by atomic nitrogen recovery mechanism. However, the present method has some significant flaws, including:

- negative efficiency for oxygen-contained gas mixtures, including real engine exhausting gases;
- lack of electrochemical mechanisms competing and blocking NO_x generation for hydrocarbon mixtures;
- no use for excited states of existing and new created (in the plasma core and attached flow region) nitrogen-oxygen bonds.

13. Conclusion

For the Long-Term 2026 goal it was demonstrated that **no entire engine family has yet to meet the goal** [3].

The trends and goals in aviation engines are paradoxical in relation to NO_x emissions. Turbine inlet temperatures (TIT) and overall pressure ratios (OPR) have been increasing over time in the pursuit of increasing thermal efficiency and thereby reducing the fuel consumption and CO₂ emissions [8]. While on the other hand, NO_x emissions have to be reduced, in spite of their tendency to increase with both TIT and OPR.

The residence time of the combustor must be sufficient so that CO can be fully burnt out into CO₂, but this will promote NO_x in the post-flame region that is directly related to the residence time. Therefore a strong compromise must be found to obtain satisfactory emission levels at all regimes.

The literatures reviewed for plasma combustion have shown better understanding of nonthermal and thermal enhancement effects, kinetic modelling and validation, diagnostics of excited species, plasma temperature combustion, flame regime transition, dynamics of the minimum ignition energy in gas turbine engines, scramjets, and other lean burn combustion systems. However, there are few information on effect of different plasma conditions on the combustion and ignition processes. The data on plasma low temperature are also limited. There are inadequate kinetic models and tools to adequately simulate plasma combustion and ignition processes. Thus, further research studies on the application of plasma in wide range of engine operations are still required.

Combustion phenomena and flame regimes involving new combustion concepts, plasma assisted combustion, and flames at extreme conditions have been analysed.

Modern engines are using more premixed and volumetric ignition modes than high temperature premixed and diffusion flame modes in conventional engines. The combustion characteristics and engine performance of advanced engines are strongly affected by fuels and fuel molecular structures. Low temperature and high pressure chemistry plays a critical role in affecting the control of heat release rate and knocking of engines. Recent turbulent flame studies of large hydrocarbon fuels revealed that low temperature ignition can lead to different turbulent flame regimes and different turbulent flame speeds. The existing Borghi turbulent flame diagram does not include the flame regimes involving large ignition Damköhler number at elevated temperature. The previous studies of turbulent flame regimes have been limited to high temperature thin flame regime. Future studies in turbulence combustion in engines need to emphasize how low temperature chemistry affects the turbulent flame regimes, propagation speeds, and turbulence-chemistry interaction, especially at high pressure and high Reynolds number [13].

Non-equilibrium plasma can significantly enhance low temperature ignition and combustion, and extend combustion limits. The fundamental process of plasma assisted combustion has been advanced by advanced laser diagnostics of plasma generated excited molecules, intermediate species, and radicals. However, there is still a large knowledge gap in low temperature chemistry and cool flames. Many fundamental combustion phenomena involving low temperature ignition and flames with fuel and thermal stratifications are not well understood at

high pressure. Moreover, there is a large uncertainty of kinetic mechanisms in extreme conditions [13].

Multi-scale and multi-physics modelling using detailed kinetic mechanism remains to be a challenging issue. Many methods using time splitting, path flux and graph analysis, adaptive chemistry, solution mapping, tabulation, and multi-timescales have been developed. These methods significantly increased the computation efficiency. Future research in model reduction needs address the large number of species needed to be carried in adaptive chemistry reduction, parallelization of model reduction method, and reduction of computation time for transport and convection calculations [13].

Elementary reactions and combustion strongly depends on pressure. Unfortunately, many existing kinetic mechanisms still use the rate constants at high pressure limit. Future challenges are: 1) Experimental validation of kinetic mechanism and elementary rate constant measurements at high pressure kinetics (1~50atm) and low temperature conditions (500~1100K); 2) Large hydrocarbon and oxygenated fuel chemistry and pressure dependent RO₂ and QOOH reaction pathways; 3) Improvement of uncertainty in ab-initio quantum chemistry calculations; and 4) Development of automatic search of high pressure reaction pathways and kinetic mechanism from the first principle [13].

It has been demonstrated that non-equilibrium plasma is a promising technology to enhance the performance of combustion at low temperature, ultra-lean, and high speed flow conditions. Different kinetic enhancement mechanisms were proposed including the effect of ion chemistry, the chemistry of excited species, and the additional production of atoms and radicals. The effect of radical production (such as O, H) from the plasma discharge on ignition and combustion has been widely recognized. Advanced laser diagnostic techniques have also been developed and applied to investigate the production of radicals from the discharge. These techniques significantly improved our understanding. However, the diagnostics are still very challenging for plasma assisted combustion research owing to the large uncertainty and very limited number of species of the measurements. In situ quantification of important intermediate species produced during the discharge and combustion process is very critical. Beyond the effect of radical addition, the effect of ion and excited species chemistry is still largely unknown. One example is the excited O₂ (O₂(¹_aΔ_g)). There are many recent efforts to model the effect of O₂(¹_aΔ_g) on the combustion system. But due to the unknown reaction pathways and rate constants of O₂(¹_aΔ_g) with hydrocarbons, especially the quenching effect, large uncertainties remain for the models and conclusions. Those species can introduce new unknown reaction pathways into the combustion system and their effects are difficult to quantify. In addition, the electron impacts on hydrocarbons are largely unknown except for some simple molecules. So a challenging target in further fundamental studies is how to isolate the plasma kinetics, which has extremely short time scales as compared with the conventional combustion kinetics. Therefore, different effects can be investigated [11].

One important feature of plasma assisted combustion is that combustion can be sustained at low temperature conditions where it cannot exist in conventional combustion systems. Since most combustion kinetic mechanisms are not validated at low temperature conditions (below 700 K), the uncertainty of the combustion kinetic mechanisms in this temperature range is very

large and difficult to estimate. The development of reliable combustion kinetic mechanisms requires a large amount of data at those conditions which can be easily modelled. With the fundamental understanding of the enhancement mechanisms of plasma on combustion, the plasma itself can be further optimized and tailored to facilitate different applications [11].

Practical combustion systems always experience a broad range of pressures. The typical working conditions for plasma and combustion systems are not aligned with each other. Most of the research about plasma assisted combustion has been conducted at low pressures (below 1 atm). With the increase of pressure, the instability of plasma discharge starts to develop and will cause a non-uniform structure of the discharge. A reliable high pressure plasma technology is very important towards the application of this technology in practical systems [11].

Despite the remaining many challenges and unknowns, recent work has demonstrated the principal enhancement mechanisms of plasma assisted combustion. It can be concluded that plasma is a promising technology to enhance ignition and combustion and can be used in novel aerospace application, designing innovative engines and energy conversion systems and enhancing the combustion properties of different fuels [11].

The behaviour of excited particles, especially ones at intermediate excitement levels, and ionized reagents in medium with relatively high hydrocarbon radicals concentrations and large amount of simultaneous reactions, is weakly explored. The role of plasma- and discharge-generated reagents (uncommon or completely inexistent in conventional flames) in NO_x generation, suppression and decomposition can be crucial and can provide the reduction of thermal and fast generation of nitrogen oxides by an order of magnitude.

The key problems are, first, the development of kinetic mechanisms of excited and ionized reagents NO_x suppression in zone with temperature above 1800K, and second, the development of discharge stimulation principle and devices for providing of necessary flow conditions and the concentrations of key reagents. Both goals need deep research of physical chemistry and thermodynamic of discharge stimulation of high temperature flames, which will give a ground for development the DENOX technology concept #1, i.e. electrochemical suppression of NO_x generation in primary combustion zone.

Also the contemporary microwave methods of NO_x reduction are focusing on almost low temperature catalysis only and are hardly applicable for gas turbine engines. Direct plasma intervention in the NO generation/decomposition has shown prominent results for non-oxygen mixtures only and isn't fitted for real gas flow yet. The most potential method involving microwave abilities for multistep excitement of nitrogen - oxygen chemical bond according to frequencies resonance hasn't been applied for now and will be in the core of the DENOX technology concept #2 focused on electromagnetic decomposition of NO_x molecules in engine exhaust

So both technology concepts of the DENOX project are beyond state-of-art and are aiming the leading edge of gas turbine engine NO_x reduction science.

References

1. H. C., Mongia, and W. G. A. E. Dodds. "Low emissions propulsion engine combustor technology evolution past, present and future." 24th Congress of International Council of the Aeronautical Sciences, Yokohama, Japan, Aug. 2004.
2. Environment Branch of the International Civil Aviation Organization (ICAO). ICAO environmental report 2013. Technical report, ICAO, 2013.
3. N Dickson. Local air quality and ICAO engine emissions standards, Available at: http://www.icao.int/Meetings/EnvironmentalWorkshops/Documents/2014-Kenya/4-1_LAQ_Technology_notes.pdf 2014.
4. ACARE. Advisory council for aviation research and innovation in Europe activity summary 2014.
5. vd Bank, Ralf, et al. Organisation of European aeronautic ultra-low NOx combustion research, Available at: http://icas.org/ICAS_ARCHIVE/ICAS2006/PAPERS/066.PDF
6. European Aviation Environmental Report 2019, Available at: <http://www.easa.europa.eu/node/15672>
7. Flightpath ACARE. 2050-Europe's Vision for aviation. Advisory Council for Aeronautics Research in Europe; 2011.
8. Yin F, Rao AG. Performance analysis of an aero engine with interstage turbine burner. In: Proceedings of the 23rd ISABE conference, Manchester, UK; 2017 Sep 3-8.
9. Perpignan, A. A., Rao, A. G., & Roekaerts, D. J. (2018). Flameless combustion and its potential towards gas turbines. *Progress in Energy and Combustion Science*, 69, 28-62.
10. Starikovskiy A, Aleksandrov N. 2012. Plasma-assisted ignition and combustion. *Progress in Energy and Combustion Science*, 39: 61-110.
11. Sun W, Ju Y. 2013. Nonequilibrium plasma-assisted combustion: a review of recent progress. *J Plasma Fusion Res.*, 89: 208-219.
12. Dolmatov D. A. 2018. Principles of thermal and electrochemical burning of hydrocarbon fuels in combustion chambers of gas-turbine engines. Thesis for the scientific degree of Doctor of Technical Sciences by specialty 05.05.03 – engines and power plants. National aerospace university "Kharkiv aviation institute", MES of Ukraine, Kharkiv. [in Russian]
13. Yiguang Ju. Recent progress and challenges in fundamental combustion research. *Advances in Mechanics*, 2014, 44: 201402
14. Alrashidi, A.M., Adam, N.M., Hairuddin, A.A. and Abdullah, L.C., 2018. A review on plasma combustion of fuel in internal combustion engines. *International Journal of Energy Research*, 42(5), pp.1813-1833.
15. M Prather, R Sausen, AS Grossman, JM Haywood, D Rind, and BH Subbaraya. Potential climate change from aviation. *Aviation and the Global Atmosphere. A Special Report of IPCC Working Groups I and III*. Cambridge University Press, Cambridge, UK, pages 185–215, 1999.

16. C.P. Fenimore. Formation of nitric oxide in premixed hydrocarbon flames. Symposium (International) on Combustion, 13(1):373-380, 1971.
17. C.P. Fenimore. Reactions of fuel-nitrogen in rich flame gases. Combustion and Flame, 26(C):249-256, 1976.
18. T.C. Lieuwen and V. Yang. Gas Turbine Emissions. Cambridge Aerospace Series. Cambridge University Press, 2013.
19. P Glarborg, AD Jensen, and J E Johnsson. Fuel nitrogen conversion in solid fuel fired systems. Progress in Energy and Combustion Science, 29(2):89-113, 2003.
20. J. A. Miller, M. J. Pilling, and J. Troe. Unravelling combustion mechanisms through a quantitative understanding of elementary reactions. Proceedings of the Combustion Institute, 30(1):43-88, 2005.
21. Konnov, A. A. (2009). Implementation of the NCN pathway of prompt-NO formation in the detailed reaction mechanism. Combustion and Flame, 156(11), 2093-2105.
22. Jaravel, T. (2016). Prediction of pollutants in gas turbines using large eddy simulation (Doctoral dissertation)
23. M. C. Drake, J. W. Ratcliffe, and R. J. Blint. Measurements and modeling of Flame front NO formation and superequilibrium radical concentrations in laminar high-pressure premixed flames. Symposium (International) on Combustion, 23(1):387-395, 1991.
24. J. M. Bozelli and A. M. Dean. Direct studies of some elementary steps for the formation and destruction of nitric oxide in the HNO system. International Journal of Chemical Kinetics, 1995.
25. F. Biagioli and F. G• uthe. Effect of pressure and fuel-air unmixedness on NOx emissions from industrial gas turbine burners. Combustion and Flame, 151(1-2): 274-288, 2007.
26. A.H. Lefebvre and D.R. Ballal. Gas Turbine Combustion: Alternative Fuels and Emissions, Third Edition. Taylor & Francis, 2010.
27. T. Doerr. Combustor Fundamentals and Key Issues in Future Combustor Technology — Berlin – FORUM-AE - non CO2 Mitigation Technology Workshop, March 2017. Available at: http://www.forum-ae.eu/system/files/03_futurecombtech_rrperspective_2017_handout.pdf
28. Liu, Y., Sun, X., Sethi, V., Nalianda, D., Li, Y. G., & Wang, L. (2017). Review of modern low emissions combustion technologies for aero gas turbine engines. Progress in Aerospace Sciences, 94, 12-45.
29. Lieuwen T.C. Physics Of Premixed Combustion-Acoustic Wave Interactions, Combustion Instabilities In Gas Turbine Engines: Operational Experience, Fundamental Mechanisms, and Modeling, Progress in Astronautics and Aeronautics, 2005, pp. 315-366.
30. Lean Combustion Technology and Control. 2nd Edition, Academic Press, 2016, 280 p., ISBN 978-0-12-804557-2.
31. Kundu K.P., Penko P.F., Yang S.L. Simplified Jet-A/Air Combustion Mechanisms for Calculation of NOx Emissions. ASME Journal of Engineering for Gas Turbines and Power, 1998, pp. 535-545.

32. Wang T.S. Thermophysics Characterization of Kerosene Combustion. *Journal of Thermophysics and Heat Transfer*, 2001, no 2, pp. 140-147.
33. Khosravyel Hossaini, M. (2013). Review of the new combustion technologies in modern gas turbines. In *Progress in Gas Turbine Performance*. IntechOpen.
34. Puggelli, S., 2018. Vers une approche unifiée pour la simulation aux grandes échelles d'écoulements réactifs, diphasiques et turbulents (Doctoral dissertation, Normandie).
35. Faber, J., Greenwood, D., Lee, D., Mann, M., De Leon, P.M., Nelissen, D., Owen, B., Ralph, M., Tilston, J., van Velzen, A. and van de Vreede, G., 2008. Lower NO_x at higher altitudes policies to reduce the climate impact of aviation NO_x emission. CE Delft Solutions for environment, economy and technology.
36. Stickles, R. and Barrett, J., 2013. TAPS II Combustor Final Report-Technology Assessment Open Report. DTFAWA-1C-00046, FAA Countinuous Lower Energy, Emissions and Noise (CLEEN) Technologies Development.
37. Mongia, H., 2003. TAPS: a fourth generation propulsion combustor technology for low emissions. In *AIAA International Air and Space Symposium and Exposition: The Next 100 Years* (p. 2657).
38. Marinov, S., Kern, M., Merkle, K., Zarzalis, N., Peschiulli, A., Turrini, F. and Sara, O.N., 2010, October. On swirl stabilized flame characteristics near the weak extinction limit. In *ASME Turbo Expo 2010: Power for Land, Sea, and Air* (pp. 259-268). American Society of Mechanical Engineers.
39. Kern, M., Marinov, S., Habisreuther, P., Zarzalis, N., Peschiulli, A. and Turrini, F., 2011, January. Characteristics of an ultra-lean swirl combustor flow by LES and comparison to measurements. In *ASME 2011 Turbo Expo: Turbine Technical Conference and Exposition* (pp. 321-330). American Society of Mechanical Engineers.
40. Andreini, A., Caciolli, G., Facchini, B., Picchi, A. and Turrini, F., 2015. Experimental investigation of the flow field and the heat transfer on a scaled cooled combustor liner with realistic swirling flow generated by a lean-burn injection system. *Journal of Turbomachinery*, 137(3), p.031012.
41. Lieberman, M.A. and Lichtenberg, A.J., 2005. Principles of plasma discharges and materials processing. John Wiley & Sons.
42. Bogaerts, A., Neyts, E., Gijbels, R. and Van der Mullen, J., 2002. Gas discharge plasmas and their applications. *Spectrochimica Acta Part B: Atomic Spectroscopy*, 57(4), pp.609-658.
43. J. R. Roth, *Industrial Plasma Engineering*, vol. 1: Institute of Physics Publishing, 1997.
44. D. Z. Pai, D. A. Lacoste, and C. O. Laux, "Nanosecond repetitively pulsed discharges in air at atmospheric pressure-the spark regime," *Plasma Sources Sci. Technol.*, vol. 19, no. 6, 2010.
45. D. L. Rusterholtz, D. A. Lacoste, G. D. Stancu, D. Z. Pai, and C. O. Laux, "Ultrafast heating and oxygen dissociation in atmospheric pressure air by nanosecond repetitively pulsed discharges," *J. Phys. D. Appl. Phys.*, vol. 46, no. 46, p. 464010, Nov. 2013.

46. D. Z. Pai, D. A. Lacoste, and C. O. Laux, "Transitions between corona, glow, and spark regimes of nanosecond repetitively pulsed discharges in air at atmospheric pressure," *J. Appl. Phys.*, vol. 107, 2010.
47. D. Z. Pai, G. D. Stancu, D. A. Lacoste, and C. O. Laux, "Nanosecond repetitively pulsed discharges in air at atmospheric pressure - The glow regime," *Plasma Sources Sci. Technol.*, vol. 18, no. 4, 2009.
48. S. V Pancheshnyi, D. A. Lacoste, A. Bourdon, and C. O. Laux, "Ignition of Propane-Air Mixtures by a Repetitively Pulsed Nanosecond Discharge," *IEEE Trans. Plasma Sci.*, vol. 34, no. 6, pp. 2478–2487, Jun. 2006.
49. K. (Ken) Ostrikov, "Control of energy and matter at nanoscales: challenges and opportunities for plasma nanoscience in a sustainability age," *J. Phys. D: Appl. Phys.*, vol. 44, no. 17, p. 174003, May 2011.
50. D. Z. Pai, K. (Ken) Ostrikov, S. Kumar, D. A. Lacoste, I. Levchenko, and C. O. Laux, "Energy efficiency in nanoscale synthesis using nanosecond plasmas," *Sci. Rep.*, vol. 3, no. 1, p. 1221, Dec. 2013.
51. R. Dawson and J. Little, "Characterization of nanosecond pulse driven dielectric barrier discharge plasma actuators for aerodynamic flow control," *J. Appl. Phys.*, vol. 113, no. 10, p. 103302, Mar. 2013.
52. J. R. Roth, D. M. Sherman, and S. P. Wilkinson, "Electrohydrodynamic Flow Control with a Glow-Discharge Surface Plasma," *AIAA J.*, vol. 38, no. 7, pp. 1166–1172, Jul. 2000.
53. D. V. Roupasov, A. A. Nikipelov, M. M. Nudnova, and A. Y. Starikovskii, "Flow Separation Control by Plasma Actuator with Nanosecond Pulsed-Periodic Discharge," *AIAA J.*, vol. 47, no. 1, pp. 168–185, Jan. 2009.
54. Minesi, N., Stepanyan, S. A., Mariotto, P. B., Stancu, G. D., & Laux, C. O. (2019). On the arc transition mechanism in nanosecond air discharges. In *AIAA Scitech 2019 Forum* (p. 0463).
55. A. Lo et al., "Streamer-to-spark transition initiated by a nanosecond overvoltage pulsed discharge in air," *Plasma Sources Sci. Technol.*, vol. 26, no. 4, p. 45012, Jun. 2017.
56. D. Packan. 2003, Repetitive nanosecond glow discharge in atmospheric pressure air, Ph.D. Thesis, Stanford University.
57. D.Z. Pai, Nanosecond repetitively pulsed plasmas in preheated air at atmospheric pressure, PhD Thesis, Ecole Centrale Paris, Châtenay-Malabry, France, 2008.
58. Melle. Kaddouri Farah (2011) Development of advanced optical diagnostics for the study of ultrafast kinetics of oxygen production by nanosecond discharges in atmospheric pressure air. PhD thesis.
59. CUI Wei, REN YiHua, 2017. New-concept swirl flame dynamics coupling plasma and particles. *Science Foundation in China*, Vol. 25(2), pp.61-80.
60. Fridman, A. A.; Rusanov, V. D. Theoretical basis of nonequilibrium near atmospheric-pressure plasma chemistry. *Pure Appl. Chem.* 1994, 66, 1267.

61. Roh, H. S.; Park, Y. K.; Park, S. E. Superior decomposition of NO over plasma-assisted catalytic system induced by microwave. *Chem. Lett.* 2000, 578.
62. Tang, J.; Zhang, T.; Liang, D.; Sun, X.; Lin, L. Conversion of NO to N₂ in continuous microwave discharge. *Chem. Lett.* 2000, 916.
63. Tang, J.; Zhang, T.; Wang, A.; Ren, L.; Yang, H.; Ma, L.; Lin, L. Removal of NO by microwave discharge with the addition of CH₄. *Chem. Lett.* 2001, 140.
64. Reid, D. W. Chemical catalysis with RF power mechanisms, systems and costs. *Res. Chem. Intermed.* 1994, 97.
65. Sathiamoorthy, G.; Kalyana, S.; Finney, W. C.; Clark, R. J.; Locke, B. R. Chemical reaction kinetics and reactor modeling of NO_x removal in a pulsed streamer corona discharge reactor. *Ind. Eng. Chem. Res.* 1999, 38, 1844.
66. Suib, S. L.; Brock, S. L.; Marquez, M.; Luo, J.; Matsumoto, H.; Hayashi, Y. Efficient catalytic plasma activation of CO₂, NO, and H₂O. *J. Phys. Chem. B* 1998, 102, 9661.
67. Masuda, S. Pulse corona induced plasma chemical processes A horizon of new plasma chemical technologies. *Pure Appl. Chem.* 1988, 60, 727.
68. Mok, Y.S.; Ham, S.W. Conversion of NO to NO₂ in air by a pulsed corona discharge process. *Chem. Eng. Sci.* 1998, 53 (9), 1667.
69. Mok, Y. S.; Ham, I. S. Role of organic chemical additives in pulsed corona discharge process for conversion of NO. *J. Chem. Eng. Jpn.* 1998, 31 (3), 391.
70. Takaki, K.; Jani, M. A.; Fujiwara, T. Removal of nitric oxide in flue gases by multipoint to plane dielectric barrier discharge. *IEEE Trans. Plasma Sci.* 1999, 27 (4), 1137.
71. Kim, H.H.; Takashima, K.; Katsura, S.; Mizuno, A. Low temperature NO_x reduction process using combined systems of pulsed corona discharge and catalysis. *J. Phys. D: Appl. Phys.* 2001, 34, 604.
72. Broer, S.; Hammer, T. Selective catalytic reduction of nitrogen oxides by combining a nonthermal plasma and a V₂O₅WO₃/TiO₂ catalyst. *Appl. Catal. B* 2000, 28 (2), 101.
73. Tang, J., Zhang, T., Ma, L., & Li, N. (2003). Direct decomposition of NO activated by microwave discharge. *Industrial & engineering chemistry research*, 42(24), 5993-5999.
74. Bak M.S., Do H., Mungal M.G. Cappelli M.A. Plasma-assisted stabilization of laminar premixed methane/air flames around the lean flammability limit, *Combustion and Flame*, vol.50, no 36. 159:3128–3137, 2012.
75. Sasaki K., Shinohara K. Transition from equilibrium to nonequilibrium combustion of premixed burner flame by microwave irradiation, *Phys. D: Appl. Phys.*, 2012, vol. 45., no 45, 455202.
76. DeFilippo A., Saxena S., Rapp V.H., Dibble R.W., Chen J.Y., Nishiyama A., Ikeda, Y. Extending the Lean Stability Limits of Gasoline Using a Microwave-Assisted Spark Plug, *SAE Technical Paper*. doi: 10.4271/2011-01-0663
77. Rapp V.H., DeFilippo A., Saxena S., Chen J.Y., Dibble R.W., Nishiyama A., Moon A., Ikeda Y. Extending Lean Operating Limit and Reducing Emissions of Methane Spark-Ignited

Engines Using a Microwave-Assisted Spark Plug. *Journal of Combustion*, Volume 2012, no 5, pp.1-8.

78. Tanoue K., Kuboyama T., Moriyoshi Y., Hotta E., Shimizu N., Imanishi Y., Iida K. Extension of Lean and Diluted Combustion Stability Limits by Using Repetitive Pulse Discharges, SAE Technical Paper, 2010, 12 p. <https://doi.org/10.4271/2010-010173>.

79. Starikovskaia S. 2006. Plasma assisted ignition and combustion. *Journal of Physics D: Applied Physics*, 39: 265-299.

80. Y. Ju, W. Sun. Plasma assisted combustion: Dynamics and chemistry. *Progress in Energy and Combustion Science*. 48 (2015), 21-83. <http://dx.doi.org/10.1016/j.pecs.2014.12.002>.

81. Sun W., Uddi M., Won S.H., Ombrello T., Carter C., Ju Y. Kinetic effects of non-equilibrium plasma-assisted methane oxidation on diffusion flame extinction limits, *Combustion and Flame*, 2012, vol. 159, pp. 221–229.

82. Starik A.M., Kuleshov P.S., Sharipov A.S., Strelnikova V.A., Titova N.S. On the influence of singlet oxygen molecules on the NO_x formation in methane-air laminar flame, *Proceedings of the Combustion Institute*, 2013, vol. 34, Issue 2, pp. 3277–3285.

83. Shibkov V.M., Aleksandrov A.A., Chernikov V.A., Ershov A.P., Shibkova L.V. Microwave and Direct-Current Discharges in High-Speed Flow: Fundamentals and Applications to Ignition, *Journal of Propulsion and Power*, 2009, vol. 25, no. 1, pp. 123-137.

84. Pertl F.A., Smith J.E. Electromagnetic design of a novel microwave internal combustion engine ignition source, the quarter wave coaxial cavity igniter, *Proceedings of the Institution of Mechanical Engineers, Part D: Journal of Automobile Engineering*, 2009, pp.1405-1417.

85. Sun W., Won S.H., Ombrello T., Carter C., Ju Y. Direct ignition and S-curve transition by in situ nano-second pulsed discharge in methane/oxygen/helium counterflow flame, *Proceedings of the Combustion Institute*, 2013, vol. 34, Issue 1, pp.847-855.

86. Bulat P.V., Minin O.P., Volkov K.N.. Numerical simulation of optical breakdown in a liquid droplet induced by a laser pulse, *Acta Astronautica*, 2017. doi: <https://doi.org/10.1016/j.actaastro.2017.11.029>.

87. Michael J.B., Dogariu A., Shneider M.N., Miles R.B. Subcritical microwave coupling to femtosecond and picosecond laser ionization for localized, multipoint ignition of methane/air mixtures, *Journal of Applied Physics*, 2010, vol. 108, Issue 9, Article Number: 093308 <http://dx.doi.org/10.1063/1.3506401>

88. Grachev, L. P., Bulat, P., Esakov, I. I., Bulat, M. P., Volobuev, I. A., & Upyrev, V. V. 2018. Method for Burning Super-Poor Fuel Mixtures in the Combustion Chamber of the Energy Microturbine by Means of the Streamer Discharge. *PROBLEMELE ENERGETICII REGIONALE*, (2), 70-84.

89. Bulat, M., Bulat, P., Denissenko, P., Esakov, I., Grachev, L., Volkov, K., & Volobuev, I. 2019. Experimental study of microwave streamer discharge ignition of premixed air/fuel mixtures. *IEEE Transactions on Plasma Science*, 47(1), 57-61.

90. Dec J E. 2009. Advanced compression ignition engine understanding the in-cylinder processes, *Proc. Combust. Inst.* 32: 2727-2742.

91. Uddi M, Jiang N, Mintusov E, Adamovich I V, Lempert W R. 2009. Atomic oxygen measurements in air and air/fuel nanosecond pulse discharges by two photon laser induced fluorescence. *Proceedings of the Combustion Institute*, 32: 929-936.
92. Won S H, Windom B, Jiang B, Ju Y. 2014. The role of low temperature fuel chemistry on turbulent flame propagation. *Combustion and Flame*, 161: 475-483.
93. Ju Y, Maruta K. 2011. Microscale combustion: Technology development and fundamental research. *Progress in Energy and Combustion Science*, 37: 669-715.
94. Fernandez-Pello A C. 2002. Micropower generation using combustion: issues and approaches. *Proceedings of the Combustion Institute*, 29: 883-899.
95. Schott G L. 1965. Observations of the structure of spinning detonation. *Physics of Fluids*, 8: 850.
96. Bykovskii F A, Zhdan S A, Vedernikov E F. 2006. Continuous spin detonations. *Journal of Propulsion and Power*, 22: 1204-1216.
97. Ohkura Y, Rao P M, Zheng X. 2011. Flash ignition of Al nanoparticles: Mechanism and applications. *Combustion and Flame*, 158: 2544-2548.
98. Sabourin J L, Dabbs D M, Yetter R A, Dryer F L, Aksay I A. 2009. Functionalized graphene sheet colloids for enhanced fuel/propellant combustion. *ACS nano*, 3: 3945-3954.
99. Sun W Q, Won S H, Gou X L, Ju Y. 2014. Multi-scale modeling of dynamics and ignition to flame transitions of high pressure stratified n-heptane/toluene mixtures. *Proceedings of Combustion Institute*, 35.
100. Nayagam V, Dietrich D L, Ferkul P V, Hicks M C, Williams F A. 2012. Can cool flame support quasi-steady alkane droplet burning? *Combustion and Flame*, 159: 3583-3588.
101. Sun W, Uddi M, Ombrello T, Won S H, Carter C, Ju Y. 2011. Effects of non-equilibrium plasma discharge on counterflow diffusion flame extinction. *Proceedings of the Combustion Institute*, 33: 3211-3218.
102. Stancu G D, Janda M, Kaddouri F, Lacoste D A, Laux C O. 2009. Time-Resolved CRDS Measurements of the N₂ (A³Σ⁺ u⁺) Density Produced by Nanosecond Discharges in Atmospheric Pressure Nitrogen and Air. *The Journal of Physical Chemistry A*, 114: 201-208.
103. Sun W, Won S H, Ju Y. 2014. In situ plasma activated low temperature chemistry and the S-curve transition in DME/Oxygen/Helium Mixture, *Combustion and Flame*.
104. Xu B, Ju Y. 2009. Studies on non-premixed flame streets in a mesoscale channel. *Proceedings of the Combustion Institute*, 32: 1375-1382.
105. Sugiyama Y, Matsuo A. 2013. Numerical study of acoustic coupling in spinning detonation propagating in a circular tube. *Combustion and Flame*, 160: 2457-2470.
106. Pilla G, Galley D, Lacoste D A, Lacas F, Veynante D, Laux C O. 2006. Stabilization of a turbulent premixed flame using a nanosecond repetitively pulsed plasma. *Plasma Science, IEEE Transactions on*, 34: 2471-2477.
107. Ombrello T, Won S H, Ju Y, Williams S. 2010a. Flame propagation enhancement by plasma excitation of oxygen. Part I: Effects of O₃. *Combustion and Flame*, 157: 1906-1915.

108. Ombrello T, Won S H, Ju Y, Williams S. 2010b. Flame propagation enhancement by plasma excitation of oxygen. Part II: Effects of O₂(a¹Δ_g). *Combustion and Flame*, 157: 1916-1928.
109. Singleton D, Pendleton S J, Gundersen M A. 2011. The role of non-thermal transient plasma for enhanced flame ignition in C₂H₄-air. *Journal of Physics D: Applied Physics*, 44: 022001.
110. Matsubara Y, Takita K. 2011. Effect of mixing ratio of N₂/O₂ feedstock on ignition by plasma jet torch. *Proceedings of the Combustion Institute*, 33: 3203-3209.
111. Leonov S B, Savelkin K V, Firsov A A, Yarantsev D A. 2010. Fuel ignition and flame front stabilization in supersonic flow using electric discharge. *High Temperature*, 48: 896-902.
112. Little J, Takashima K, Nishihara M, Adamovich I, Samimy M. 2010. High lift airfoil leading edge separation control with nanosecond pulse driven DBD plasma actuators. *AIAA paper*, 4256: 2010.
113. Lacoste D A, Moeck J P, Paschereit C O, Laux C O. 2013. Effect of plasma discharges on nitric oxide emissions in a premixed flame. *Journal of Propulsion and Power*, 29: 748-751.
114. Serbin S, Mostipanen A, Matveev I, Tropina A. 2011. Improvement of the gas turbine plasma assisted combustor characteristics. In 49th AIAA Aerospace Sciences Meeting including the New Horizons Forum and Aerospace Exposition (pp. 4-7)., AIAA-paper 2011-61.
115. Sun W, Chen Z, Gou X, Ju Y. 2010. A path flux analysis method for the reduction of detailed chemical kinetic mechanisms. *Combustion and Flame*, 157: 1298-1307.
116. Williams S, Gupta M, Owano T, Baer D S, O'Keefe A, Yarkony D R, Matsika S. 2004. Quantitative detection of singlet O₂ by cavity-enhanced absorption. *Optics letters*, 29: 1066-1068.
117. Ombrello T, Qin X, Ju Y, Gutsol A, Fridman A, Carter C. 2006. Combustion enhancement via stabilized piecewise nonequilibrium gliding arc plasma discharge. *AIAA journal*, 44: 142-150.
118. Ombrello T, Ju Y, Fridman A. 2008. Kinetic ignition enhancement of diffusion flames by nonequilibrium magnetic gliding arc plasma. *AIAA Journal*, 46: 2424-2433.
119. W.S. Choi, Y. Neumeier, J. Jagoda, Stabilization of a combustion process near lean blow off (LBO) by an electric discharge, in 42nd Aerospace Sciences Meeting and Exhibit, AIAA 2004982. 2004: Reno, Nevada.
120. A. Bourig. 2009. Combustion Modification by Non-Thermal Plasma. Thesis for the degree of Doctor-Engineer.
121. D. Han, M.G. Mungal, Simultaneous measurement of velocity and CH layer distribution in turbulent non-premixed flames. *Proc. Combust. Inst.*, 2001. 28: p. 261-267.
122. Muñiz, M.G. Mungal, Effects of heat release and buoyancy on flow structure and entrainment in turbulent nonpremixed flame. *Combustion and Flame*, 2001. 126(1-2): p. 14021420.
123. C.D. Carter, J.M. Donbar, J.F. Driscoll, Simultaneous CH-PIV imaging of turbulent nonpremixed flames. *Appl. Phys. B*, 1998. 66(1): p. 129-132.

124. S. Prakash, S. Nair, T.M. Muruganandam, Y. Neumeier, T. Lieuwen, J. Seitzman, B.T. Zinn, Acoustic sensing and mitigation of lean blow out in premixed flames, in 43rd AIAA Aerospace Sciences Meeting and Exhibit. AIAA-2005-1420. 2005: Reno, Nevada.
125. S. Tachibana, S. Zimmer, Y. Kurosawa, K. Suzuki, The effects of location of secondary fuel injection on the suppression of combustion oscillation, in 2nd Asian Joint Conference on Propulsion and Power. 2005: Kitakyushu, Japan.
126. R.W. Schefer, M. Namazian, J. Kelly, Velocity measurements in a turbulent nonpremixed bluff-body stabilized flame. *Combust. Sci. Technol.*, 1987. 56(4-6): p. 101-138.
127. D.T. Yegian, R.K. Cheng, Development of a lean premixed low swirl burner for low NOx practical applications. *Combust. Sci. Technol.*, 1998. 139(1-6): p. 207-227.
128. S. Archer, A.K. Gupta, The role of confinement on flow dynamics under fuel lean combustion conditions, in 2nd International Energy Conversion Engineering Conference. AIAA 2004-5617. 2004: Providence, Rhode Island.
129. W. Kim, H. Do, M.G. Mungal, M.A. Cappelli, Optimal discharge placement in plasma-assisted combustion of a methane jet in cross flow. *Combustion and Flame*, 2008. 153: p. 603-615.
130. H.F. Calcote, Electrical properties of flames: burner flames in transverse electric fields *Proc. Combust. Inst.*, 1949. 3(1): p. 245-253.
131. H.F. Calcote, C.H. Berman, Increased methane-air stability limits by a DC electric field, in *Fossil Fuel Combustion Symposium*. 1989, p.25-31: Houston, Texas.
132. G.P. Tewari, J.R. Wilson, Experimental study of the effects of high frequency electric fields on laser-induced flame propagation. *Combustion and Flame* 1975. 24(2): p. 159-167.
133. C.S. Maclatchy, R.M. Clements, P.R. Smy, An experimental investigation of the effect of microwave radiation on a propane-air flame. *Combustion and Flame*, 1982. 45: p. 161-169.
134. S.H. Won, M.S. Cha, C.S. Park, S.H. Chung, Effect of electric fields on reattachment and propagation speed of tribrachial flames in laminar coflow jets. *Proc. Combust. Inst.*, 2007. 31: p. 963-970.
135. F.J. Weinberg, K. Hom, A.K. Oppenheim, K. Teichman, Ignition by plasma-jet. *Nature*, 1978. 272: p. 341-343.
136. F.B. Carleton, I.M. Vince, F.J. Weinberg, Structure and extinction of near-limit flames in a stagnation flow. *Proc. Combust. Inst.*, 1983. 19: p. 1523-1531.
137. A.J.J. Lee, F.J. Weinberg, A novel ignition device for the internal combustion engine. *Nature*, 1984. 311: p. 738-740.
138. S.A. Bozhenkov, S.M. Starikovskaia, A.Yu. Starikovskii, Nanosecond gas discharge ignition of H₂ and CH₄ containing mixtures. *Combustion and Flame*, 2003. 133: p. 133-146.
139. E.I. Mintoussov, S.V. Pancheshnyi, A.Y. Starikovskii, Propane-air flame control by nonequilibrium low temperature pulsed nanosecond barrier discharge, in 42nd AIAA Aerospace Sciences Meeting and Exhibit. 2004: Reno, Nevada
140. D. Galley, G. Pilla, D. Lacoste, S. Ducruix, F. Lacas, D. Veynante, C.O. Laux, Plasma-enhanced combustion of a lean premixed air-propane turbulent flame using a nanosecond

repetively pulsed plasma, in 43rd AIAA Aerospace Sciences meeting and Exhibit, AIAA 20051193. 2005.

141. N. Chintala, A. Bao, G. Lou, I.V. Adamovich, Measurements of combustion efficiency in nonequilibrium RF plasma-ignited flows. *Combustion and Flame*, 2006. 144(4): p. 744-756.

142. W. Kim, H. Do, M.G. Mungal, M.A. Cappelli, Plasma-discharge stabilization of jet diffusion flames. *IEEE Trans. Plasma Sci.*, 2006. 34(6): p. 2545-2551.

143. Wu, L. (2013). *Kinetic Studies of Non-equilibrium Plasma-assisted Ignition and Combustion*. Drexel University.

144. Bahr, D.W., 1987. Technology for the design of high temperature rise combustors. *Journal of propulsion and power*, 3(2), pp.179-186.

145. Suo, J., Yu, H. and Zheng, L., 2017. Experimental Study on Lean Blowout of a High Temperature Rise Combustor. In 55th AIAA Aerospace Sciences Meeting (p. 1056).

146. Liu Xingjian, He Liming, Yi Chen, Lei Jianping, Deng Jun Emission characteristics of aviation kerosene combustion in aero-engine annular combustor with low temperature plasma assistance. *Thermal Science 2018 OnLine-First Issue 00*, Pages: 138-138. <https://doi.org/10.2298/TSCI171002138L>

147. Xing-Jian, L., Li-Ming, H., Jin-Lu, Y. and Hua-Lei, Z., 2015. Experimental investigation of effects of airflows on plasma-assisted combustion actuator characteristics. *Chinese Physics B*, 24(4), p.045101. http://cpb.iphy.ac.cn/article/2015/cpb_24_4_045101.html

148. Liming, H. E., Yi, C. H. E. N., Jun, D. E. N. G., Jianping, L. E. I., Li, F. E. I., & Pengfei, L. I. U. (2019). Experimental study of rotating gliding arc discharge plasma-assisted combustion in an aero-engine combustion chamber. *Chinese Journal of Aeronautics*. 32(2), pp. 337-346. <https://doi.org/10.1016/j.cja.2018.12.014>

149. Baldur Eliasson. *Nonequilibrium Volume Plasma Chemical Processing*. IEEE TRANSACTIONS ON PLASMA SCIENCE, VOL. 19, NO. 6, DECEMBER 1991

150. Chang, J. S. (2008). *Physics and chemistry of plasma pollution control technology*. *Plasma Sources Science and Technology*, 17(4), 045004.

151. Fridman, A. (2008). *Plasma Chemistry*, Cambridge University Press, Cambridge, USA, ISBN-13 978-0-521-84735-3

152. Penetrante, B. M. & Schultheis, S. E. (1993). *Non-Thermal Plasma Techniques for Pollution Control*, NATO ASI Series, Vol. G34, Springer, Part A and B, Berlin, Germany, ISBN 0258-2023

153. H.H. Kim, 2004, Nonthermal plasma processing for air-pollution control: A historical review, current issues, and future prospects. *Plasma Processes and Polymers*, Vol. 1, pp. 91-110, ISSN 1612-8850.

154. Djaouani, N., Lemerini, M., & Dahham, O. S. (2018). Numerical Analysis of the Chemical Reactions Effects on NO_x Conversion under Various Reduced Electric Fields. *INTERNATIONAL JOURNAL OF NANOELECTRONICS AND MATERIALS*, 11(3), 271-282.

155. Mir Agha Mousavi, (2017) Gas Turbine Combustion Chamber Analysis with Regard to the Effects of the Plasma Space, *Pal. Jour. V.16, I.3, No.2 2017*, 351-366.

156. Dae Hoon Lee, Kwan-Tae Kima , Hee Seok Kang, Young-Hoon Song , Jae Eon Park, 2013, "Plasma-assisted combustion technology for NO_x reduction in industrial burners," *Environ. Sci. Technol.*, 2013, 47 (19), pp 10964–10970. DOI: 10.1021/es401513t
157. Dolmatov, D. and Hajivand, M., 2018. On Low-Emission Annular Combustor Based on Designing of Liner Air Admission Holes. *Bulletin of the National Technical University "KhPI". Series: Power and Heat Engineering Processes and Equipment.* No. 13(1289), pp. 83-94.
158. Clean Cky2. Innovation Takes Off. Thematic Topics. Toulouse, May 2018. <https://www.cleansky.eu/sites/default/files/inline-files/CS2CFP08ID-thematic-topics.pdf>
159. Zadeh, J.E., Balegh, H. and Fallahi, R., 2016, September. Electromagnetic DORT time reversal dielectric spectroscopy. In 2016 8th International Symposium on Telecommunications (IST) (pp. 437-441). IEEE.
160. Dadhich, N., 2000. Electromagnetic duality in general relativity. *General Relativity and Gravitation*, 32(6), pp.1009-1023.
161. L.B. Ibraguimova, G.D. Smekhov, O.P. Shatalov, Recommended rate constants of chemical reactions in H₂-O₂ gas mixture with electronically excited species O₂(a¹Δ_g), O(¹D), OH(²Σ⁺) involved, in Institute of Mechanics of Lomonosov, Moscow State University, Moscow. 2003, <http://www.chemphys.edu.ru/pdf/2003-01-20-001.pdf/>.
162. Shuang-chen Ma , Juan-juan Yao , Li Gao , Xiao-ying Ma & Yi Zhao (2012) Experimental study on removals of SO₂ and NO_x using adsorption of activated carbon/microwave desorption, *Journal of the Air & Waste Management Association*, 62:9, 1012-1021, DOI: 10.1080/10962247.2012.695320
163. C.-Y. CHA Microwave induced reactions of SO₂ and NO_x decomposition in the char-bed, *Res. Chem. Intermed.* Vol. 20, No. 1, pp. 13-28 (1994)
164. M. Baeva, H. Gier, A. Pott, J. Uhlenbusch, J. Hoschele, and J. Steinwandel (2001) Studies on Gas Purification by a Pulsed Microwave Discharge at 2.46 GHz in Mixtures of N₂/NO/O at Atmospheric Pressure, *Plasma Chemistry and Plasma Processing*, Vol. 21, No. 2, 2001
165. Jian Luo, Steven L. Suib, Manuel Marquez, Yuji Hayashi, and Hiroshige Matsumoto (1998) Decomposition of NO_x with Low-Temperature Plasmas at Atmospheric Pressure: Neat and in the Presence of Oxidants, Reductants, Water, and Carbon Dioxide, *J. Phys. Chem. A*, 1998, 102 (41), pp 7954–7963

Appendix 2. Reaction scheme for hydrogen oxidation involving electronically-excited oxygen molecules

This MSU kinetic model has been obtained by Ibraguimova et al. [161]. Units are in mole-cm-sec-cal.

Reaction mechanism

Table A2.1 – Rate constants of reactions in an H/O system with particles in ground state. Dimensions are in (cm³/mol)m – 1/s, m is the order of reaction [161].

No.	Reactions	Domain of validity $\Delta T, 10^3 \text{ K}$	A	n	E, K	$\Delta \log k$
1	$\text{H}_2 + \text{O}_2 \rightarrow \text{H} + \text{HO}_2$	1.0-2.5	1.94E+14	0	29770	0.2
	$\text{H} + \text{HO}_2 \rightarrow \text{H}_2 + \text{O}_2$	0.25 – 2.0	2.39E+13	0.1	711	0.2
2	$\text{H}_2 + \text{O}_2 \rightarrow \text{O} + \text{H}_2\text{O}$	1.0 – 2.5	3.0E+13	0	35000	-
3	$\text{H}_2 + \text{O}_2 \rightarrow \text{OH} + \text{OH}$	0.76 – 2.5	4.47E+11	0	17338	0.5
	$\text{OH} + \text{OH} \rightarrow \text{H}_2 + \text{O}_2$	0.25 – 3.0	1.7E+13	0	24100	0.8
4	$\text{H}_2 + \text{M} \rightarrow \text{H} + \text{H} + \text{M}$					
	M=Ar	1.0-8.0	2.23E+14	0	48350	0.2
	M=H ₂	1.0-8.0	3.46E+14	0	48350	0.24
	M=O ₂	1.0-8.0	3.46E+14	0	48350	0.5
	M=H ₂ O	0.6-2.0	8.48E+19	-1.1	52530	0.7
	$\text{H} + \text{H} + \text{M} \rightarrow \text{H}_2 + \text{M}$					
	M=Ar	0.5-2.5	6.48E+17	-1	0	0.5
M=H ₂	0.3-5.0	9.72E+16	-0.6	0	0.5	
M=H ₂ O	0.3-2.0	1.0E+19	-1	0	0.7	
M=H	0.3-5.0	3.2E+15	0	0	0.5	
5	$\text{O}_2 + \text{M} \rightarrow \text{O} + \text{O} + \text{M}$					
	M=Ar	2.0-4.1	1.5E+18	-1	59380	0.17
	M=O ₂	2.0-5.0	9.8E+24	-2.5	59380	0.3
	M=O	2.0-5.0	3.5E+25	-2.5	59380	0.4
	M=O ₃ , H ₂ O	2.0-5.0	1.2E+19	-1	59380	1
	$\text{O} + \text{O} + \text{M} \rightarrow \text{O}_2 + \text{M}$					
	M=Ar	0.3-4.0	1.89E+13	0	-900	0.11
	M=O ₂	0.3-4.0	1.5E+16	-0.41	0	0.23
	M=O	0.3-4.0	5.34E+16	-0.41	0	0.2
	M=O ₃	0.3-4.0	1.3E+14	0	-900	0.8
6	$\text{H}_2 + \text{O}_2 + \text{O}_2 \rightarrow \text{HO}_2 + \text{HO}_2$	0.5 – 3.0	2.0E+17	0	13000	-
7	$\text{H}_2 + \text{OH} \rightarrow \text{H} + \text{H}_2\text{O}$	0.2-4.1	2.53E+8	1.48	1700	0.5
	$\text{H}_2\text{O} + \text{H} \rightarrow \text{H}_2 + \text{OH}$	0.5-2.5	1.87E+14	0	10433	0.3
8	$\text{OH} + \text{OH} \rightarrow \text{H}_2\text{O} + \text{O}$	0.25-4.1	1.5E+9	1.14	50	0.2
	$\text{H}_2\text{O} + \text{O} \rightarrow \text{OH} + \text{OH}$	0.25-3.0	5.75E+13	0	9052	0.2
9	$\text{O}_2 + \text{H} \rightarrow \text{OH} + \text{O}$	0.3-5.3	8.65E+14	-0.24	8200	0.1
	$\text{OH} + \text{O} \rightarrow \text{H} + \text{O}_2$	0.16-2.5	8.91E+12	0	-251	0.3
10	$\text{H}_2 + \text{O} \rightarrow \text{OH} + \text{H}$	0.3-4.1	5.1E+4	2.67	3160	0.5
	$\text{OH} + \text{H} \rightarrow \text{O} + \text{H}_2$	0.3-2.5	4.88E+3	2.8	1950	0.3
11	$\text{O}_2 + \text{O} + \text{M} \rightarrow \text{O}_3 + \text{M}$					
	M=Ar	0.2-2.5	4.3E+12	0	-1050	0.6
	M=O ₂	0.2-3.0	3.26E+19	-2.06	0	0.6
	M=O	0.22-3.0	2.28E+15	-0.5	-700	0.3
M=O ₃	0.22-3.0	1.67E+15	-0.51	-700	0.36	

	$O_3+M \rightarrow O_2+O+M$					
	M=Ar	0.2-3.0	2.48E+14	0	11430	0.1
	M=O ₂	0.3-3.0	1.54E+14	0	11600	-
	M=O	0.2-3.0	2.48E+15	0	11430	
	M=O ₃	0.3-3.0	4.4E+14	0	11600	0.2
12	$O_2+H+M \rightarrow HO_2+M$					
	M=Ar	0.3-4.1	6.1E+17	-0.8	0	0.5
	M=O ₂	0.5-3.0	2.7E+18	-1	0	0.7
	M=H ₂	0.3-2.0	2.09E+18	-0.8	0	0.5
	M=H ₂ O	0.3-2.0	1.56E+18	-0.8	0	0.5
	$HO_2+M=O_2+H+M$					
	M=Ar	20.5-3.0	2.1E+15	0	23000	0.2
	M=O ₂	0.5-3.0	2.8E+15	0	23000	0.3
13	$H_2O_2+M \rightarrow OH+OH+M$					
	M=Ar	0.95-1.5	6.0E+16	0	22900	0.3
	M=H ₂	0.50-2.5	3.2E+17	0	23820	-
	M=H ₂ O ₂	0.5-0.95	2.51E+18	0	24154	-
	$OH+OH+M=H_2O_2+M$					
	M=Ar	0.3-3.0	6.33E+23	-2.53	42	
	M=H ₂ O	0.3-0.4	1.44E+18	0	0	0.4
14	$H+OH+M \rightarrow H_2O+M$					
	M=Ar	0.3-3.0	8.3E+21	-2	0	0.3
	M=H ₂	0.5-3.0	2.0E+20	-1	0	-
	M=OH	1.74-1.86	8.34E+15	0	0	-
	M=H ₂ O	0.3-3.0	1.4E+23	-2	0	0.5
	$H_2O+M=H+OH+M$					
	M=Ar	0.3-2.5	4.0E+23	-2.2	59000	0.6
	M=O ₂	2.0-6.0	3.5E+15	0	52920	0.5
	M+H ₂ O	2.0-5.0	1.6E+17	0	57491	0.3
15	$H+O+M \rightarrow OH+M$	0.3-2.5	4.71E+18	-1	0	0.7
	$OH+M=O+H+M$					
	M=Ar, O ₂	0.3-2.5	2.41E+15	0	50000	0.7
16	$OH+O+M \rightarrow HO_2+M$					
	M=Ar	0.3-2.5	8.0E+16	0	0	2.0
17	$OH+H_2O \rightarrow H_2+HO_2$	0.25-3.0	7.9E+9	0.43	36100	1.4
18	$O_2+OH \rightarrow O+HO_2$	0.3-2.5	2.23E+13	0	26500	0.5
	$HO_2+O \rightarrow OH+O_2$	0.22-2.5	1.75E+13	0	-200	0.3
19	$HO_2+H \rightarrow OH+OH$	0.3-4.1	1.69E+14	0	440	0.4
	$OH+OH \rightarrow H+HO_2$	0.25-2.5	1.2E+13	0	20200	1.0
20	$OH+HO_2 \rightarrow H_2O+O_2$	0.25-4.1	2.85E+13	0	-250	0.13
	$H_2O+O_2 \rightarrow OH+HO_2$	0.5-3.0	5.6E+13	0.17	36600	1.5
21	$OH+O_3 \rightarrow O_2+HO_2$	0.22-2.5	9.6E+11	0	1000	0.6
22	$O_2+O_2 \rightarrow O_3+O$	0.25-3.0	1.2E+13	0	50500	0.6
	$O_3+O \rightarrow O_2+O_2$	0.2-1.0	4.82E+12	0	2060	0.3
23	$O_2+OH \rightarrow H+O_3$	0.25-3.0	4.4E+7	1.44	38600	2.0
	$O_3+H \rightarrow OH+O_2$	0.2-2.0	6.87E+13	0	437	0.7
24	$HO_2+O_3 \rightarrow OH+O_2+O_2$	0.2-1.0	1.66E+11	-0.284	1000	0.45
25	$H_2+HO_2 \rightarrow H_2O_2+H$	0.3-2.5	3.01E+13	0	13100	0.5
	$H+H_2O_2 \rightarrow HO_2+H_2$	0.3-1.0	1.69E+12	0	1890	0.3
26	$H_2+H_2O_2 \rightarrow H_2O+OH+H$	0.5-3.0	8.69E+12	0.5	18347	-
27	$H_2O_2+O_2 \rightarrow HO_2+HO_2$	0.3-2.5	5.42E+13	0	20000	0.7
	$HO_2+HO_2 \rightarrow H_2O_2+O_2$	0.3-2.5	1.8E+12	0	0	0.5
28	$H+H_2O_2 \rightarrow H_2O+OH$	0.3-1.0	1.02E+13	0	1800	0.3
	$OH+H_2O \rightarrow H+H_2O_2$	0.4-1.0	2.4E+14	0	40500	1.0
29	$H_2O+HO_2 \rightarrow OH+H_2O_2$	0.3-2.5	2.8E+13	0	16500	0.3
	$OH+H_2O_2 \rightarrow H_2O+HO_2$	0.3-1.45	4.46E+12	0	477	0.5
30	$H_2O+O_2 \rightarrow O+H_2O_2$	0.5-2.5	3.4E+10	0.52	44800	1.4
	$O+H_2O_2 \rightarrow H_2O+O_2$	0.3-2.5	8.4E+11	0	2130	1
31	$H_2O_2+O \rightarrow OH+HO_2$	0.28-1.0	1.08E+12	0	2000	0.35

Table A2.2 – Rate constants of supplementary reactions in an H/O system with particles in electronically excited state. Dimensions are in (cm³/mol)^m – 1/s, m is the order of reaction [161].

No.	Reactions	$\Delta T, 10^3 K$	A	n	E, K	$\Delta \log k$
32	$OH^* + H_2 \rightarrow H_2O + H$	1.0-2.5	1.0E+14	0	276	-
33	$OH^* + M \rightarrow OH + M$					
	M=Ar	1.0-2.5	2.9E+9	0.5	0	-
	M=O ₂ ,H ₂	1.0-2.5	2.9E+11	0.5	0	-
	M=H ₂ O	1.0-2.5	2.9E+13	0.5	0	-
34	$OH^* \rightarrow OH + hv$		1.4E+6	0	0	-
35	$H_2 + HO_2^* \rightarrow H_2O + OH^*$	1.0 -2.2	4.8E+19	-1.7	19000	-
36	$O + H + M \rightarrow OH^* + M$					
	M=Ar	1.0-2.5	3.0E+18	-1	0	-
	M=O ₂ ,H ₂	1.0-2.5	3.0E+18	-1	0	-
	M=OH	1.0-2.5	1.5E+19	-1	0	-
37	$O + H + M \rightarrow OH^* + M$					
	M=Ar	1.0-2.5	1.5E+18	-1	0	-
	M=H ₂ ,O ₂	1.0-2.5	4,77E+18	-1	0	-
38	$OH^* + O_2 \rightarrow O_3 + H$	1.0-2.5	2.3E+12	0.5	0	-
39	$OH^* + O_2 \rightarrow HO_2 + O$	0.5-3.0	1.2E+12	0.5	0	-
40	$OH^* + H_2O \rightarrow H_2O_2 + H$	0.5-3.0	7.5E+12	0	276	-
41	$O_2^* + M \rightarrow O + O + M$	1.0-3.0	2.6E+18	0	48188	-
42	$O_3^* + M \rightarrow O_2^* + O + M$	0.3-3.0	1.3E+14	0	11400	-
	$O_2^* + O + M \rightarrow O_3^* + M$	0.3-3.0	6.9E+12	0	-1050	-
43	$HO_2^* + M \rightarrow O_2^* + H + M$	0.2-2.2	6.9E+14	0	23000	-
	$O_2^* + H + M \rightarrow HO_2^* + M$	0.2-2.2	1.5E+15	0	-500	-
44	$O_2^* + M \rightarrow O_2 + M$					
	M=Ar	0.3	5.0E+3	0	0	-
	M=H ₂	0.3	2.7E+6	0	0	-
	M=O ₂	0.5-2.0	1.0E+6	0	0	-
	M=O,H	0.5-2.0	4.2E+8	0	0	-
	M=OH,H ₂ O,HO ₂ ,H ₂ O ₂	0.5-2.0	3.4E+6	0	0	-
45	$H + HO_2^* \rightarrow O_2^* + H_2$	0.3-2.5	4.8E+7	1.67	3162	-
46	$O^* + O_2 \rightarrow O + O_2$	0.3	6.03E+12	0	0	0.4
47	$O_2^* + O_3 \rightarrow O_2 + O_2 + O$	0.28-2.0	3.13E+13	0	2840	-
48	$O_2^* + H_2 \rightarrow H_2O + O^*$	0.5-2.5	3.5E+13	0	20000	-
49	$O_2^* + O_2 \rightarrow O_3 + O$	0.3-2.5	1.2E+13	0	39604	-
50	$O_2^* + H \rightarrow OH + O$	0.25-2.5	1.1E+14	0	3188	-
	$OH + O \rightarrow O_2^* + H$	0.3-2.5	5.8E+12	0	6224	-
51	$O_2^* + H_2 \rightarrow OH + OH$	0.25-2.5	1.7E+15	0	17000	-
52	$O_2^* + OH \rightarrow H + O_3$	0.25-2.5	4.4E+7	1.44	27225	-
53	$O_2^* + OH \rightarrow O + HO_2$	0.25-2.5	1.3E+13	0	17000	-
54	$O_3 + OH \rightarrow HO_2 + O_2$	0.25-2.5	4.8E+11	0	1000	-
55	$O_3 + HO_2 \rightarrow OH + O_2 + O_2$	0.25-2.5	1.0E+10	0	1000	-
56	$HO_2 + HO_2 \rightarrow H_2O_2 + O_2$	0.25-2.5	9.0E+12	0	500	-
57	$O_2 + O \rightarrow O_2^* + O$	0.3	1.2E+13	0	0	-
58	$O^* + H_2 \rightarrow OH + H$	0.1-2.1	8.7E+13	0	-14	-
59	$HO_2^* + H \rightarrow H_2O + O^*$	1.0-2.5	1.7E+12	0.46	678	-
60	$O^* + M \rightarrow O + M$					
	M=Ar	0.11-0.33	3.0E+11	0	0	-
	M=O ₂	0.2-0.35	1.93E+13	0	67	-
	M=O	0.298	3.0E+12	0	0	0.3
61	$O^* + H_2O \rightarrow OH + OH$	0.2-0.35	1.3E+14	0	0	-
62	$O^* + O_3 \rightarrow O + O + O_2$	0.2-1.0	7.9E+13	0	0	-

Appendix 3. Influence of reactions rate on conversion NOx species

Table A3.1 – Main reactions contributing to generation and destruction of NOx and their rate constants. (The units of rate constants are in $\text{cm}^3 \cdot \text{molecule}^{-1} \cdot \text{s}^{-1}$ for two body reactions, whereas $\text{cm}^6 \cdot \text{molecule}^{-2} \cdot \text{s}^{-1}$ for three body reactions) [154].

	Reactions	Rate constants
R1	$e + \text{O}_2 \rightarrow \text{O} + \text{O} + e$	$k_1 = 15 \times 10^{-9}$
R2	$e + \text{N}_2 \rightarrow \text{N} + \text{N} + e$	$k_2 = 2.05 \times 10^{-11}$
R3	$e + \text{H}_2\text{O} \rightarrow \text{OH} + \text{H} + e$	$k_3 = 3.35 \times 10^{-10}$
R4	$e + \text{CO}_2 \rightarrow \text{CO} + \text{O} + e$	$k_4 = 8.7 \times 10^{-11}$
R5	$\text{N}(^2\text{D}) + \text{O}_2 \rightarrow \text{NO} + \text{O}$	$k_5 = 5.2 \times 10^{-12}$
R6	$\text{N} + \text{O}_3^- \rightarrow \text{NO} + \text{O}_2 + e$	$k_6 = 5.0 \times 10^{-10}$
R7	$\text{O} + \text{NO}_3^- \rightarrow \text{NO} + \text{O}_3 + e$	$k_7 = 1.5 \times 10^{-10}$
R8	$\text{NO} + \text{O}_4^- \rightarrow \text{NO}_3^- + \text{O}_2$	$k_8 = 2.5 \times 10^{-10}$
R9	$\text{NO} + \text{O}_3^- \rightarrow \text{NO}_3^- + \text{O}$	$k_9 = 1.0 \times 10^{-11}$
R10	$\text{NO} + \text{O}_3^- \rightarrow \text{NO}_2^- + \text{O}_2$	$k_{10} = 2.6 \times 10^{-12}$
R11	$\text{H} + \text{NO}_2 \rightarrow \text{NO} + \text{OH}$	$k_{11} = 1.15 \times 10^{-10}$
R12	$\text{NO} + \text{HO}_2 \rightarrow \text{NO}_2 + \text{OH}$	$K_{12} = 1.1 \times 10^{-11}$
R13	$\text{N} + \text{NO}_3^- \rightarrow \text{NO}_2 + \text{NO} + e$	$K_{13} = 5.0 \times 10^{-10}$
R14	$\text{NO}_2^- + \text{N}_2\text{O}_5 \rightarrow 2\text{NO}_2 + \text{NO}_3^-$	$k_{14} = 7.0 \times 10^{-10}$
R15	$\text{N} + \text{O}_2^- \rightarrow \text{NO}_2 + e$	$k_{15} = 5.0 \times 10^{-10}$
R16	$\text{NO}_2 + \text{O}_3^- \rightarrow \text{NO}_2^- + \text{O}_3$	$k_{16} = 7.0 \times 10^{-11}$
R17	$\text{NO}_2 + \text{O}_3^- \rightarrow \text{NO}_3^- + \text{O}_2$	$k_{17} = 2.0 \times 10^{-11}$
R18	$\text{NO}_2 + \text{O}_2^- \rightarrow \text{NO}_2^- + \text{O}_2$	$k_{18} = 7.0 \times 10^{-10}$
R19	$\text{NO}_3^- + \text{O}_4^+ \rightarrow \text{NO}_3 + \text{O}_2 + \text{O}_2$	$k_{19} = 1.0 \times 10^{-7}$
R20	$\text{NO}_3^- + \text{NO}^+ \rightarrow \text{NO}_3 + \text{N} + \text{O}$	$k_{20} = 1.0 \times 10^{-7}$
R21	$\text{OH} + \text{HNO}_3 \rightarrow \text{NO}_3 + \text{H}_2\text{O}$	$k_{21} = 1.3 \times 10^{-13}$
R22	$\text{NO}_3 + \text{O}_2^- \rightarrow \text{NO}_3^- + \text{O}_2$	$k_{22} = 5. \times 10^{-10}$
R23	$\text{NO}_3 + \text{OH} \rightarrow \text{NO}_2 + \text{HO}_2$	$k_{23} = 2.6 \times 10^{-11}$
R24	$\text{NO}_3 + \text{NO}_2^- \rightarrow \text{NO}_2 + \text{NO}_3^-$	$k_{24} = 5.0 \times 10^{-10}$
R25	$\text{H}_2\text{O} + \text{O}(^1\text{D}) \rightarrow 2\text{OH}$	$k_{25} = 2.3 \times 10^{-10}$
R26	$\text{H} + \text{O}_3 \rightarrow \text{OH} + \text{O}_2$	$k_{26} = 2.8 \times 10^{-11}$
R27	$\text{H} + \text{O}^- \rightarrow \text{OH} + e$	$k_{27} = 6.5 \times 10^{-10}$
R28	$\text{HO}_2 + \text{O}_3 \rightarrow \text{OH} + 2\text{O}_2$	$k_{28} = 2.0 \times 10^{-15}$
R29	$\text{OH} + \text{O}_3 \rightarrow \text{HO}_2 + \text{O}_2$	$k_{29} = 6.5 \times 10^{-14}$
R30	$\text{OH} + \text{NO}_2 \rightarrow \text{HNO}_3$	$k_{30} = 3.5 \times 10^{-11}$
R31	$\text{OH} + \text{HO}_2 \rightarrow \text{H}_2\text{O} + \text{O}_2$	$k_{31} = 1.1 \times 10^{-10}$
R32	$\text{OH} + \text{NO}_2 + \text{O}_2 \rightarrow \text{HNO}_3 + \text{O}_2$	$k_{32} = 2.2 \times 10^{-30}$